Unterschrift des Betreuers

TECHNISCHE UNIVERSITÄT WIEN
Vienna University of Technology

DIPLOMARBEIT

Modification of Poly(vinyl alcohol) for Two Photon Polymerisation via Thiol-Ene Chemistry

Ausgeführt am Institut für
Angewandte Synthesechemie
der **Technischen Universität Wien**

unter der Anleitung von
Ao.Univ.Prof. Dipl.-Ing. Dr.techn. Robert **Liska**
und
Projektass. Branislav **Husár**, PhD

durch
Daniel **Bomze**, BSc
Friedlgasse 40/20, A-1190 Wien

Wien, 16. Oktober 2013

Unterschrift des Studenten

“Alle Menschen sind klug - die einen vorher, die anderen nachher.”

- Voltaire

Firstly, I want to thank Professor Robert Liska for giving me the possibility to write my diploma thesis in his research group and for supervising me during the last year. Also my second supervisor Branislav Husár deserves my thankfulness. Furthermore I want to thank my colleagues from the Institute of Applied Synthetic Chemistry and especially from the division of macromolecular chemistry for the numerous interesting discussions, cheerful moments and pleasant working atmosphere.

I want to thank Peter Gruber for supporting me while working with Two-Photon Polymerisation apparatus and for the LSM measurements. Also Marica Markovic, who performed the toxicology analysis and cell culturing deserves my gratefulness.
Further on I want to thank Viktoria Schwarz for her work during her Bachelor Thesis. Under my supervision, she did most of the photorheology characterisation of the prepared PVA derivatives. With her accurate and assiduous work together with her bright mind she helped me a lot to finish my thesis successfully.

Michelle, my girlfriend, who gives me the support I need in difficult situations and always has the right words in the right time to cheer me up deserves the most gratitude. Without you, Michelle, I would not have been able to write this thesis.
Also I want to thank my dear friends, who always stick by me and bring me pleasant time.

Last but not least I want to thank my family and particularly my parents Susanne and Immanuel. They all believed in me and always gave me support, help and motivation when I needed it.

Thank you all very much!

Abstract

Tissue engineering is a part of biomedical engineering which has the aim to replace removed or unhealthy tissue until the body has rebuilt it completely. A high priority of tissue engineering is the production of synthetic tissue that resembles real tissue as much as possible. Biocompatibility is defined as "the ability of a material to perform with an appropriate host response in a specific application" and is of uttermost importance for any material that should be used in the field of tissue engineering.

In this thesis, novel modifications of the synthetic polymer poly(vinyl alcohol) (PVA) were developed for usage in the field of biomedical engineering. Poly(vinyl alcohol) is a non-toxic (FDA approved [U.S. Food and Drug Administration]), watersoluble polymer that has already been modified by a bunch of different functional groups. The aim was to produce novel low toxic PVA macromers modified with reactive carbon-carbon double-bonds on the one hand and thiol groups on the other. These macromers should be photopolymerised via thiol-ene chemistry and finally used as material for the application in two-photon polymerisation. The advantages of thiol-ene chemistry over free radical polymerisation in general are: quantitative yields; only small concentrations of relatively benign catalysts; rapid reaction rates. Furthermore, this approach works in bulk or green solvents; it is insensitive to water and oxygen; and usually requires no cleanup.

To form the hydrogels, an additive manufacturing technique (AMT, formerly known as rapid prototyping) was used - two photon polymerisation (2PP). The benefits of two photon polymerisation are the possibility to create almost unlimited complex shapes with a resolution of less than 1 μm. In comparison to other stereolithographic techniques, there is no need for supporting material to form shapes with overhang.

In this thesis PVA was modified with allyl succinic anhydride as well as with norbornene anhydride to produce macromers with reactive ene groups. Further PVA was modified with γ-thiobutyrolactone to yield macromers with thiol groups. Toxicity studies have shown that the material exhibits almost no cell-toxicity, when used in concentrations of 1% and 0.1% for 24 hours. The cross-linked hydrogels were studied concerning their swellability and have shown a high mass swell ratio. Photorheology was used to optimize mixtures concerning reactivity based on their thiol-to-ene ratio, photoinitiator concentration and macromer content. Also the storage stability of the macromer mixtures with different concentrations of pyrogallol as inhibitor has been investigated. Finally processing windows for 2PP of selected mixtures were determined. PVA-Norbornene showed excellent results for the application in biomedical engineering.

Zusammenfassung

Als Teilgebiet der Biomedizintechnik soll Tissue Engineering entferntes oder erkranktes Gewebe ersetzen, bis der Körper es vollständig nachgebildet hat. Vorranging ist dabei, dass das synthetische Gewebe dem natürlichen Gewebe so stark als möglich ähnelt und eine gute Biokompatibilität (das ist die Fähigkeit, im Wirtsystem keine negativen Reize zu entfalten) aufweist. In Rahmen dieser Arbeit wurden neue Modifikationen von Polyvinylalkohol (PVA) hergestellt. Diese Substanzen sind potentielle Kandidaten für biomedizintechnische Anwendungen. PVA ist ein ungiftiges, wasserlösliches, synthetisches Polymer, das bereits mit einer Vielzahl an funktionellen Gruppen umgesetzt worden ist. Das Ziel dieser Arbeit war es, neue PVA Makromere herzustellen, welche sowohl mit reaktiven Kohlenstoff-Kohlenstoff-Doppelbindungen als auch mit Thiolgruppen ausgestattet sind. Die hergestellten Macromere sollten mittels Thiol-Ene Chemie durch Photopolymerisation vernetzt und als Material für die Zwei-Photonen-Polymerisation eingesetzt werden. Die Vorteile von Thiol-Ene Polymerisation gegenüber freier radikalischer Polymerisation sind quantitative Umsätze, schnelle Reaktionsraten sowie die Insensititvität gegenüber Sauerstoff und Wasser. Weiters benötigt Thiol-Ene Chemie nur kleine Katalysator-Konzentrationen, die Reaktionen laufen in wässrigen oder umweltverträglichen Lösungsmitteln ab und benötigen überdies meistens keine Aufreinigung der Produkte. Um die Quervernetzung der Hydrogele herzustellen, wurde Zwei-Photonen-Polyermisation (2PP) benutzt, eine Form der Additive Manufacturing Technologies (AMT). Der Vorteil von 2PP liegt in der Fähigkeit, auch sehr kompliziert geformte Strukturen, selbst mit Überhang, herzustellen, ohne dabei Stützmaterial zu benötigen. Dieses Stützmaterial muss bei anderen AMT Verfahren nach der Strukturierung entfernt werden. Außerdem ist mittels 2PP eine Auflösung von unter 1 μm erreichbar. Im Rahmen dieser Arbeit wurde die Synthese von mit Allylbernsteinsäureanhydrid und Nobornenanhydrid modifiziertem PVA entwickelt, wie auch die Synthese von PVA-derivaten mit γ-Thiolbutyrolacton. Toxizitätsstudien haben gezeigt, dass die Makromere in Konzentration von 1% und 0.1% keine Zelltoxizität aufweisen. Weiters wurden mittels Photorheologie der Einfluss von Thiol zu Ene Verhältnis, Makromer-Konzentration und Photoinitiator-Konzentration sowie die Lagerungsstabilität mit unterschiedlichen Konzentrationen von Pyrogallol als Inhibitor untersucht. Schließlich wurden noch Prozessfenster von ausgewählten Mischungen für die Anwendung als Material für 2PP ermittelt. Es hat sich gezeigt, dass PVA-Norbornen ausgezeichnete Resultate in Bezug auf Reaktivität und Eignung für 2PP aufweist und damit ein potentielles Material für die Biomedizintechnik darstellt.

Contents

Introduction

1 Tissue Engineering and Hydrogels

According to the yearly report of the Eurotransplant[1] organisation, responsible for coordination of organ transplants in Europe, the average time on the waiting list for a patient waiting for a kidney is over 42 months; for a heart, lung or liver it is about 15 months. While the number of transplants is almost constant for the last years, the number of patients on the waiting lists is constantly increasing. This shortage of transplantable organs on the one hand and the need for tissue that has to be replaced after trauma or disease on the other hand is the main reason for the need of tissue engineering. Tissue engineering has the aim to replace removed or unhealthy tissue until the body has rebuilt it completely.
A quite recent paper from Zopf et al.[2] clearly shows the ability of tissue engineering in saving lives. In their paper they describe the production and implantation of a 3D printed bioresorbable airway in an infant with tracheobronchomalacia, which is a condition in newborns which manifests itself with dynamic airway collapse and respiratory insufficiency. After 21 days from the implantation of the synthetic airway splint made of poly(caprolactone), the child could be discharged from hospital in good condition. One year after the surgery no unforeseen problems concerning the splint arised. This example shows how up to date this type of research and development is.
This is also represented from the high amount of current review papers on this topic.[3–8] Although there are many types of tissue that has to be replaced, in this thesis only tissue engineering for soft tissue will be considered. As replacement for soft tissue, hydrogels are used most commonly. Hydrogels have received very high attention due to their innate structural and compositional similarities to the extracellular matrix (ECM).[8] The ECM together with the interstitial space and basement membrane are building the mechanical framework for natural tissue. The ECM consists of two main structures: the collagen fibers which are formed as bundles and extend through interstitium providing durability, and the proteoglycan filaments which are coiled structures consisting of a protein chain in the center and glucoseaminoglycanes covalently bonded to this center (e.g. hyaluronic acid). The latter interconnect the cells and bind cations because of their negative charge.[9] Hydrogels are three-dimensional networks of hydrophilic polymers, that are cross-linked to form insoluble polymer structures. Being usually soft and elastic due to their water content, they are used for many biomedical applications.[4] Besides modified natural polymers like agarose, alginate, chitosan, fibrin, collagen and hyaluronic acid, also synthetic monomers

were used to produce hydrogels. Synthetic precursors for hydrogels are among others poly(ethylenglycol) (PEG), poly(vinyl alcohol) (PVA), poly(2-hydroxethyl methacrylate) (PHEMA).[8]

The first use of hydrogels in vivo were contact lenses made of PHEMA by Wichterle[10] developed in 1950s.

The primary purpose of the tissue scaffold is the promotion of tissue regeneration, therefore the hydrogels must meet the basic requirements of biocompatibility which are according to Agrawal[11]:

- no or very limited immunological response;
- non toxicity to the surrounding cells;
- no foreign body response;
- biodegradability (in some cases);
- permit cell attachment;
- degradation products have to be non-toxic and excretable;
- have appropriate mechanical properties for the indicated application;
- change in mechanical properties with degradation should be compatible with the regeneration process;

According to Williams[12] biocompatibility can be defined as "the ability of a material to perform with an appropriate host response in a specific application". Hydrogels in regenerative medicine are currently used as scaffolds to provide structural integrity; as tissue barriers; bioadhesives; as drug depots; for delivering bioactive agents and to encapsulate and deliver cells. Here the two main purposes concerning tissue engineering should be described in further detail:

Scaffolds:

Hydrogels are especially convenient for scaffolds because their mechanical properties can be adapted to mimic those of natural tissue. So they are used to provide bulk or mechanical constitution to a tissue construct, where cells are suspended within the three dimensional gel or adhered directly to the gel. It has been shown that cell adhesion is better in charged gels than in uncharged ones.[8] Furthermore, the modification of hydrogel precursors with the RGD adhesion peptide sequence (arginine, glycine, aspartic acid) showed a much better binding towards cells. Also an enhanced cellular migration, proliferation, growth and organization were reported by Shin[13] and Hersel.[14]

Cell encapsulation:

Allografts (transplantations from another individual of same species) bear the problem of immuno response which leads to rejection of the organ or tissue. To circumvent this reaction the cells that are supposed to be transplanted can be encapsulated with hydrogels. This allows diffusion of oxygen, nutrients and metabolic waste products from

and to the cell while providing immuno-isolation. For development of an artificial pancreas, the islets of Langerhans were encapsulated via interfacially photopolymerisation of poly(ethylenglycol) diacrylate (PEGDA). It has been observed that with an adequate reduction of the hydrogel thickness the diffusion was high enough that the cell remained viable while the hydrogel retained its immuno-isolation function.[15]

Barriers:

The use of barriers in the healing process of injured tissue should reduce post-operative adhesion formation as well as thrombosis or restenosis following vascular injury. For prevention of tissue adhesion, hydrogel layers were placed as coatings on the tissue surface. It showed that the hydrogel layers where highly resistant to protein adsorption and diffusion as well as to cell adhesion. To prevent thrombosis and restenosis the tunica intima (innermost layer of blood vessels) was coated via interfacial photopolymerisation with hydrogels. These materials prevented thrombosis and reduced intima thickening (a measure of restenosis) significantly.[16]

For most applications a controllable breakdown of the scaffolds is desired and needed to achieve better results in biomimetics. The reason is that the organism is constantly renewing its cells which can be seen in wound-healing and rebuilding of the bones by osteoclasts and osteoblasts. With degradeable hydrogels one can facilitate two main problems of Tissue engineering: the long-term stability of the implant and the ingrowth of cells. If the implant should stay forever in the body, much more considerations about the ability to adapt of the implant have to be done. While ageing, the body constantly changes its shape and size, which long lasting implants would also have to do.

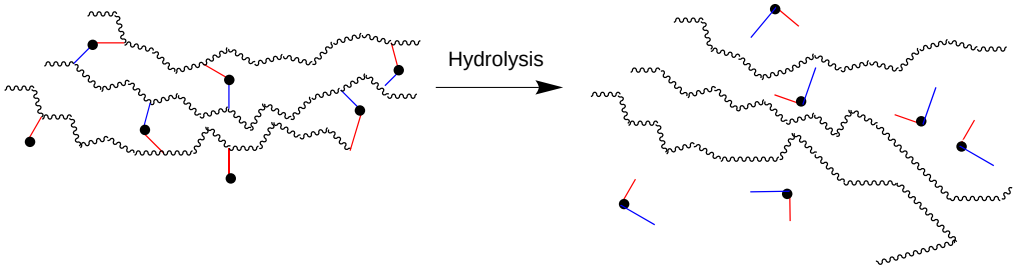

Figure I.1.1: Hydrolysis process of a cross-linked hydrogel

Figure I.1.1 shows the process of hydrolysis in cross-linked hydrogels. As can be seen the polymer network undergoes scission at different bonds where it cross-linked before (black blobs mark the cross-linking points).

With controllable degradation, the hydrogel yields the proliferating cells which can remodel the scaffold as needed. It has to be noted that for special applications like cartilage or corneal replacement, degradation is not necessary nor desired. Ideally the rate of cell growth and the degradation of the scaffold should be identical.

Techniques for the production of hydrogel scaffolds are emulsification, micromolding, and Additive Manufacturing Technologies (AMT). Emulsification was an early method to produce hydrogel microspheres. The precursors were put in an hydrophobic medium and the hydrophilic phase was broken up by agitation resulting in small droplets that form the

microsphers. The size of the microsphere can be controlled with the agitation conditions. There are some drawbacks concerning this technique: the shape of the formed gels is limited to spheres and heterogeneity of the formed hydrogels.
Micromolding will form the hydrogel based on the structure of the mold, which enables additional control of size and heterogeneity of the gels. With this technique the production of nanoscale hydrogel structures with controlled shape and size is possible in reproducible manner.
Other production techniques are the AMT methods, which allow the production of objects with virtually no limit of complexity of the shape and no need for tools or molds. Stereolithography (a type of AMT) is based on the solidification of liquid formulations upon irradiation with light. The structures are built layer by layer by curing the formulation and adding new formulation to the top of the cured resin. Among this techniques are stereolithography with UV-lasers (SLA), digital light processing (DLP) and two photon polymerisation (2PP). The main difference between SLA and DLP on the one hand and 2PP on the other hand is the way how layers can be produced. SLA and DLP are based on the addition of one layer to the next with the drawback that shapes with overhang can only be produced with the use of supporting material, which has to be removed after the production process. Also the possible resolution of SLA (20 µm)[17] and DLP (40 µm)[18] cannot compete with 2PP (1.5 µm).[19] A detailed view on the technique of two photon polymerisation is given in the following section.

2 Two-Photon Polymerisation

Two-photon polymerisation (2PP) is an additive manufacturing technology based on laser-induced curing of cross-linkable formulations. The term additive manufacturing technology (AMT) refers to a production technique which allows the production of parts in low quantities up to unique pieces. The structure of the produced part can be constructed using computer aided design (CAD).[20] The former term for AMT was rapid prototyping, which should not be used anymore because not only prototypes are produced with these technique.

A great advantage of 2PP compared to other AMTs is the enormous resolution - up to nanometer scale - in which the parts can be produced. This is especially important for one of the most important applications of 2PP: Tissue engineering. As mentioned in the previous section, the structure of synthetic ECM is crucial for the cell growth.

For 2PP a radiation source, a suitable photoinitiator (PI) for starting the polymerisation process and a cross-linkable mixture is needed. A suitable two-photon photoinitiator is a molecule that absorbs two photons (Two-photon absorption [2PA]) and converts to a higher energy state. From this state it should convert all the energy towards initiating radicals. In general these molecules consist of electron donors and electron acceptors which are linked to a chromophore.

The energy of the photons is added to each other so that with two photons of 800 nm wavelength the same energy level can be reached as with one photon of 400 nm.

This is especially convenient because organic tissue has a minimum of absorption at 800 nm which allows the deep penetration of radiation in the tissue and thus 2PP at the place of destination. Figure I.2.2 displays the Jablonski diagram indicating processes that compete with radical formation that initiates polymerisation.

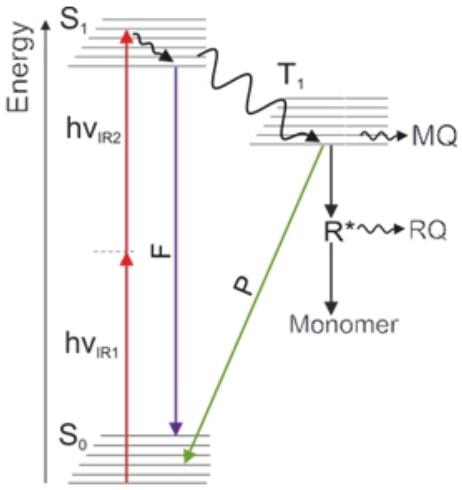

Figure I.2.2: Jablonski diagram for 2PA and initiation reducing processes including fluorescence (F), phosphorescence (P), monomer quenching (MQ) and radical quenching (RQ)

As can be seen in Figure I.2.2, the energy of two photons is added to each other, thus resulting in an excitation of a molecule from ground state S_0 to excited state (S_1).

From this S_1 state the molecule can relax and looses its excitation energy via fluorescence (F) or can convert to a excited triplet state (T_1). Again more than one possibility is available for relaxing from T_1 to ground state S_0: The molecule can release a photon and phosphorescence (P) occurs, or can quench monomers or radicals, or else it finally starts the radical reaction. Thus a good PI should reduce all factors mentioned before that reduce the rate of radical initiation.
The radiation source is needed to excite the photosensitive chromophore of the PI in the focal point of a microscope objective and in this way triggers the two-photon induced chain-reaction polymerisation. The reaction only occurs in a very confined region called volumetric pixel (voxel) which leads to the before mentioned very high resolution. The main difference between one-photon (OPA) and two- or multi-photon absorption (TPA, MPA) is the probability of two photons hitting the chromophore of an initiator at the same time (within a time frame of 10^{-15}s)[21], which is described impressively by Denk[22]: Rhodamine B is a good one-photon and two-photon absorber. In bright sunlight this molecule absorbs about one photon per second through a one-photon process whereas a photon pair (two-photon process) is only absorbed every 10 million years. In the entire age of the universe no three-photon absorption is expected.

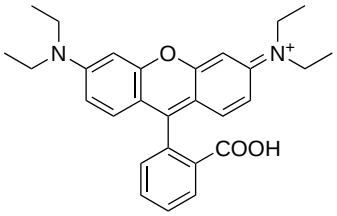

Figure I.2.3: Structure of dye Rhodamine B

Thus a laser with high output energy is needed for this process to happen in a reasonable amount of time. With the invention of tightly focused femtosecond (fs) pulsed laser like Ti:S (Titanium-Saphire) lasers the requirements were met to do 2PP.[20]
The following Figure shows a cuvette filled with Rhodamine solution with 2 beams passing through it.

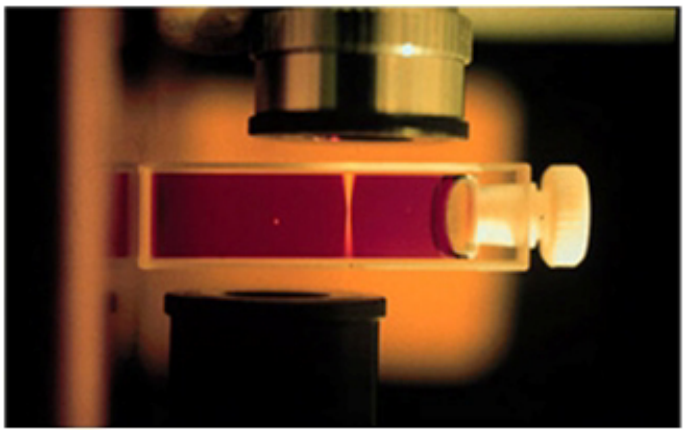

Figure I.2.4: TPA (left) and OPA (right) of fluorescence dye solution[23]

Figure I.2.4 illustrates the difference between OPA and TPA on a laserbeam going through a cuvette with fluorescence dye. On the right part the whole beam can be seen going through the cuvette which is a normal one-photon absorption. In constrast, on the left part of the cuvette only a very small lighted point can be seen. Only in this very small volume, absorption and therefore fluorescence occurs. This process is due to two-photon absorption and shows well the difference between OPA and TPA.

Photopolymerisation:
Photopolymerisation is one form of radical polymerisation, which is in this case initiated by photoinitiators.

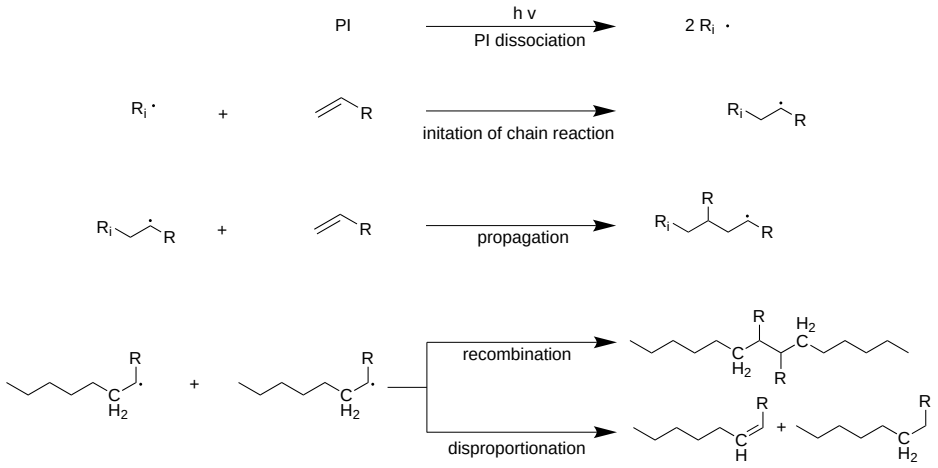

Figure I.2.5: Mechanism of photopolymerisation

In Figure I.2.5 the mechanism of photopolymerisation is displayed. The reaction starts with the cleavage of a PI to form two initiator radicals. These radicals can start the radical polymerisation of the monomer and leads to propagation. Termination of the polymerisation process is because of recombination of two radicals or because of disproportionation. Typical monomers that can be used for photopolymerisation are hexanediol diacrylate (HDDA), pentaerythritol tetraacrylate (PETTA), trimethylolpropane triacrylate (TTA) and ethoxylated trimethylolpropane triacrylate (ETA).[24] They are shown in Figure I.2.6.

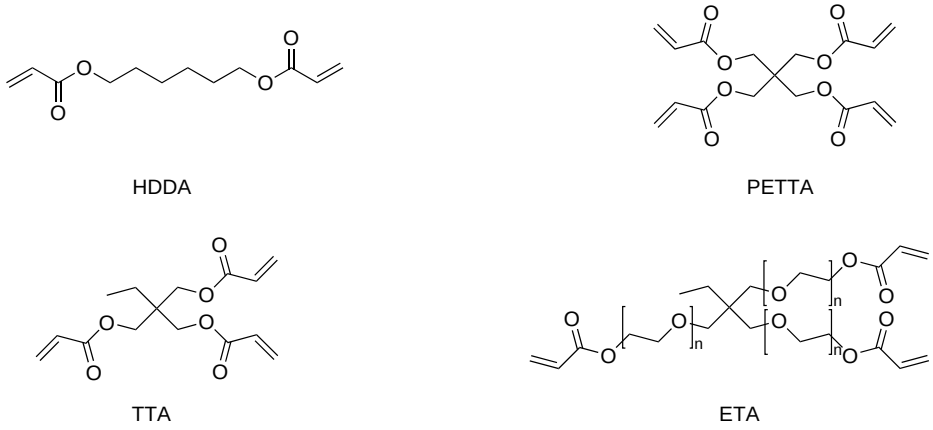

Figure I.2.6: Structures of photopolymerisable monomers which have been studied for their suitability in tissue engineering

These monomers are hydrophobic and therefore unsuitable for preparation of hydrogels. Another problem with these monomers concerning the application for tissue engineering is their cell toxicity.
For for the production of photopolymerisable hydrogels macromers with two or more reactive groups are used.[16]

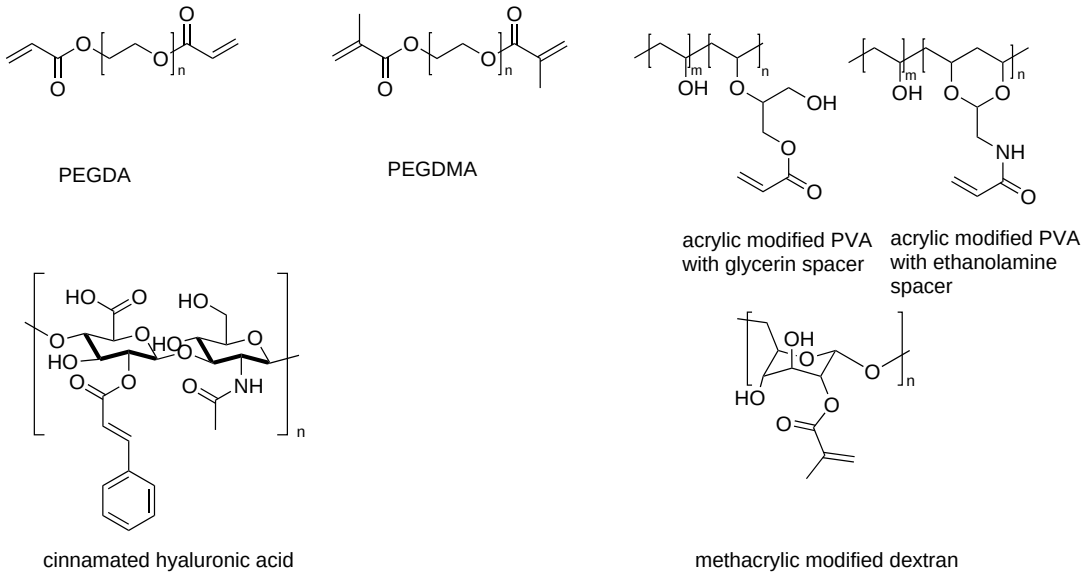

Figure I.2.7: Structures of macromers modified with acrylic acid, methacrylic acid and cinnamic acid

Figure I.2.7 shows structures from a selection of synthesized macromers which have been used for the production of hydrogels in tissue engineering. Sawhney[25] et al. developed photopolymerisable mixtures of poly(ethylen glycol)-co-poly(lactic acid) diacrylate to build biodegradable hydrogels that adhere to surrounding tissue if polymerised in contact with the tissue and are not adhesive at all if polymerised prior to contact with the tissue. This phenomenon is most likely due to interpenetration of the built hydrogel with the surrounding tissue, which does not happen in the case of prior to contact polymerisation.
Poly(ethylen glycol) dimethacrylate (PEGDMA) was successfully used by Elisseeff[26] to

encapsulate ovine and bovine chondrocytes via photopolymersation of PEGDMA. The number of cells decreased at the beginning of the encapsulation, but stabilized further on. Also, it showed that the cells built new, functional extracellular matrix, which increased over time. Therefore their conclusion was that this system is feasible for tissue engineering.

The natural polysaccharide hyaluronic acid was modified by Matsuda[27] with cinnamic acid groups to produce a hydrogel barrier in order to prevent adhesion between injured natural tissues, what normally would retard the healing process. They covered the peritoneum of rats with the hydrogel and no signs of tissue adhesion could be seen after one week; some adhesion could be observed 2 weeks after implantation.

The swellability and morphology of swollen and unswollen modified dextran hydrogels were studied by Kim[28]. They modified dextran with methacrylic moieties and cross-linked their formulation via irradiation with UV-light. They discovered differences concerning the morphology between the swollen and unswollen gels as well as a strong heterogeneity of the pore size. With decreasing intensity of the UV light, depending on penetration depth of the light, the pore size increased as a sign of lower cross-linking density.

3 Thiol-Ene Chemistry

The reaction between carbon-carbon double bonds and thiol-groups is nothing revolutionary new. For example, the vulcanization of rubber tires with sulfur was patented in the mid-19th century.[29] However, the use of thiol-ene polymerisation in polymer chemistry avoided some serious drawbacks of classical free radical polymerisation which suffers from inhibition by oxygen,[30] volume relaxation and stress development,[31] complex polymerisation kinetics[32] and formation of highly heterogeneous networks.[33] According to the concept of Sharpless et al.[34] from 2001, one can think of thiol-ene reactions of click reactions. The characteristics of click reactions are

- high yields;
- byproducts (if formed) must be removable with non-chromatographic methods;
- insensitivity to oxygen and water;
- mild reaction conditions;
- solventless or aqueous conditions;
- orthogonality with other common organic synthesis reactions;
- regio- and stereo specificity;
- amenability to a wide variety of readily available starting materials;

As the thiol-ene reaction achieves quantitative yields; requires only small concentrations of relatively benign catalysts; has rapid reaction rates; works in bulk and green solvents; is insensitive to water and oxygen, requires usually no cleanup and yields a single regioselective product, this reaction can truly be seen as click-reaction.[35] Another argument that pushed this reaction type was the commercial availability of starting materials on the one hand and the ease of synthesising products for this purpose.
There are two general types of reactions between thiols and carbon-carbon double bonds. Firstly, the radical addition of thiols to nonactivated carbon-carbon double bonds which are mostly referred as thiol-ene free radical addition, and second the Michael-type nucleophilic addition of anionic thiyls.[36] The first type uses radical initiators while the second involves anionic initiation. The storage stability of thiol-ene formulations is very poor unless stored with suitable inhibitors. Esfandiari et al.[37] showed that with an inhibition system covering both modes of reaction (radical and nucleophilic Michael addition), an increase in shelflife time stability up to 110 days is possible.

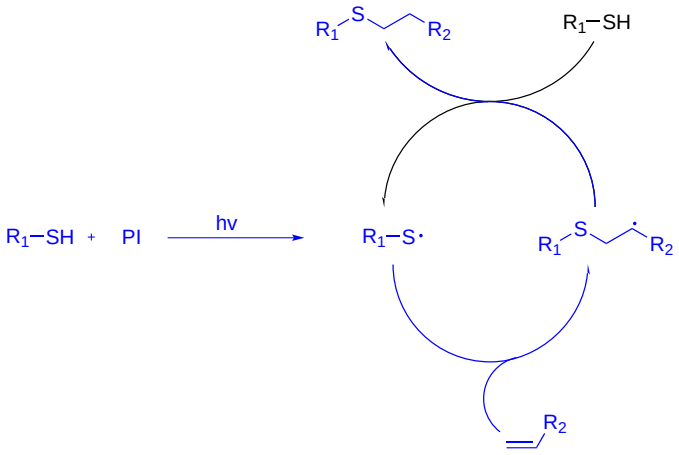

Figure I.3.8: Reaction mechanism of the free radical thiol-ene reaction with alternating chain transfer

Figure I.3.8 depicts the thiol-ene reaction as a step-growth-reaction; no homopolymerisation takes place during the reaction, which leads to conversions up to 100% unless not otherwise limited (e.g. mass-transfer limitation). If one compares the addition of the same thiol to electron-rich (e.g. vinyl ethers) and electron-poor enes (e.g. styrenes), the addition is much faster in case of electron-rich double bonds.[38] The initiation of thiol-ene reactions can be done via thermal initiation or light induced with photoinitiators. It was found that using photochemical conditions lead to faster and, in many cases quantitative reactions.[36] According to the review of Hoyle et al.,[38] thiol-ene reactions were successful with norbornenes, vinyl ethers and esters, allyl ether and esters, (meth)acrylates, unsatured esters, (substituted) maleimides and many other monomeres. But also the modification of natural products with thiol groups or with double bonds has been done and the products were very effective as reactive components in thiol-ene systems.[39]
The use of modified natural polymers has the advantage of using sustainable materials with adjustable properties according to one's needs. Applications of thiol-ene polymers range from surface modification, high energy absorbing materials to hydrogels with biomaterial application. The latter can be used for cell encapsulation, tissue engineering, drug delivering systems and many more.

Objective

There are a bunch of natural and synthetic polymers, which have been modified for the production of hydrogels with applications in the field of biomedicine (e.g. tissue engineering). Poly(vinyl alcohol) (PVA) is a non-toxic (FDA approved), water soluble polymer that has been modified with a variety of different functional groups. Acrylate and methacrylate modified PVA derivatives are state of the art in photocross-linkable PVA macromers as hydrogel precursors in biomedical applications. The cell toxicity of acrylic acid and the comparatively low reactivity of methacrylates are the main drawback of these substances. Hence the aim of this thesis was to develop a synthetic strategy for the modification of PVA with reactive carbon-carbon double-bond containing moieties on the one hand and with thiol groups on the other hand to yield photocross-linkable macromers. These macromers should react in a thiol-ene reaction to achieve a rapid and quantitative conversion. Also the formed hydrogels should be biodegradeable to facilitate cell growth. For this purpose the use of esters groups as linkage between PVA and the reactive groups promises good results. Also synthesis should yield different degrees of substitution of the different PVA derivatives so that the mechanical properties can be adjusted according to the need of their application.

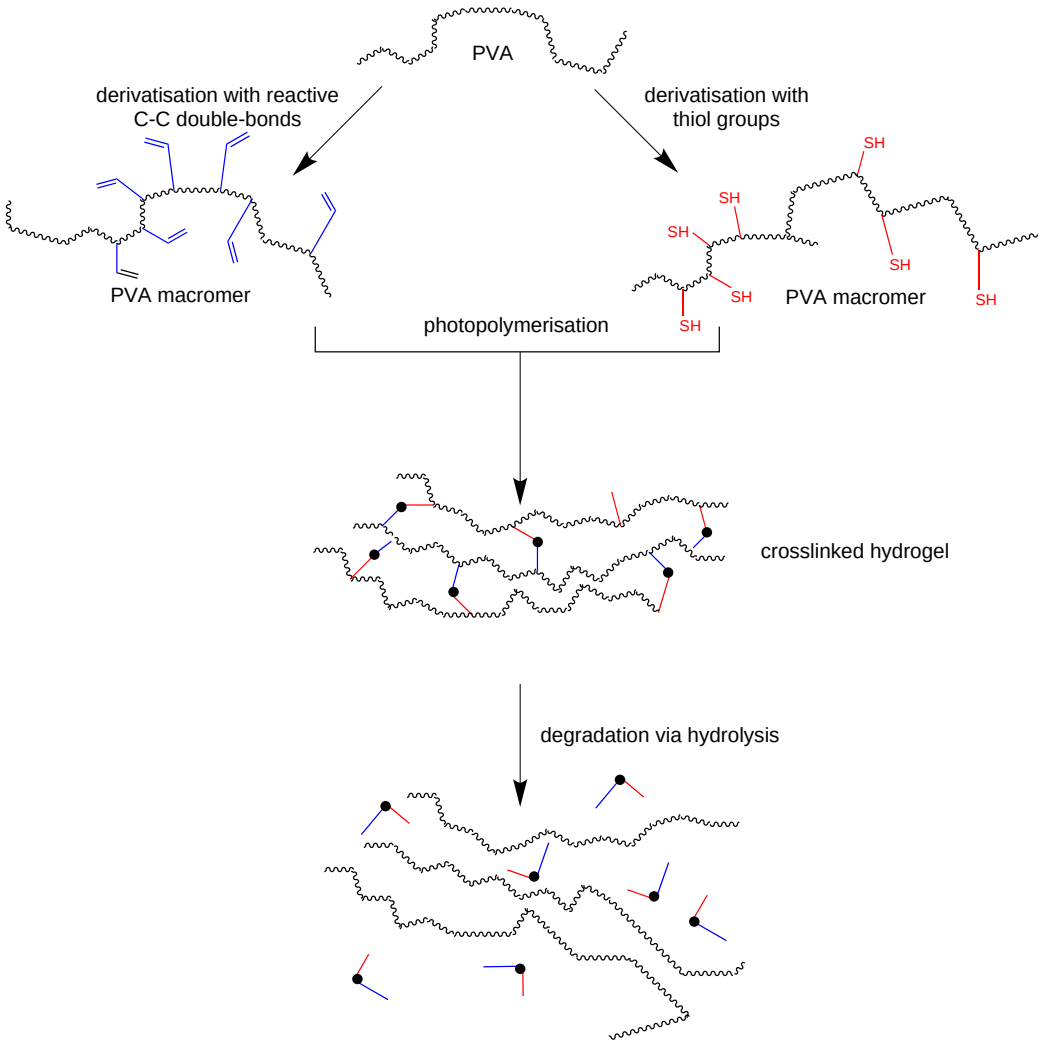

These products should be characterized by their swellability, photorheological and toxicological properties. Further the storage stability of formulations containing these molecules should be determined in dependency on different inhibitor concentrations. Finally their applicability in formation of hydrogels via two photon polymerisation should be tested and analysed.

General

1 State of the Art

Poly(vinyl alcohol) (PVA) is a watersoluble, odourless, tasteless, white and non-toxic polymer widely used in industry. It was first prepared in 1924 by Herrmann and Haehnel[40] by saponification of poly(vinyl esters) with caustic soda. This is still a widely used method for producing PVA in addition to transesterification with absolute alcohols. The direct production from its monomer, vinylalcohol, is not possible due to the fact that vinylalcohol is the tautomeric form of acetaldehyde and therefore not available. Although a bunch of other materials can be used, vinyl acetate is the most used starting material for the production of PVA. The hydrolysis or transesterification can be carried out in solution, suspension, or emulsion with alkaline or acidic catalysts.

Figure G.1.1: Structure of PVA

The properties of PVA depend on their grade of hydrolysis and molecular weight. PVA is produced commercially in 650 000 tons per year (2000) and is available with a hydrolysis grade between 70% and 99%.[40]
PVA is generally considered as non-toxic and therefore pure PVA is used in food packaging, as additive to food and for cosmetic products. The "final report on the safety assessment of polyvinyl alcohol"[41] reports a LD_{50} (oral, rat) value between 10 000 mg/kg and 215 000 mg/kg and considers PVA as safe for use in cosmetic products.
The chemical properties of PVA are according to its secondary hydroxyl groups and the most important reactions are the formation of esters,[42] ethers[43] and acetals.[44] Physical cross-linking of PVA is possible with repeated freeze-and-thaw cycles.[45] Chemically cross-linking is done either by direct cross-linking of the hydroxyl groups with glutaraldehyde,[46] epichlorohydrin,[47] diglycidyls[48] or by incorporation of polymeriseable functionalities.
The following part considers publications in the field of PVA modification with the purpose of producing cross-linked hydrogels. First modifications of PVA which can be cross-linked without irradiation are shown and later on photocross-linkable PVA derivatives are discussed.

Modification of PVA with less toxic substances than (meth)acrylates was done by Chaouat et al.[49] They used sodium trimetaphosphate (STMP), a largely accepted food cross-linker, to form membrane devices for implantable vascular grafts.

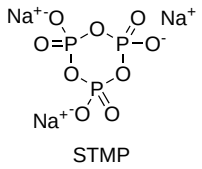

Figure G.1.2: Structure of Chaouat's cross-linker: sodium trimetaphosphate

Differently from all methods mentioned before in this section, this process cross-linked PVA without any prior modification. To a solution of PVA and STMP in water an aqueous sodium hydroxide solution was added and the resulting solution was poured on a Petri dish. The water of this solution was evaporated at room temperature during 24 hours resulting in a thin film. The cross-linked film was washed with water to remove unreacted STMP and sodium hydroxide. It showed that the produced PVA derivatives possessed high mechanical strength and were used to replace the infrarenal aorta of a rat. No mechanical nor thrombotic complication occurred within one week, even without anticoagulant or antiplatelet treatment.
Fernández et al.[50] modified PVA with the use of acid chlorides. They used 1,3-dimethyltetrahydropyrimidin-2(1*H*)-one urea (DMPU) as a solvent for the reaction of PVA with 3,5-dinitrobenzoyl chloride.

Figure G.1.3: Structure of the dinitrobenzoyl derivative of PVA synthesised by Fernández and their used solvent N,N'-dimethylpropylene urea

The purification was done by repeated precipitation steps. Degrees of substitution up to 86% were obtained with this method. Comparing vinyl acetate-vinyl alcohol copolymer products derived from base-catalyzed transesterification to the products obtained in DMPU, they found that the sequence distributions were quite different. For the products prepared in DMPU a distribution close to random could be observed, whereas the products from the transesterification where block copolymers.

Similar to Tsuda, Gimenez et al.[51] synthesised vinyl alcohol-vinyl ester copolymers via Schotten-Baumann esterification with cinnamoyl, benzoyl, p-toloyl and phenylacetyl chloride. Also cross-linking of the yielded polymers was carried out with the use of isocyanates like hexamethylenediisocyanate (HMDI) or toluene-2,4-diisocyanate (TDI) and dianhydrides like Epiclon B-4400.

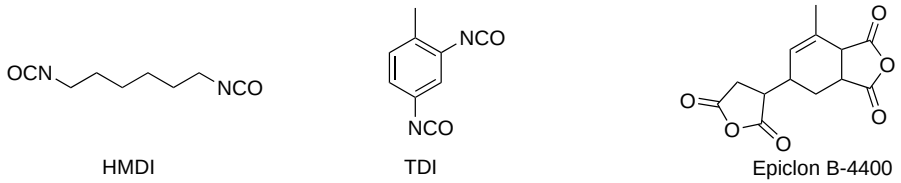

Figure G.1.4: Structures of the cross-linkers used by Gimenez: HMDI, TDI and Epiclon B-4400

They investigated the influence of the degree of substitution (DS) and therefore the amount of remaining hydroxy groups on the cross-linking process. It was shown that the lower the DS, the higher is the reaction enthalpy for the cross-linking process. Also the glass transition temperature (T_g) is depending on the percentage of remaining hydroxy groups: the more hydroxy groups are left, the higher T_g gets.

Crosslinking of PVA via 1,3-dipolar azide-alkyne cycloaddition was also done by Ossipov et al.[52] in 2006. They modified PVA with the help of 1,1'-carbonyldiimidazole (CDI) and amines terminated with azides or alkynes respectively.

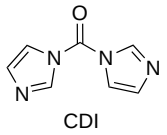

Figure G.1.5: Structure of 1,1'-carbonyldiimidazole

The so produced PVA derivatives were dissolved separately and formed a hydrogel upon mixture together with a Cu(I) catalyst. It was importent for them to produce only PVA derivatives with a low DS (1-5%), in order to remain water-soluble.

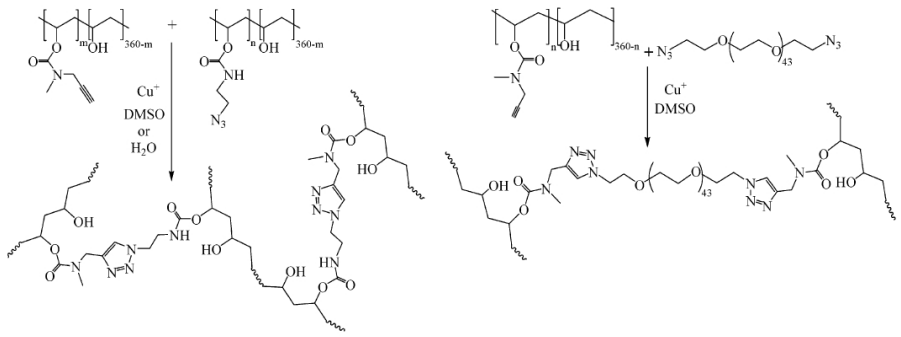

Figure G.1.6: Alkyne and azide modified PVAs in the cross-linking process, synthesised by Ossipov et al.[52]

They did the cross-linking with modified PVA-azides as well with low-molecular PEG-diazides which is shown in Figure G.1.6. There they showed that the mechanical properties of these hydrogels cannot only be controlled by varying the weight-fraction but also by changing the functionality (i.e. the number of functional groups) of the cross-linking molecule.

Another way for forming hydrogels in situ was developed by Ossipov et al.[53] in 2007. Similar to their preceding work, they modified PVA with acetaldehyd groups and with hydrazone groups, to cross-link this hydrogel formulation in situ. The modification with acetaldehyde was again done with CDI and 3-amino-1,2-propanediol to form a carbamate bonded primary alcohol. This alcohol was subsequently oxidised with $NaIO_4$ to form the aldehyde. In parallel, PVA was modified with CDI and glycine ethyl ester hydrochloride together with hydrazine to form the PVA-hydrazide.

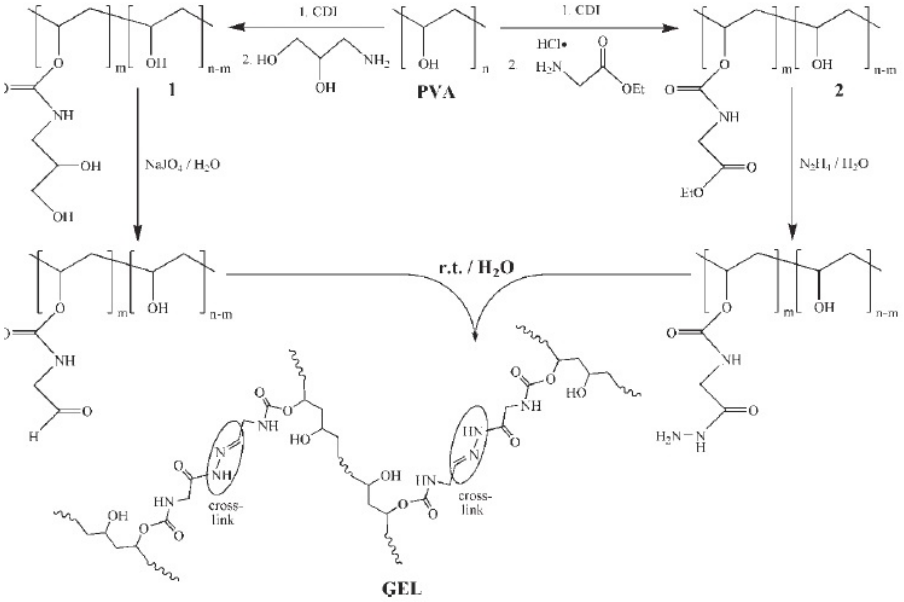

Figure G.1.7: Aldehyde and hydrazide modified PVAs in the cross-linking process, synthesised by Ossipov et al.[53]

For cell encapsulation, the two modified PVA were separately dissolved in water, and murine neuroblastoma N2a cells were added to the solution of PVA hydrazone. Upon mixture the solutions gelled and the formed gels were put in well plates for analysing. It showed that the cells were viable for 4 days but were not able to proliferate during this time. According to Ossipov et al., a reason for this is the fact that this gels are not degradable, a property which is critical for tissue engineering.
A bit different approach than they did before was done by Ossipov et al.[54] in 2008, when they managed to modify PVA with nucleophilic groups (aminooxy, thiol, cysteine) as well as with electrophilic groups (maleimide, acrylamide, 2-haloacetyl, semicarbazide) and form hydrogels out of aqueous solutions upon mixture. The produced gels showed no significant cytotoxicity when testing with human dermal fibroblast cells.
In 1964 Tsuda[55] developed a way to produce photosensitive polymers based on PVA and cinnamic acid.

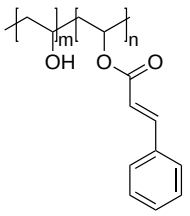

Figure G.1.8: Structure of the cinnamic acid derivative of PVA synthesised by Tsuda

The only solvent dissolving PVA available to Tsuda was water, so the reaction was designed in a Schotten-Baumann[56] way using a two-phased heterogeneous reaction.

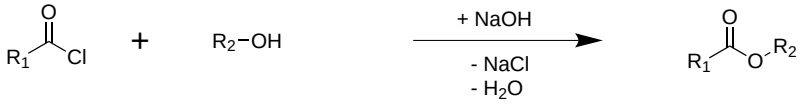

Figure G.1.9: Schotten-Baumann esterification of a carboxylic acid chloride with an alcohol catalysed by sodium hydroxide

For this purpose the PVA was dissolved in water and the cinnamoyl chloride in methylethylketone in the presence of alkali hydroxides. This two-phased reaction mixture was cooled, so that the hydrolysis of the acid chloride was reduced. The product could be collected at the phase boundary and was purified by centrifugation and precipitated with petrol ether. Tsuda also observed that the addition of surfactants lowered the yield because of an increased hydrolysis of the acid chloride. Although not mentioned in the paper, it is very likely that the products from this procedure will not have a homogeneous distribution of the ester groups because of inhomogeneous reaction conditions.
Mühlebach[57] et al. developed a method for modifying PVA with 2-vinyl-4,4-dimethylazlactone as well as with acrylic and methacrylic acid with the purpose of creating hydrogels for soft contact lenses.

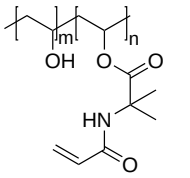

Figure G.1.10: Structure of 2-vinyl-4,4,-dimethylazlactone modified PVA synthesised by Mühlebach

They carried out the reaction in water as solvent and used concentrated hydrochloric acid as catalyst. As an example a degree of substitution of 2% (concerning the (meth)acrylate ester) is mentioned, but this can be varied over a wide range according to Mühlebach. The modification with azlactone was done in dimethylsulfoxide (DMSO) as solvent and with 1,8-diazabicyclo[5.4.0]undec-7-ene (DBU) as catalyst. Similarly an exemplary DS of 6% is stated and again the variation was possible over a wide range. With this methods they were able to produce well-defined starting materials for the cross-linking reaction by UV irradiation with Irgacure 2959 as photoinitiator (PI).

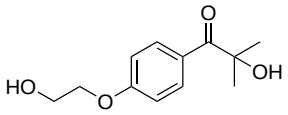

Figure G.1.11: Structure of the PI Irgacure 2959

The cross-linked hydrogels showed excellent mechanical and optical properties which make them well-suited materials for the production of contact lenses.
Nuttelman[58] et al. synthesised a graft macromer of PVA and poly(lactic acid) (PLA) with methacrylate end-caps.

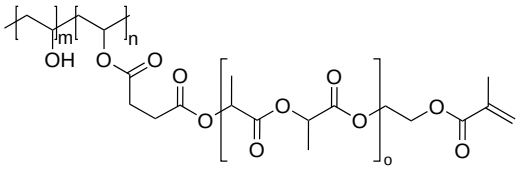

Figure G.1.12: Structure of methacrylate modified PVA, synthesised by Nuttelman

This strategy involved the advantages of PVA (high water content, tissue like elasticity and ability to attach a variety of molecules) and PLA (degradability, ability to photocross-link and hydrophobicity) without involving the disadvantages (PVA: no cell adhesion possible without modification, PLA: stiff and brittle) of them. Therefore they grafted poly(lactic acid)-co-poly(ethylene glycol) polymers to PVA, yielding brush-like macromers. These degradable grafts have been end-capped with photocross-linkable methacrylate groups and they concluded, that this material has a high potential for tissue engineering due to the ability to control the rate of network degradation, mass erosion profile and its bulk chemical properties.
Bourke[59] et al. used PVA modified with acrylamide in order to produce nondegradable, photocross-linked hydrogels for drug release in wound healing applications. They evaluated the capabilities of protein permeability with using trypsin inhibitor as model substance. Their conclusion was that the release profile of proteins can be tailored by modifying three major parameters: solid content, initial protein load and incorporation of hydrophilic fillers.
Martens[60] et al. synthesised and characterized PVA modified with acrylic acid.

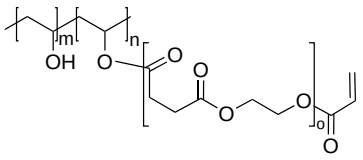

Figure G.1.13: Structure of acrylate modified PVA, synthesised by Martens

Their aim was to produce a photocross-linkable PVA macromer with hydrolytically cleavable ester groups and they managed to introduce low-molecular spacers made of succinic acid and ethylene glycol to improve the degradability.

2 Synthesis of modified PVA derivatives

2.1 Modification of PVA with itaconic acid (PVA-IA)

Itaconic acid (IA) is a naturally occurring compound that can be produced from distillation of citric acid. IA is non toxic (LD_{50} (oral, rat) = 2969 mg/kg)[61] and produced in multi ton amounts via fermentation of *Aspergillus terreus*,[62] therefore it is quite cheap. Also there is literature[63–66] describing the cross-linking of macromers, that were modified with IA. Ohnishi[65] described the synthesis of amphiphilic monomers containing itaconic acid as polymerisable center esterified with a hydrophobic (but oxygen permeable) tris(trimethylsiloxy)silyl group on one side and a hydrophilic methoxyethyl moiety on the other side. This amphiphilic itaconic monomers were homo- and co-polymerised with N-vinylpyrrolidone to form translucent, oxygen permeable membranes for contact lenses. But their conclusion was that the produced membranes were inferior compared to similar products containing maleic acid as polymerisable center.
According to Ramos et al.,[64] the modification of pentaerythritol with itaconic acid was successful with sulfuric acid as catalyst, although with quite low yields because of the formation of oligomers.
In Leonard's book on vinyl and diene Monomers,[67] there is already stated that itaconic anhydride and derivatives can be polymerised either via free radical polymerisation with peroxides or by radiation initiation with UV light.
Copolymers with methylmethacrylate and itaconic anhydride were produced by Milanovic et al.[63] via free radical polymerisation to produce amphiphilic polymers. For their behalf they modified the copolymer by amidation with di-n-butyl-amine to yield itaconamic acid with complete conversion. It is also stated that the percentage of amidation is not depending of the copolymer composition.
In a review from Tate[68] polymerisation of itaconic anhydride, itaconic acid and itaconic esters are described. The derivatives are used as protective and decorative coatings, synthetic fibers, oil additives and rigid plastics. Also the isomerisation between itaconic acid, mesaconic acid and citraconic acid, which takes places in presence of strong bases is mentioned.

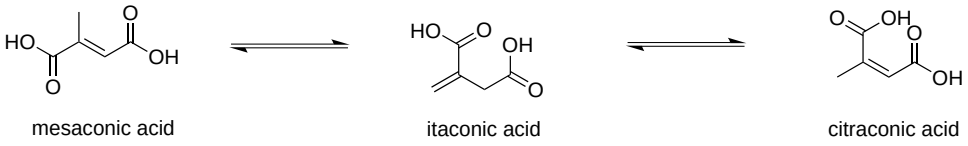

Figure G.2.14: Isomerisation of mesaconic, itaconic and citraconic acid

Beside isomerisation, also decarboxylation of itaconic acid is described in another paper by Tate.[69] Here the influence of DS and temperature on the decarboxylation of solutions of itaconic acid polymers is described.
Tate also mentioned that esters from itaconic acid can be produced by reaction of the anhydride with alcohols, to selectively obtain monoesters. Beside the direct polymerisation of itaconic acid and anhydride to its polymeric product, also grafting of nylon 66

yarns was carried out. For that purpose nylon yarn was soaked in an itaconic acid solution and irradiated with electrons, which produced a nearly quantitative polymerisation. Also copolymers of itaconic acid derivatives with styrene, methylmethacrylate, acrylnitrile, vinylchloride and vinylacetate are known according to Tate.[69]
There is already a lot of literature concerning itaconic acid as source of cross-linkable compounds. But since, to the best of our knowledge, there is no literature about the modification of PVA with IA, it was our choice to modify PVA with itaconic acid to form cross-linkable macromers. Figure G.2.15 shows the target structure of modified PVA.

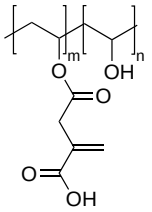

Figure G.2.15: Target structure of PVA, modified with IA

2.1.1 Model reaction for synthesis (1)

First some model reactions were carried out for implementing a way to create an ester of PVA and IA. IA was used as itaconic anhydride (IAH) for this synthesis. For the first experiment, ethylene glycol was used as a difunctional alcohol in analogy to Elbert et al.[70] synthesis of 1*H*,1*H*,2*H*,2*H* -perfluorododecyl itaconate with $ZnCl_2$ as catalyst in dry toluene. Ethylenglycol was used because its a difunctional alcohol, but has convenient boiling point and molecular weight that allows widely common analysis methods like TLC, GC-MS or ^{1}H-NMR for being used with it. Since ethylene glycol is a primary alcohol, conditions that do not work with ethylene glycol would for sure not work with PVA, which has only considerably less reactive secondary hydroxy groups.

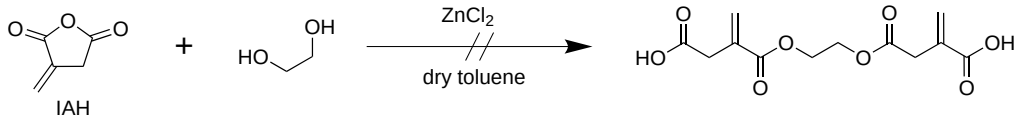

The IAH was fractionally distilled in vacuo prior to usage. Ethylenglycol was stirred for five days over sodium sulfate and distilled afterwards. The reaction was carried out under argon atmosphere. Therefore IAH (2.25 eq.) was dissolved together with ethylene glycol (1 eq.) in dry toluene and $ZnCl_2$ was added subsequently. The reaction was heated to reflux over night and after evaporation of the toluene, a yellow oil was yielded. The extraction with chloroform and ether was not successful, and with methanol a yellow solid precipitated. The methanol was filtered off and the solid was dried in vacuo. NMR showed that there was no conversion at all.
As another method, the esterification with pyridine as catalyst and solvent was tried, in analogy to Wathier's[71] esterification of PEG with succinic anhydride. Additionally 0.2 wt% of pyrogallol (Pyr) was added to prevent homopolymerisation during reaction.

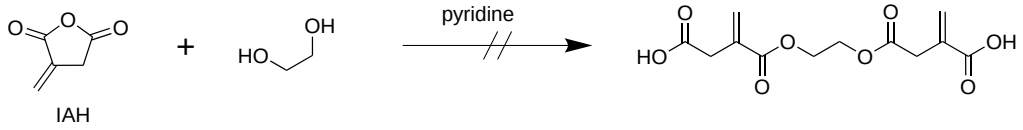

Directly after mixing the components the reaction mixture turned black. It was heated to reflux over night. Afterwards a sample of it was taken and GC-MS showed no sign of conversion.
A further trial of esterification was carried out in THF with triethylamine (TEA) with 4-dimethylaminopyridin (DMAP) as catalyst in analogy to Gou et al.[72]

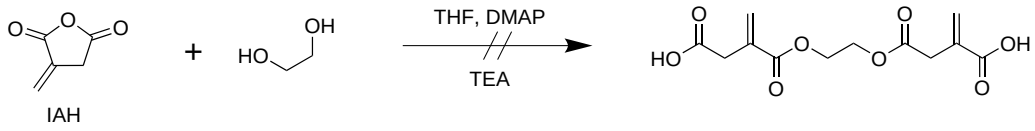

Ethylenglycol was mixed with 4 equivalents of IAH in THF on an ice bath, 10 mg TEA and 128 mg of DMAP were added subsequently to the mixture together with 0.2% of pyrogallol. The whole reaction was carried out under argon atmosphere and was stirred over night at 35°C. Again GC-MS showed no signal of the desired product.
Finally, some classical esterification conditions with acidic catalysts were tested with para-toluenesulfonic acid,[73] sulfuric acid[74] and camphor-10-sulfonic acid. All reactions were carried out in dry toluene and under argon atmosphere.

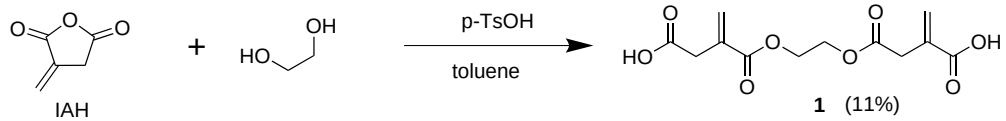

IAH (1.12 eq.) was mixed with ethylene glycol in dry toluene and 0.25% of para-toluenesulfonic acid (based on IAH) was added subsequently. The reaction was stirred at room temperature. After 6 days, no further conversion could be observed with TLC, so water was added and the mixture was extracted with ethylacetate. The organic phase was dried and the solvent removed in vacuo. It yielded NMR pure 4-(2-((2-carboxyallyl)oxy)ethoxy)-2-methylene-4-oxobutanoic **(1)** acid as white solid in 11% yield.

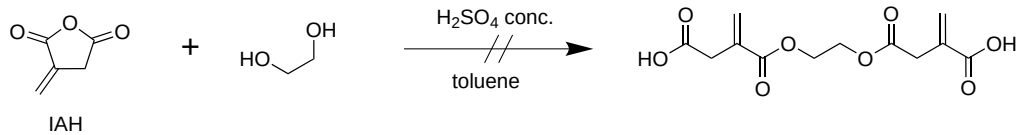

IAH (1.12 eq.) was mixed with ethylene glycol in dry toluene and 0.25% of concentrated sulfuric acid (base on IAH) was added. The reaction was stirred under argon atmosphere at room temperature. GC-MS showed only minimal signs of conversion so the reaction was not carried out any longer.

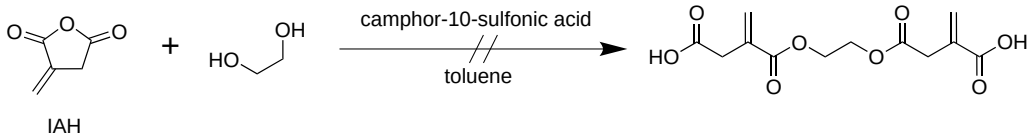

Also a trial with camphor-10-sulfonic acid was carried out. Again IAH (1.12 eq.) was mixed with ethylene glycol in 10 mL toluene and 0.25% of camphor-10-sulfonic acid (based on IAH) were added. After six days of reaction the reaction mixture was hydrolysed with conc. HCl and water, and extracted three times with ethylacetate. After removal of the solvent a white solid was obtained. ^{1}H-NMR showed only conversion of one alcohol group to the ester and therefore cannot be considered a successful method. Also an experiment without catalyst was done, which showed no conversion at all after 6 days, so no work-up was done. From these methods, p-TsOH was the only catalyst that gave the desired product, although in a quite low yield.

2.1.2 Modification of PVA with itaconic acid

Based on the model reaction, PVA should be modified in a similar way. As PVA is completely insoluble in toluene, a different solvent had to be found first.
The choice of solvent is quite limited since there are only few solvents (water, dimethylsulfoxide (DMSO), N-methyl-2-pyrrolidone, ethylene glycol), that dissolve PVA in an acceptable way.[75,76]
According to Tacx et al.[75], DMSO has the best solvent abilities for PVA of all tested solvents and since DMSO is a standard solvent with also very good solving abilities for other compounds, our choice was to use DMSO for the reaction.

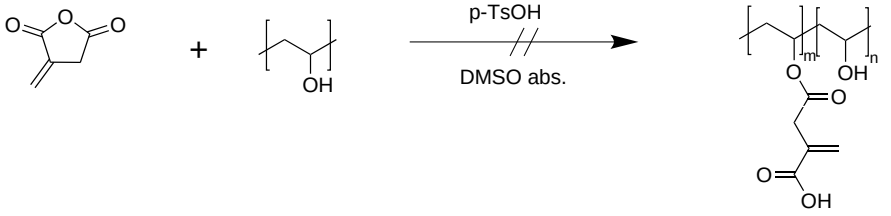

For the modification of PVA with itaconic acid PVA was dissolved together with p-TsOH and pyrogallol in anhydrous DMSO. The mixture was heated under argon atmosphere to 60°C for about an hour until a clear solution was formed. Afterwards IAH was added and stirred at 60°C for 4 days. The solution got darker during reaction and was dark brown at the end. The mixture was dialysed against deionized water for workup.
During the dialysis precipitation occurred. The precipitate was filtered off the solution and yielded 180 mg of a brownish solid.
It showed that the precipitate was not soluble in water, aqueous sodium bicarbonate solution, aqueous sodium hydroxide, methanol, DMSO, THF, chloroform, acetone and acetonitrile. No further investigations were done concerning this precipitate.
From the aqueous solution of the dialysis the water was removed and NMR showed only

very little conversion of below 4%. Also the overall yield was unacceptably low: from 110 mg of PVA used for the reaction, only 28 mg of PVA derivative were recovered and most of it was completely insoluble.
Also a rerun of the synthesis did not improve the result in any way. Although a homopolymerisation of itaconic acid is very unlikely under these conditions, because of the added pyrogallol, it is the only explanation for the failure of this synthesis.

2.1.3 Model reactions for thiol-ene polymerisation

In parallel of the trials for modifying PVA with IA the concept of thiol-ene reaction was tested for itaconic acid in NMR tube experiments.

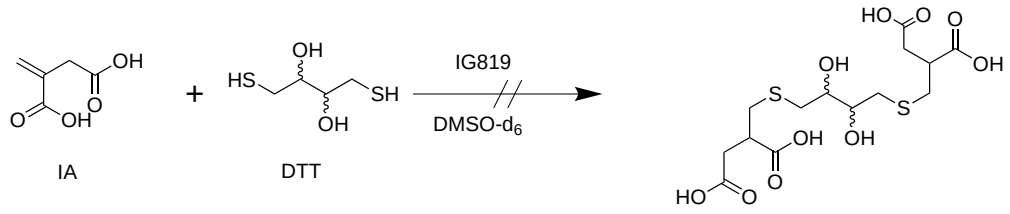

For this purpose itaconic acid was dissolved with 1 eq. of dithiothreitol (DTT) and 2% of Irgacure 819 (IG819, based on IA and DTT) in deuterated dimethylsulfoxide (DMSO-d_6). After all components were dissolved completely, 1/3 of this solution were transferred into each of three NMR tubes. One of these tubes was not irradiated at all, the second one was irradiated for 30 s and the third for 15 min. For detailed explanations about the used setup for irradiation of the samples see corresponding section in Experimental Part. Later on, ^{1}H-NMR measurements of the solutions were performed which showed that no reaction at all occurred and only exchange of hydrogen and deuterium could be observed. A second experiment was carried out as before, but with N-acetyl-L-cysteine (ACC) instead of dithiothreitol.

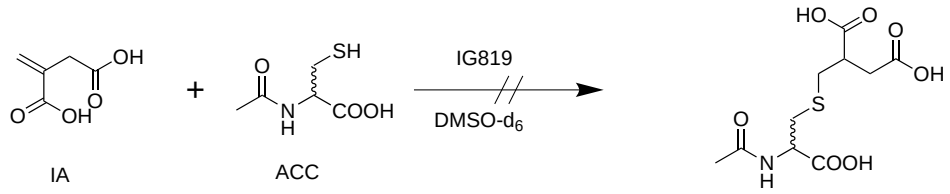

Here itaconic acid was dissolved together with ACC (1 eq.) in DMSO-d_6 with 2 wt% of IG819. Again the solution was divided and transferred into 3 NMR tubes. After irradiation of 0 s, 30 s and 15 min, ^{1}H-NMR spectra were measured. Also here no reaction could be observed.

2.2 Modification of PVA with maleic acid (PVA-MA)

Since the modification as well as the thiol-ene reaction of itaconic acid failed completely an alternative had to be found. Therefore maleic acid was chosen, due to the low toxicity[77] (LD_{50} (oral, rat): 708 mg/kg) and low price in purchase.

2.2.1 Model reaction for synthesis

At first a model reaction with methanol was carried out analogous to Sabitha et al.[78] with borontrifluoride as catalyst. They performed lewis acid catalysed ring-opening reactions of cyclic anhydrides with alcohols.

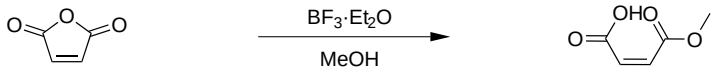

Maleic acid was dissolved in methanol (15 eq.) and under magnetic stirring, 0.5 eq. of borontrifluoride-etherate were added dropwise. Afterwards the reaction mixture was stirred at room temperature for 10 min. Since TLC showed almost complete conversion, the reaction mixture was poured onto saturated sodium bicarbonate solution and washed with diethylether. The aqueous phase was acidified with conc. HCl to a pH of 2 and subsequently extracted with diethylether. The organic phase was dried and the solvent evaporated. *(Z)*-4-methoxy-4-oxobut-2-enoic acid was obtained as colourless oil in 22% yield. NMR confirmed the purity of the product.

2.2.2 Model reactions for thiol-ene polymerisation

Again some model reactions for the thiol-ene polymerisation were carried out with maleic acid. Thiocure PETMP (pentaerythritol tetra-3-mercaptopropionate) and ACC were used as thiols.

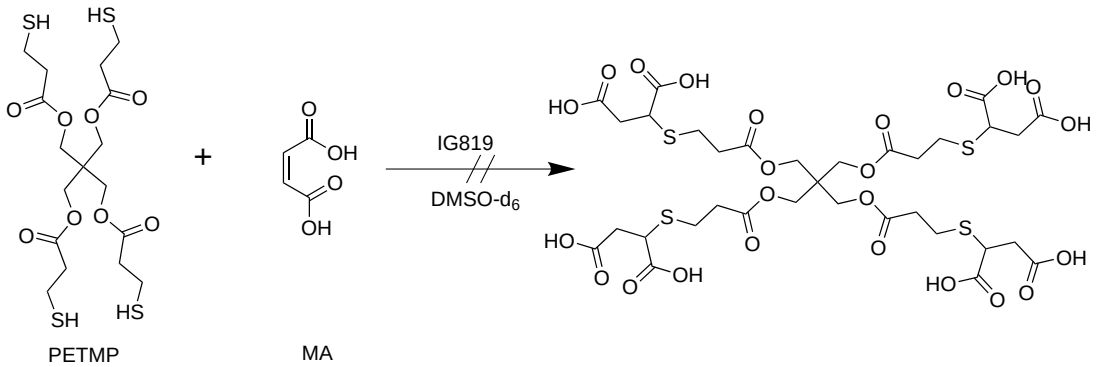

For the reaction of the tetrathiol PETMP with MA both substances (equimolar based on functional groups) together with 2% of IG819 were dissolved in DMSO-d_6. After five minutes everything was dissolved cleanly, the solution was divided into three portions and transferred to three NMR tubes. As mentioned above the tubes were irradiated for 0 s, 30 s and 300 s at 80% intensity. NMR showed no sign of thio-addition but light-induced isomerisation to fumaric acid could be clearly observed as described in literature[79]. Beside the tetrathiol PETMP, also the acetyl-protected amino acid ACC was used as thiol.

Here maleic acid together with ACC (1 eq.) was dissolved in DMSO-d_6 with 2% IG819 as PI. Also in this case, only isomerisation to fumaric acid could be observed in the NMR spectra.
To summarise, also maleic acid showed no tendency to undergo any thiol-ene reaction, so another substance had to be found.

2.3 Modification of PVA with allylsuccinic acid (PVA-Allyl)

Allylsuccinic acid has the advantage of having a free double bond in allylic position, making it more reactive than maleic acid, and has an even lower toxicity (LD_{50} (oral, rat) = 1250 mg/kg)[80] than itaconic acid. The higher reactivity is due to the terminal alkene functionality compared to internal enes like maleic acid, where the thiol-ene reaction is reversible.[38] It has also to be noted that a prediction of reactivity for thiol-ene reaction only from its electronic properties and structure is not reliable, according to Northrop.[81]

2.3.1 Model reaction for synthesis (2)

Since PVA is a secondary alcohol our approach was to use 2-propanol as model alcohol for the following modifications. Although ethylene glycol and methanol was used before it showed that the predictability was better with 2-propanol as model substance.

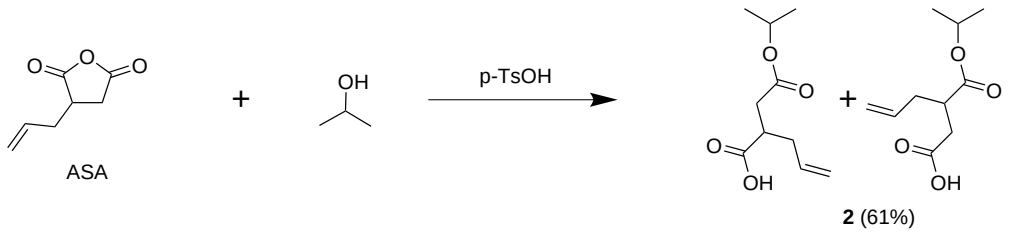

Allylsuccinic anhydride (ASA) was dissolved in 2-propanol (320 eq.) together with 0.25 wt% of p-TsOH (based on anhydride and 2-propanol) and 1000 ppm of pyrogallol (based on anhydride), to prevent premature polymerisation. This reaction mixture was stirred at 60°C for 3 days until no further conversion could be observed with TLC. After cooling to room temperature the solvent was removed in vacuum yielding the cure product as a colourless oil.
Purification was done via column chromatography yielding in NMR pure product (mixture of isomers) of **2** in 61% yield.

2.3.2 Model reactions for thiol-ene polymerisation

The thiol-ene reaction with the anhydride ASA was tested with 1-dodecanethiol in deuterated chloroform ($CDCl_3$) because the peak-overlapping from DTT in DMSO-d_6 did not allow any analysis of the reaction.
Since the boiling point of $CDCl_3$ is much lower than of DMSO-d_6, the long irradiation time had to be performed in two-minute steps with cooling to room temperature in-between.

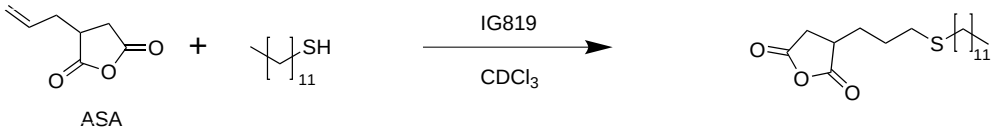

ASA and 1-dodecanethiol (1 eq.) were dissolved in $CDCl_3$ and 2% of IG819 (based on ASA and 1-dodecanethiol) in $CDCl_3$ were added subsequently. After all components have dissolved completely, 0.7 mL were transfered to each of three NMR tubes. The radiation was performed for 0 s, 30 s and 16 min at 100% intensity. The conversion was determined via ^{1}H-NMR.
After 16 min a decrease of 46% of the allylic proton signals could be observed compared to the methyl group of the dodecanethiol.
Because of the incomplete conversion the experiment was carried out again in the same way but with 20% of IG819 instead of 2%. This time the signal reduction of the allyl protons was 64%, which showed a much better result but still far away from full conversion.
Because the thiol can also react as nucleophile with the anhydride in a ring-opening reaction, a third experiment with two equivalents of the thiol and 20% of the photoinitiator was carried out. Here the conversion could be increased up to 77%.
An explanation of this still unsatisfactory conversion is the fact that chloroform is an unsuitable solvent for radical reactions. It is known that chloroform reacts with radicals to form chlorine radicals and therefore reduces the amount of desired radicals dramatically.[82]
But also the nucleophile ring-opening reaction competes with the thiol-ene reaction and therefore reduces the yield.

2.3.3 Synthesis of the PVA allylsuccinic derivative (PVA-Allyl)

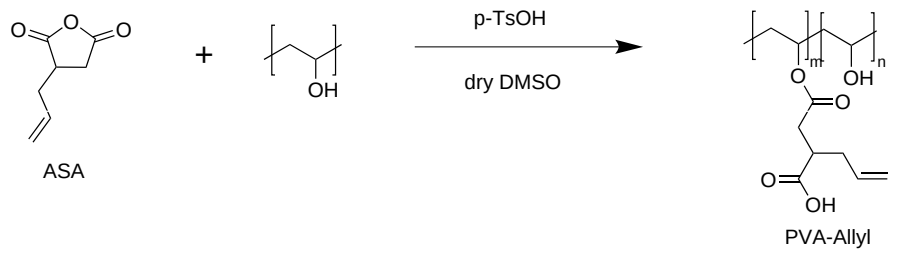

Similar to the model reaction the derivatisation of PVA with allylsuccinic anhydride was carried out in anhydrous DMSO with p-TsOH as catalyst. To prevent unwanted homopolymerisation, 1000 ppm pyrogallol was added, compared to the weight of ASA.

PVA was dissolved at 60°C in anhydrous DMSO together with 0.25% p-TsOH and 1000 ppm pyrogallol. Subsequently ASA was added dropwise to the mixture and the flask was stirred at 60°C for 3 days.
After this time, the reaction mixture was transferred to a dialysis tubing and dialysed against deionized water for purification. To neutralise the added p-TsOH the pH of the dialysing solution was kept around 7. After removal of the water the product was yielded as white to grey solid.
For further use the product was transferred into its sodium salt to increase its water solubility, and subsequently ground to produce a fine powder. This procedure also increased the solubility. Table G.2.1 shows the different degrees of substitution yielded during this theses. Only A4 and A20 were produced in larger scale and therefore examined more closely for further usage, the rest were a proof of concept and trials for different equivalents of allylsuccinic anhydride.

Table G.2.1: PVA-Allyl derivatives with degree of substitution and their abbreviations

Sample	**DS [%]**
A2	2
A4	4
A20	20
A24	24
A32	32
A54	54

2.4 Modification of PVA with norbornene (PVA-Norbornene)

Successfull thiol-ene polymerisation was already done with norbornene modified PEG by Fairbanks et al. in 2009.[83] They cross-linked norbornene modified pentaerythritol (with PEG as chain extenders) with peptides containing thiol groups (e.g. KCGGYRGCK) and resulted in cytocompatible hydrogels.

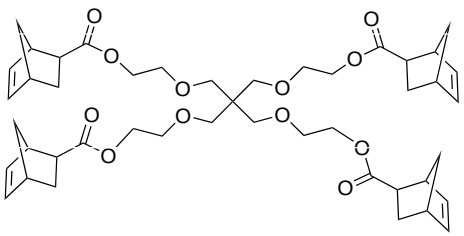

Figure G.2.16: Structure of norbornene modified pentaerythritol with PEG chain extenders, synthesised by Fairbanks

The reactions were fast and the resulting hydrogels possessed a Young's modulus similar to physiologically relevant tissues. Whereas PEG only allows the incorporation of two functional groups on a chain or PEG modified pentaerythritol allows functionalisation with 4 norbornene groups, the modification of PVA would enable producing macromers

with a high diversity of DS with norbornene as photocross-linkable group.

2.4.1 Model reaction for synthesis (3)

As model substance again 2-propanol was the alcohol of choice because of the secondary hydroxyl group. The endo-isomer was chosen, because it costs only half of the exo-isomer. In 2-propanol (80 eq.), *cis*-5-norbornene-*endo*-2,3-dicarboxylic anhydride (NAH) was dissolved together with 0.125 wt% of p-TsOH (based on amount of 2-propanol and anhydride). To prevent unwanted polymerisation of the substance 1000 ppm (based on the weight of anhydride) pyrogallol was added to the reaction mixture. The reaction was heated to 50°C and stirred under argon atmosphere. After 3 days, no further reaction could be observed. Thus the solvent was evaporated, resulting in a white solid crude product. Because TLC showed unreacted acid, the product was purified via column chromatography yielding in 26% of **3** as white solid.

2.4.2 Model reactions for thiol-ene polymerisation

For a model reaction of the thiol-ene polymerisation of the anhydride NAH, DMSO-d_6 was used as solvent. As thiol compound DTT was used, which had the drawback of overlapping peaks in the NMR.
NAH and DTT (0.5 eq.) were dissolved in DMSO-d_6 and 2% of IG 2959 was added (based on the whole formulation). This solution was divided in to three NMR-tubes that were irradiated at 100% intensity for 0 s, 30 s and 15 min.
From the signal of the carbon-carbon double bond, a conversion of 62% was calculated. But it has to be mentioned that this value is inaccurate because of the peak-broadening of the referenced peak and therefore our conclusion was a good but not quantitative conversion of this reaction.

2.4.3 Synthesis of the PVA norbornene derivative (PVA-Norbornene)

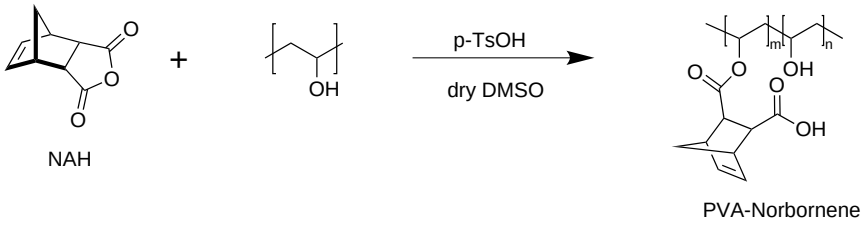

The synthesis of PVA-Norbornene was quite similar to the preparation of PVA-Allyl and carried out according to the model reaction. PVA and 0.125 wt% p-TsOH (based on amount of PVA and anhydride) were dissolved in anhydrous DMSO at 50°C while stirring under argon atmosphere for 1 hour. Subsequently NAH was dissolved in a small amount of anhydrous DMSO and added dropwise to the reaction mixture. Afterwards the reaction mixture was stirred for 48 hours at 50°C. After cooling to room temperature the solution was dialysed against deionized water for purification. To readily yield the product completely as sodium salt, the pH value in the outer dialysing-vessel was kept between 8.2 and 8.8 with sodium bicarbonate and sodium carbonate. Because these are very weak bases and the dialysis was carried out at room temperature hydrolysis is quite unlikely under this conditions.
This procedure yielded PVA-Norbornene in different DS depending on reaction time and amount of NAH. Table G.2.2 shows the different degrees of substitution and abbreviations for the PVA-Norbornene derivatives.

Table G.2.2: PVA-Norbornene derivatives with degree of substitution and their abbreviations

Sample	**DS** [%]
N7	7,5
N19	19
N23	23
N42	42,5

To have comparable results, only N7 and N19 were used for further examinations, because of the similar DS compared to A4 and A20.

2.5 Modification of PVA with γ-thiobutyrolactone (PVA-Thiol)

γ-Thiobutyrolactone (GTBL) is known as an easy-to-use reagent to obtain thiols from alcohols. For instance, de Gregori[84] has produced a methanol ester from it with triethylamine as catalyst, and Huckstep[85] has successfully synthesised methanol esters with the use of sulfuric acid as catalyst. Also GTBL is not specifically toxic - it has a LD_{50} (oral, rat) value of 1860 mg/kg.[86]

2.5.1 Model reaction for synthesis (4)

Also with GTBL, 2-propanol was the model alcohol of choice. It turned out that the esterification was not successful with de Gregori's[84] method. Instead a method according to Huckstep[85] was tried, which worked quite well.

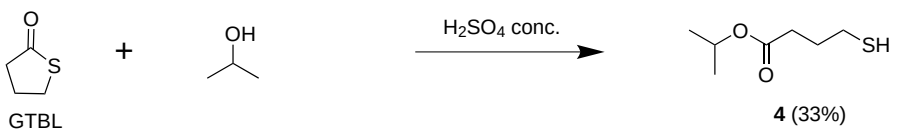

In analogy to Huckstep, GTBL was dissolved in 2-propanol (65 eq.) and a few drops of concentrated sulfuric acid were added subsequently. The flask was purged with argon and heated to 90°C for three days. GC-MS showed good conversion and the mixture was cooled to room temperature and neutralised with sodium bicarbonate. After filtration and removal of the solvent, the product was obtained as a colourless oil. Purification was carried out with column chromatography yielding in 33% of pure isopropyl 4-mercaptobutanoate **(4)** as colourless oil.

2.5.2 Synthesis of the PVA thiol derivative (PVA-Thiol)

Since the model reaction with sulfuric acid was successfull we decided to use the same catalyst also for the modification of PVA. A vast difference was still between low-molecular 2-propanol and PVA: While we were able to use 2-propanol as reactant and solvent at the same time PVA cannot be used as a solvent at all, due to a significantly higher melting point. According to the previous synthesis of PVA derivatives DMSO was here also used as solvent.
It turned out that the quite high water content of the used PVA resulting from the hydrolysation of the poly(vinyl acetate), reduces the degree of substitution reached. To avoid this drawback, a protocol for reducing the water-content of the used PVA was developed. For this purpose, the PVA is heated in fine vacuum and afterwards dissolved in anhydrous DMSO with subsequent removal of about 10% of the DMSO volume by destillation in vacuum. With this protocol, the water content could be reduced by 60%, from 5% to 2%.

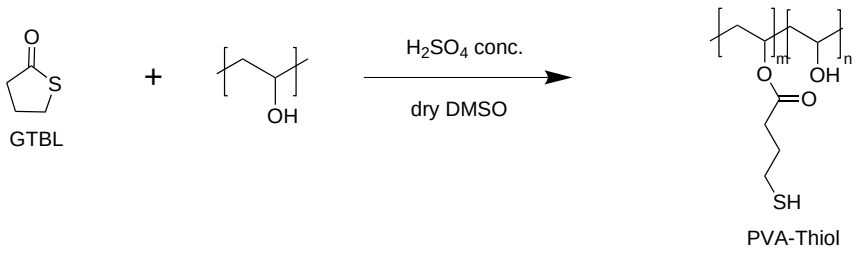

For the synthesis itself, pre-dried PVA was dissolved in anhydrous DMSO at 50°C. Afterwards approximately 10% of the solvent were distilled off in vacuum. After cooling to room temperature about 0.5 eq. (per hydroxy group of PVA) of concentrated sulfuric acid were added dropwise and stirred for 10 min.
Afterwards the thiolactone GTBL was added dropwise to the solution and heated to 90°C. The reaction mixture was stirred at 90°C for 3 days before it was cooled to room temperature. The mixture was worked up and purified via dialysis according to the standard dialysing protocol. After removal of the water the modified PVA-Thiol was yielded with different degrees of substitution (DS) according to used equivalents of GTBL. The DS was determined by ^{1}H-NMR.
For further usage, all PVA-Thiol blends were ground in a cryomill for better handling.

Table G.2.3: PVA-Thiol derivatives with degrees of substitution and their abbreviations

Sample	**DS** [%]
T1	1.5
T2	2.5
T6	6
T9	9

Only PVA-Thiol T2 und T6 were synthesised in larger scale and therefore used for further examinations.

With these PVA derivatives in hand, we wanted to examine their reactivity in thiol-ene polymerisation, their cell toxicity and their suitability for 2PP. The results of this examinations will be presented in the following sections.

3 Toxicology

3.1 Sample preparation and assay setup

The toxicity of the synthesised macromers was tested with murine fibroblastic cells (adipocytes) according to the Presto Blue cell viability reagent protocol.
For that purpose the different PVA derivatives were dissolved in Dulbecco's Modified Eagle Medium (DMEM) without serum proteins.
A detailed explanation of the assay is described in Section 3. After the preparation of the assay the sample solutions were put on the cells to treat them for exactly 24 hours. Thereafter, the medium was exchanged and the fluorescence dye Presto Blue (PB) was added. After 30 min of incubation the fluorescence was measured in order to count the living cells. All substances were analysed at least in triplicate.
The cell counting is based on the metabolic reduction of the Presto Blue dye by living cells. The reduced dye exhibits fluorescence, which is measured by a plate reader and gives quantitative information proportional to the number of living cells. Since this reduction may also occur with other reducing agents like molecules containing thiol groups, the results concerning PVA-Thiol have to be interpreted with caution.

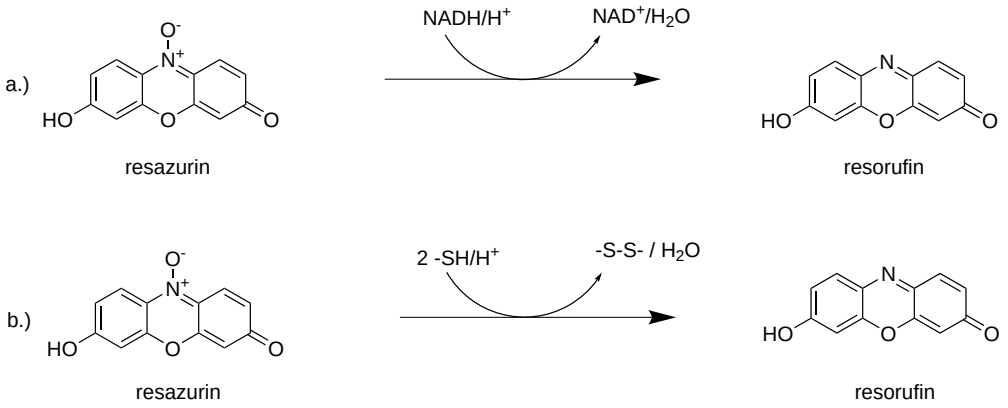

Figure G.3.17: Reduction of the dye in the Presto Blue assay a.) reduction in vivo by NADH b.) possible reduction of the dye by thiol groups

Figure G.3.17 shows the reaction of resazurin (the dye in Presto Blue assay) to the fluorescence dye resorufin. Resazurin is a blue dye with no intrinsic fluorescence value. Resorufin is red coloured and exhibits strong fluorescence at 586 nm.

3.2 Results of toxicology tests

Beside the analysed PVA-derivatives also a positive control (10% Presto Blue and 90% medium) and a negative control (medium, 10% Presto Blue and 90% DMSO) were added, so that the determination of viable cells was possible if they were not harmed at all. DMSO is highly cell-toxic if used in final concentrations above 0.25%.[87] The results from this experiment are shown in the following figures.

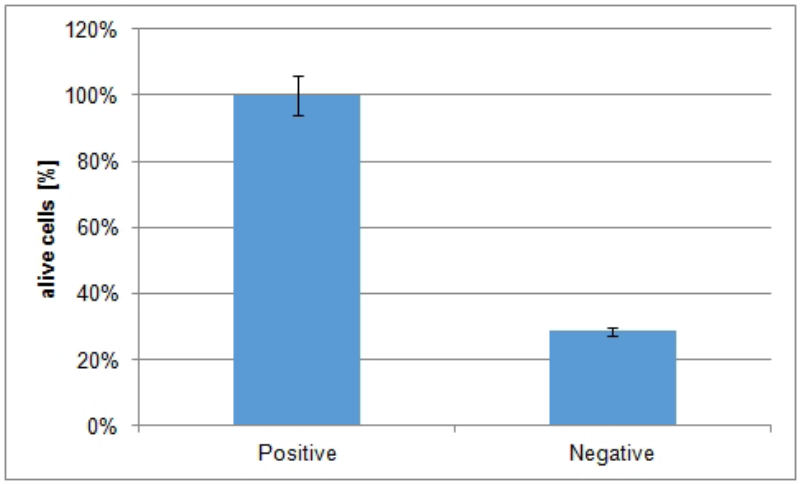

Figure G.3.18: Cell viability of a positive control sample containing only medium and dye and a negative control sample with dead cells (with DMSO, medium and dye)

All intensities were averaged and normalised to the intensity in the positive control sample of Figure G.3.18, from which also the percentage of dead cells by DMSO can be seen. The original measured data are listed in Section 3.3. Also PVA without modification was analysed concerning toxicity. The results of this analysis are shown in Figure G.3.19.

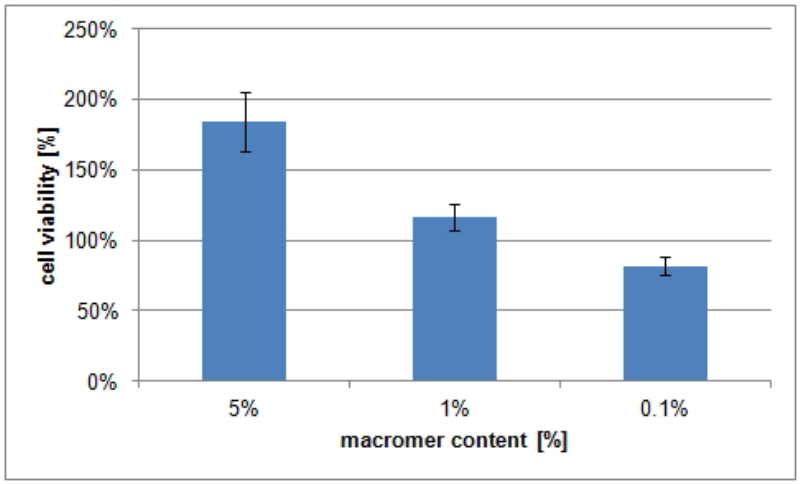

Figure G.3.19: Cell viability on stimulation with unmodified PVA in concentrations of 5%, 1% and 0.1%

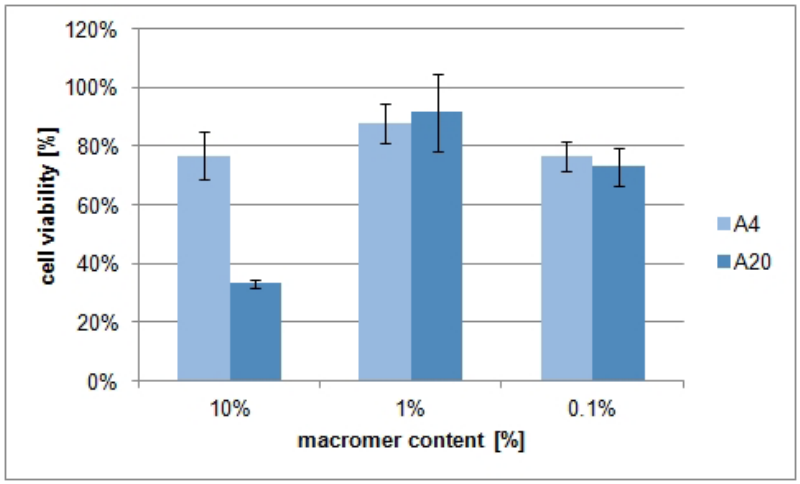

Figure G.3.20: Cell viability on stimulation with PVA-Allyl in concentrations of 10%, 1% and 0.1%

Figure G.3.20 shows the results concerning PVA-Allyl. As can be seen clearly, the toxicity of the lower substituted PVA-Allyl (A4) is by far smaller than of the higher substituted one (A20), with A20 beeing almost as toxic to the cells as DMSO and A4 with almost no toxicity. One has to keep in mind that the time of exposure and the concentration to the substances is much higher than in normal applications where the formulation would be cured in minutes to hours, which would also decrease the concentration of the substances dramatically.

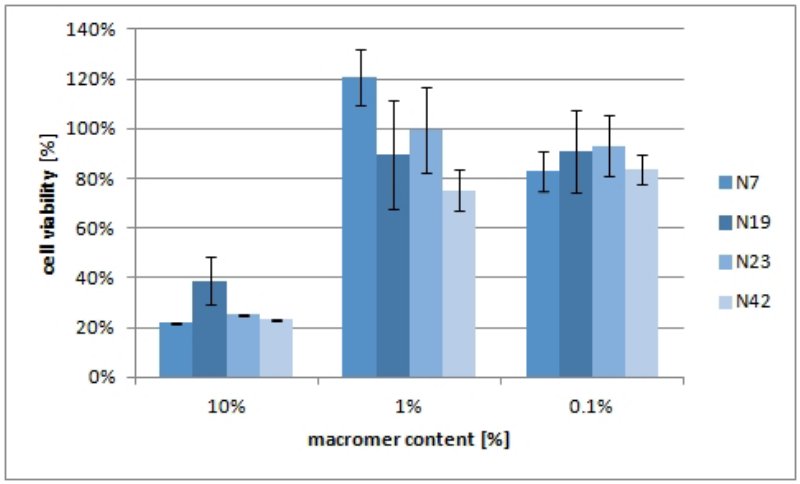

Figure G.3.21: Cell viability on stimulation with PVA-Norbornene in concentrations of 10%, 1% and 0.1%

The results from the toxicity analysis from PVA-Norbornene with different DS can be seen in Figure G.3.21. This comparison shows a significant difference between the mixtures with 10% and with 1% or below. As with PVA-Allyl, PVA-Norbornene exhibits a high toxicity if used in 10% solution for 24 hours of exposure. The differences between the DS of 1% and 0.1% macromer content is not significant.

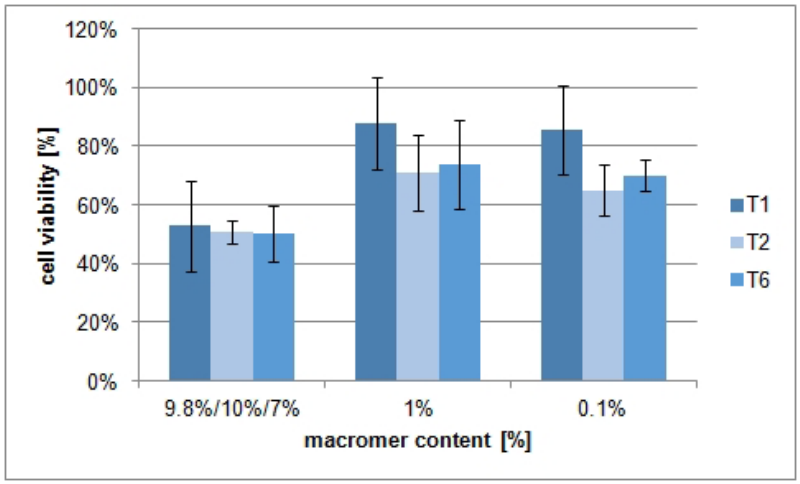

Figure G.3.22: Cell viability on stimulation with PVA-Thiol in concentrations of 10%, 1% and 0.1%

The cell viability of cells treated with PVA-Thiols of different DS is shown in Figure G.3.22. Special attention is needed for the PVA-Thiols because of the different concentration of T6: The maximum concentration of T6 in DMEM was 7%. This may also be the reason why the difference between the PVA-Thiols T2 and T6 seems not as big in Figure G.3.22 as with PVA-Allyl or PVA-Norbornene.
Here one has to keep in mind that the dye from the assay will develop its colour through reduction in the cells. Also the thiol groups from PVA-Thiol could act as reducing agent which would interfere with the assay with giving false positive results. See Figure G.3.17 for a explanation of the reduction of PVA by thiols.

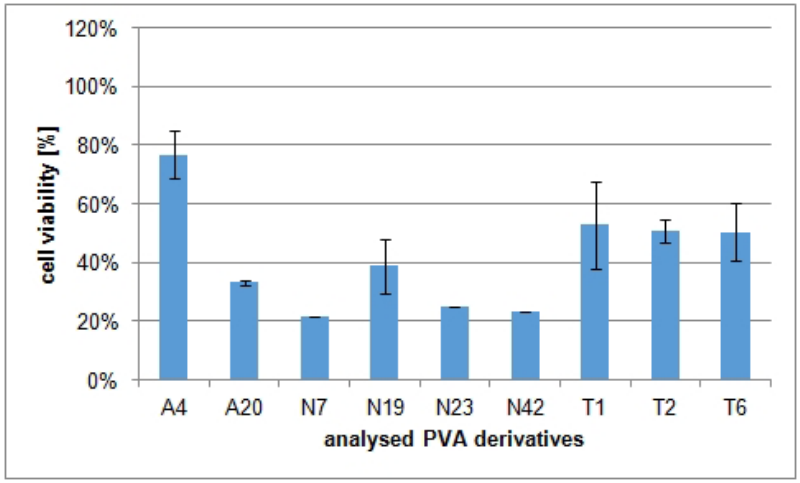

Figure G.3.23: Cell viability of the samples with 10% macromer concentration (T6 has only 7%, T1 only 9.8%)

In Figure G.3.23 all samples with 10% (7% in T6 and 9.8% in T1 respectively) macromer concentration are displayed for direct comparison. As can be seen clearly, PVA-Allyl A4 exhibits the lowest toxicity of all analysed samples with 10% macromer concentration. There is a positive trend linking DS with toxicity, for PVA-Allyl. By contrast no clear trend emerges with PVA-Norbornene, and there is no difference at all between the PVA-

Thiols T1, T2 and T6; however note that we have only a 7% solution of the T6 sample.

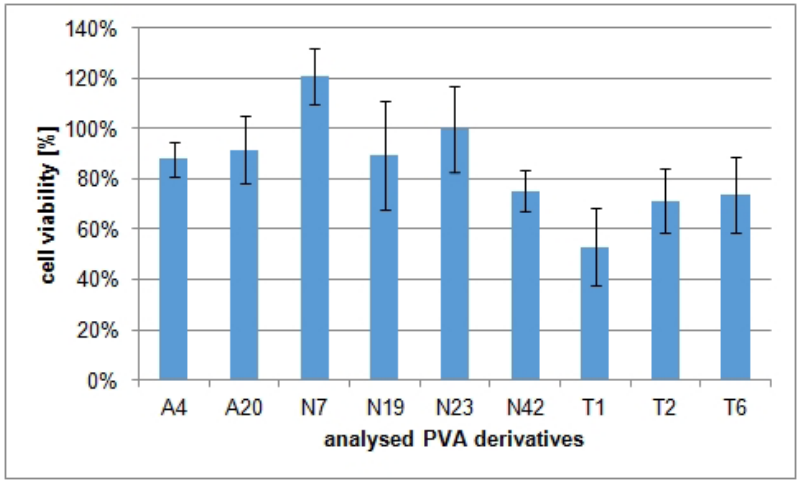

Figure G.3.24: Cell viability of the samples with 1% macromer concentration

With a higher dilution of the solutions displayed in Figure G.3.24, the toxicity decreases overall except for PVA-Thiol T1, whose toxicity stayed the same between 10% and 1%. Especially PVA-Norbornene N7, which showed the highest toxicity at 10%, has here the lowest toxicity of all analysed substances.

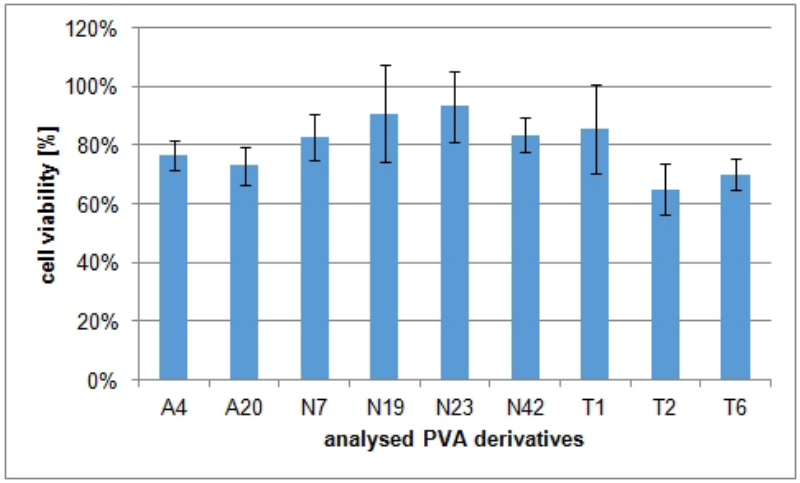

Figure G.3.25: Cell viability of the samples with 0.1% macromer concentration

Finally Figure G.3.25 shows the analysed samples with 0.1% concentration. The toxicity of the solutions with 0.1% macromer content is not significantly different from the solutions of 1% macromer content. These solutions can also be considered as not cell-toxic as well as the solutions with 1%. From all the data analysed here one can conclude that the direct toxicity from the unreacted PVA derivatives is the best in PVA-Allyl A4, especially in high concentrated solutions (10%). With decreasing concentrations the cell viability increases and the differences between the variable DS and substances vanish. PVA-Thiols have in this assay the least differences between DS and concentration concerning their toxicity, but as already mentioned, the measured data may be defective due to the possibility that the PVA-Thiols are acting as reducing agents.

Tests with cell encapsulation and cell viability studies on cross-linked polymers remain to be done in the future.

4 Rheology

4.1 Determination of optimal thiol to ene ratio

Since it is known in literature[88,89] that the ratio of thiol to ene in thiol-ene reaction has a big influence on the reactivity, conversion and properties of the final product, our first goal for the further investigations was to determine the optimal ratio of thiol to ene concerning cross-linking density and reactivity, in hydrogel systems with PVA-Allyl, PVA-Norbornene respectively and PVA-Thiol.
Therefore the increasing storage modulus during irradiation with polychromatic UV light was measured on a rheometer. The storage modulus is a good indicator for the cross-linking density of a given system and therefore the slope of the curve can be taken as benchmark for the reactivity of a photocurable system.

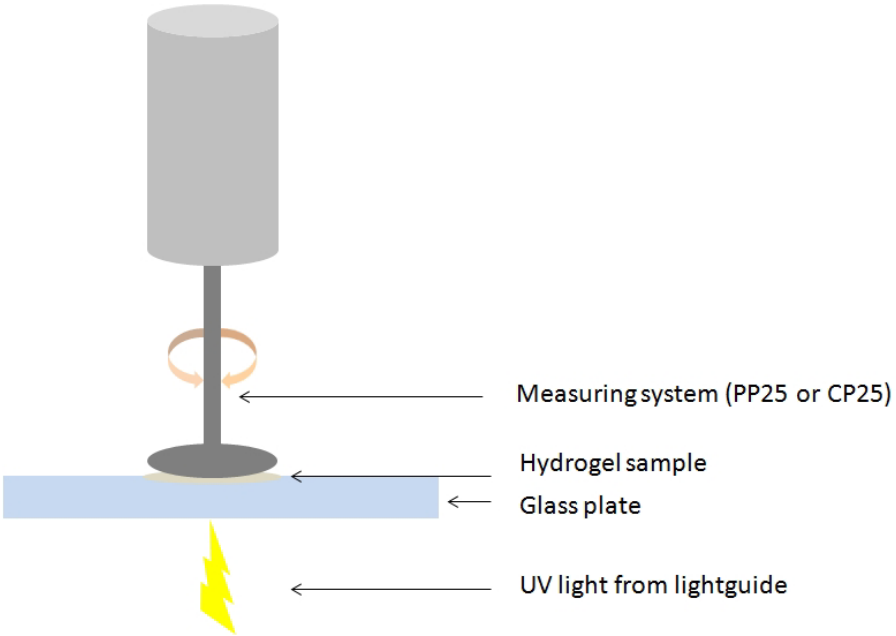

Figure G.4.26: Scheme of photo-rheometer

Figure G.4.26 shows the setting of the photo-rheometer. For detailed information of the used setup see the corresponding section in the experimental part.
In the given case the measurements were done for mixtures between PVA-Allyl A20 (DS: 20%) as ene component, dithiothreitol (DTT) and PVA-Thiol T2 (DS: 2.5%), respectively as the thiol component. Although PVA-Allyl A4 showed a significant lower toxicity, the use of A20 promised better results concerning mechaniccal properties, which was the reason for the selection of A20.

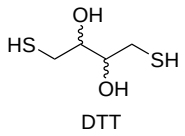

Figure G.4.27: Structure of dithiothreitol (DTT)

DTT was selected as a compound with low molecular-weight which will produce hydrogels with a high cross-linking density. The PVA-Thiol T2 is a macromer with a very low DS and will therefore result in hydrogels with a less dense network und lower cross-linking density.
All percentage specifications in the this section are weight/weight percent, if not otherwise stated.
The hydrogel mixtures were calculated to a macromer-content (DTT included) of 10% with a photoinitiator content of 0.5% based on the whole formulation. Irgacure 2959 (IG2959) was used as PI for the photorheology measurements, because it is currently the only watersoluble UV-photoinitator commercially available with the main drawback of a quite poor solubility and absorption only below 350 nm. An advantage of IG2959 is its low cytotoxicity in dark as well as during UV-curing according to Bryant et al.[90] and Williams et al.[91]
The thiol-ene ratios were investigated from 20% thiol to 120% thiol compared to ene (molar ratio of functional groups) with a stepsize of 20%. It showed that with the use of T2 only solutions up to 60% thiol-content were possible, above this amount precipitation occurred. This was not observed in the case of DTT where all concentrations were possible.
Table G.4.4 shows the content of the analysed mixtures for evaluation of the best thiol to ene ratio. The concentration of macromer and DTT was (together) 10% in water, based on the whole formulation. In all cases the PI concentration was 0.5%.

Table G.4.4: Mixtures for evaluation for the best thiol to ene ratio with A20 and DTT

Sample	**Thiol-Ene Ratio** [%]
A20DTT-20	20
A20DTT-40	40
A20DTT-60	60
A20DTT-80	80
A20DTT-100	100
A20DTT-120	120

More details about the mixtures are displayed in Table E.4.6.
As can be seen in Figures G.4.28 and G.4.29 with increasing thiol content up to 60% (molar ratio compared to ene) the storage modulus G' increases because of a higher cross-linking density.

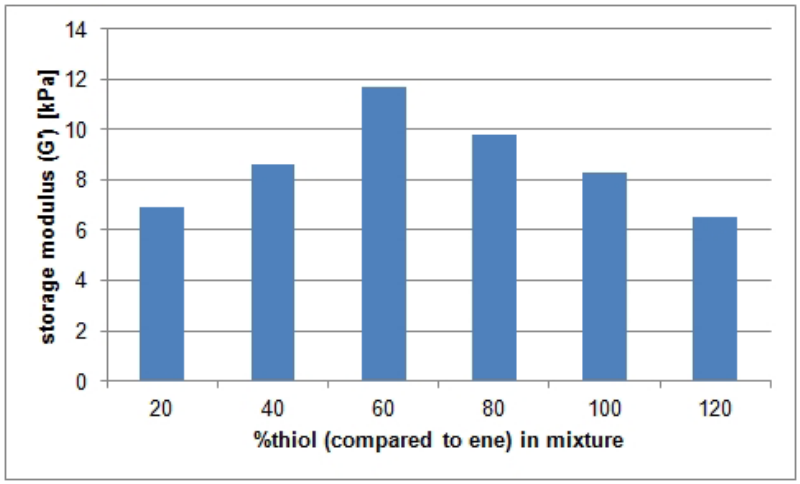

Figure G.4.28: Maximum of storage modulus G' of A20DTT mixtures with different thiol to ene ratios

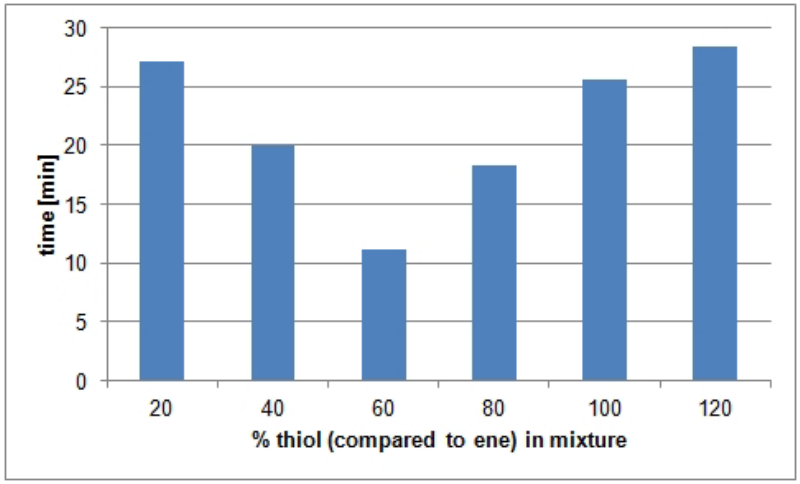

Figure G.4.29: Time after which 95% of the maximum value of G' are reached in A20DTT mixtures with different thiol to ene ratios

Only if there is sufficient thiol able to react with the PVA-Allyl, a higher value of cross-linking density can be achieved. On the other hand if there is a too high amount of thiol available, it could first lead to mono-reacted products (lower cross-linking density) which react afterwards, but much slower and incomplete because of the decreasing mobility of the formed network. By consequence, the formed network has also an increase in viscosity which will decrease the rate of diffusion and therefore reduces the maximum cross-linking density. Figures G.4.28 and G.4.29 show that there is an equilibrium of cross-linking density and decreasing mobility with a maximum of cross-linking density with 60% thiol compared to ene.

For analysis of the slope, which indicates the reactivity of a given system, a regression line was fit through the linear region of the measuring curve so that the correlation coefficient R^2 exceeded 0.98.

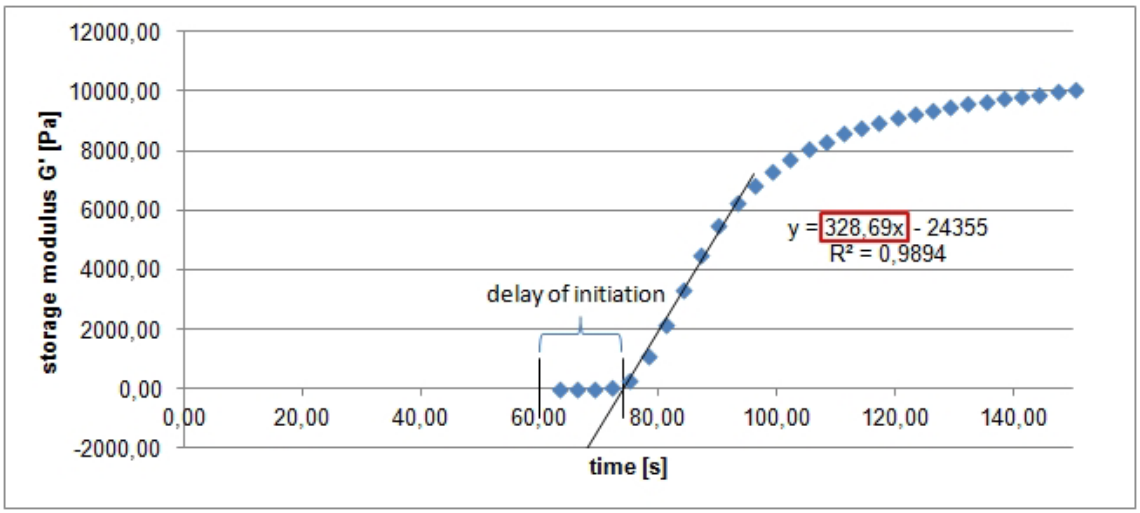

Figure G.4.30: Example of how the slope and the delay of initiation were determined

Figure G.4.30 shows how the regression line is laid trough the curve and how this curve is intersected with the abscissa to calculate the delay of initation.
In the case of reactivity the mixture with 40% thiol compared to ene (A20DTT-40) gives the best results as can be seen in Figure G.4.31 indicated by a faster increase in storage modulus.

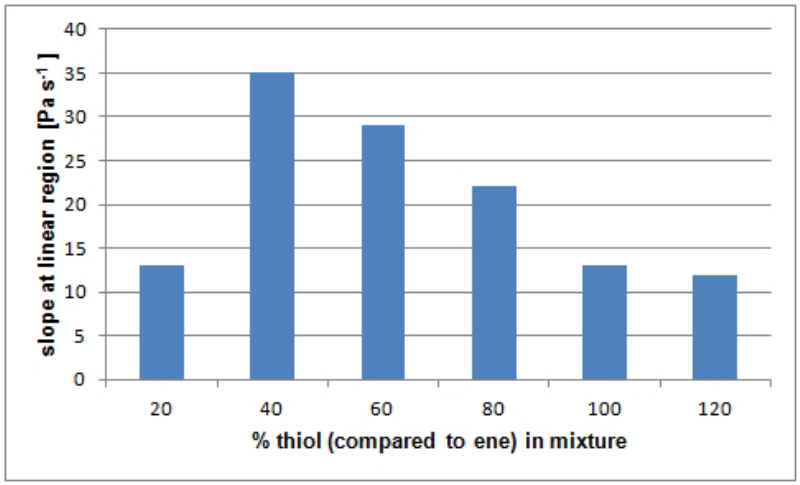

Figure G.4.31: Slope of G' in the linear region of mixture A20DTT with different thiol to ene ratios

Also the delay of initiation was analysed. With the beginning of the measurement the measuring system starts with oscillation, but without radiation. After 60 s the shutter of the UV-lamp gets opened and from this moment the initiation should start.
To analyse the point where an increase of viscosity was visible, the point of intersection of the before mentioned regression line with the abscissa is calculated and the time where no irradiation occurs (60 s in this case) was subtracted like shown in Figure G.4.30 These time intervals are compared in Figure G.4.32.

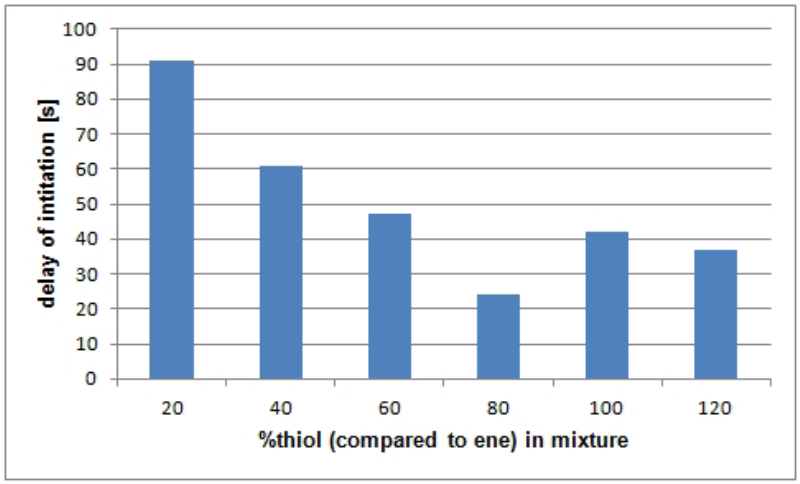

Figure G.4.32: Delay of initiation of mixture A20DTT with different thiol to ene ratios

As can be seen in Figure G.4.32 the delay of initiation is strongly dependent on the thiol-ratio with a minimal delay of 24 s with 80% thiol.
With increasing amount of thiol in the mixture, a higher number of thiyl radicals is generated in the beginning and therefore the probability for the radical to start a reaction increases. But as always in radical reactions, the rate of termination increases also with increasing radical concentration which leads to a lowest delay of reaction in equilibrium of these two effects. What emphasizes this explanation is the fact, that the reaction rate of the termination reaction is about two magnitudes bigger than the propagation rate according to Claudino's[92] research.
The same evaluation was carried out with PVA-Thiol T2 instead of DTT. Table G.4.5 gives information about the analysed ratios of substances.

Table G.4.5: Mixtures for evaluation for the best thiol to ene ratio with A20 and T2

Sample	**Thiol-Ene-Ratio** [%]
A20T2-20	20
A20T2-40	40
A20T2-60	60

Like before the overall macromer content was 10% in H_2O and the concentration of PI was 0.5% based on the whole formulation. IG2959 was used as PI for this examination. The mixtures with ratios from 80% to 120% were also prepared but a precipitate was formed upon mixture. It seems that the solubility limit is above 60% of thiol to ene at a macromer content of 10%. Additionally a thiol to ene ratio of 70% was examined, but also this solution was not homogeneous and therefore could not be measured.
A problem that occurred during the measurements was the drying of the samples due to evaporation of water. Interestingly, this only occurred in samples with T2 but not in samples with DTT. Further investigations have to be done concerning this phenomenon. To circumvent this troublesome evaporation, the edge of the measuring system was coated

with mineral oil, which performed very well in avoiding evaporation.

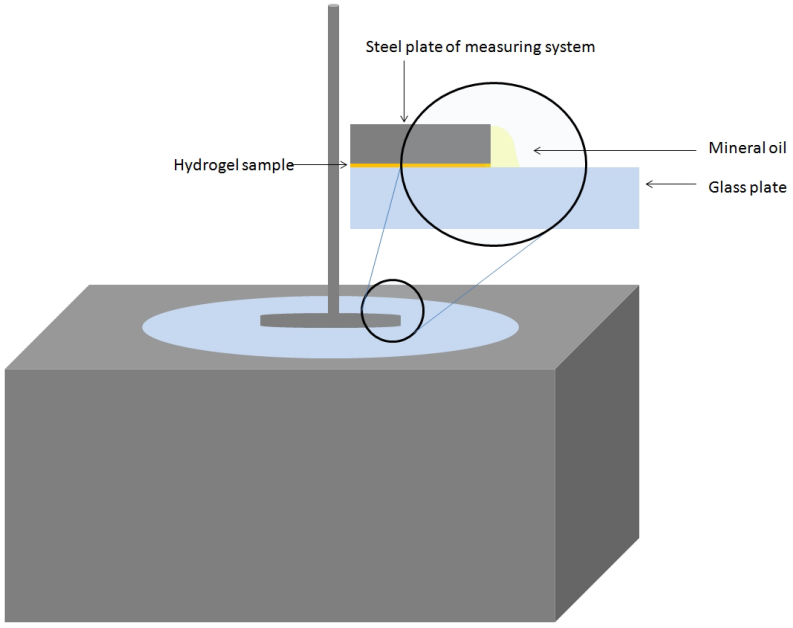

Figure G.4.33: Scheme of the rheometer setup with the mineral oil coating the measuring system

Figure G.4.33 shows a scheme of measuring system, that has been coated with mineral oil on its edges.
Again the maximum value of storage modulus G', the time to reach 95% of the maximum value of G', the slope of the storage modulus in the linear region, and the delay of initiation was determined from this samples.
From Figure G.4.34 one can see that the trend to higher storage modulus and therefore to higher cross-linking density is the same with the thiol T2 as with DTT. Although the trend between the samples is the same, the absolute value of the storage modulus differs significantly between the thiol T2 and DTT. With DTT as thiol-component (A20DTT-60) a storage modulus up to 11700 Pa could be reached where the maximum value of the mixture with T2 (A20T2-60) is 3170 Pa.
The lower cross-linking density of A20T2 is due to the relatively low DS of T2 as compared to DTT. The hydrogel mixtures A20T2 give much less dense polymeric network, which results in a lower storage modulus.

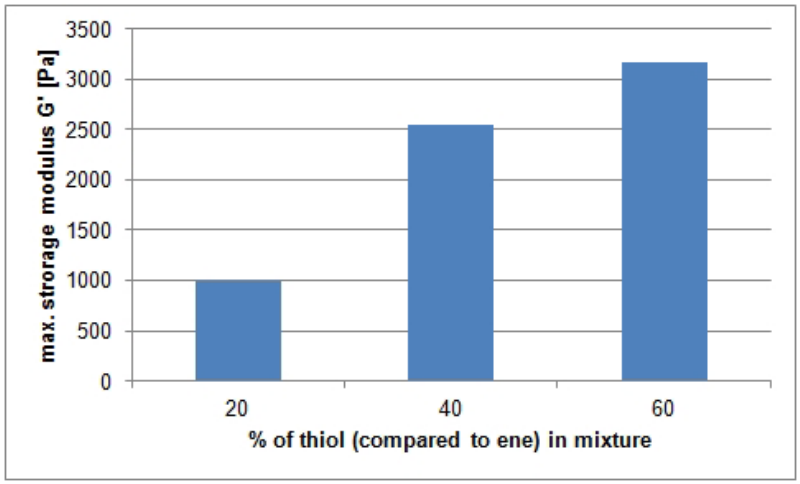

Figure G.4.34: Maximum of storage modulus G' of mixture A20T2 with different thiol to ene ratios

The time to reach 95% of the maximum value of G' is shown in Figure G.4.35.

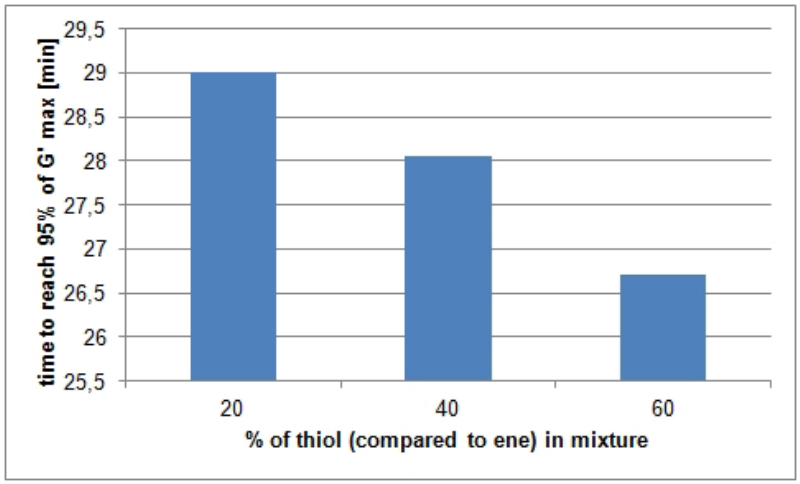

Figure G.4.35: Time after which 95% of the maximum value of G' is reached from mixture A20T2 with different thiol to ene ratios

Like before, the trend between T2 and DTT as thiol-components is similar, but the absolute values differ again. In the case of DTT, 95% of the maximum values are reached in the best case after 11 minutes (A20DTT-60), compared to 26 minutes with T2 (A20T2-60). These numbers indicate that diffusion and therefore the reaction is hindered due to the size of the involved molecules.

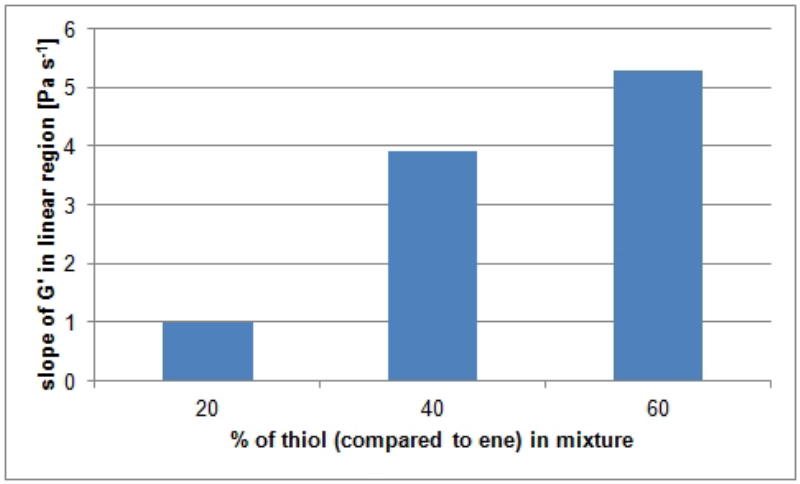

Figure G.4.36: Slope of G' in the linear region of mixture A20T2 with different thiol to ene ratios

Another difference between the DTT and T2 systems is the trend of the slope between the different thiol-ene ratios as can be seen in Figure G.4.36. Where in the case of DTT the sample A20DTT-40 had the highest slope, here it can be seen that the more thiol is in the mixture, the higher the slope gets - with a maximum in case of the A20T2-60 sample. Generally the slope is lower for the PVA-Thiol samples (A20T2) than for the samples with the dithiol DTT (A20DTT). In Figure G.4.37 the delay of initiation is shown depending on sample's thiol to ene ratio.

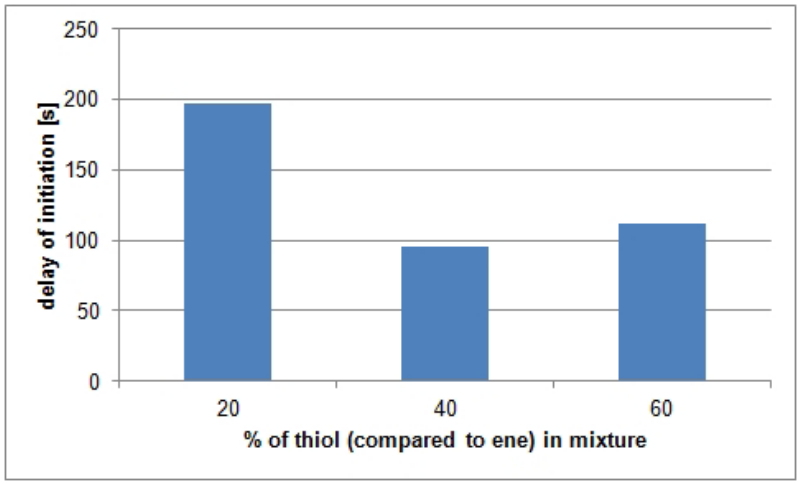

Figure G.4.37: Delay of initiation after start of irradiation

The sample A20T2-40 has the minimal delay of initiation of 95 s, but is still about 4 times higher than hydrogel mixture A20DTT-80 (24 seconds), which had the lowest delay of initiation from the DTT samples. Also the trends differ between the T2 and the DTT samples. As within the T2 samples the A20T2-40 has shown the lowest delay of initiation, whereas with DTT the sample A20DTT-80 showed the lowest delay.
Again the hindered diffusion of large macromolecules compared to the unimpeded diffusion of the small DTT molecule is the reason for the much more delayed reaction in the samples with thiol T2.

4.2 Influence of the photoinitator concentration

Beside the thiol to ene ratio also the concentration of the PI was analysed. For this purpose 4 mixtures with different concentrations of the PI IG2959 were prepared and the increase of the storage modulus was measured during irradiation with UV light.
The solutions contained PVA-Thiol T6 (DS: 6%) and PVA-Allyl A20 (DS: 20%) with a macromer concentration of 10 wt% in water. The analysed PI-concentrations are listed in Table G.4.6.

Table G.4.6: PI concentration in the analysed A20-T6 mixtures

PI concentration [%]
0.10
0.25
0.50
0.92

The value of 0.92% PI is due to the maximum solubility of the PI. Since the solutions have to be mixed together and the PVA-Thiol only dissolves on heating for a few hours, we decided to solve it in water only (without PI in it). Therefore the whole PI amount had to be dissolved in the part of the solution in which the PVA-Allyl was dissolved. Since from the PI only solutions up to 1.5 wt% could be dissolved, a final concentration of 0.92 wt% PI in the solution was the maximum that could be prepared.
Like in the last section again the maximum of the storage modulus G', the time to reach 95% of the maximum value of G', the slope in a linear area of the G' curve and the delay of initiation was determined of the mixtures. It showed that the 0.1% mixture did not start within the time used for measuring the other samples (1800 s) and on increasing the measurement time to 5400 s it did not give any reproducible results and was therefore not analysed. Figure G.4.38 shows the maximum storage modulus of each mixture.

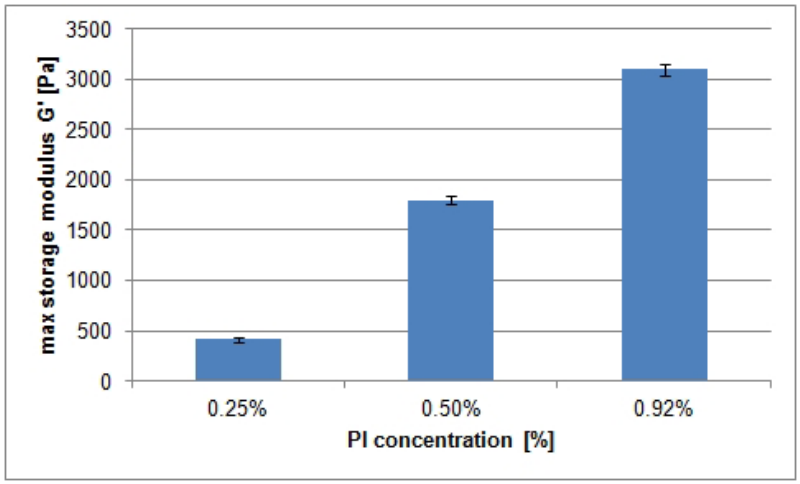

Figure G.4.38: Maximum of storage modulus G' of each mixture from A20T6 with different PI concentrations

As can be seen in Figure G.4.38, the storage modulus is strongly dependent on the PI

concentration. The higher the PI concentration was, the higher the maximum G' became. This is due to a higher degree of cross-linking in presence of more radicals.

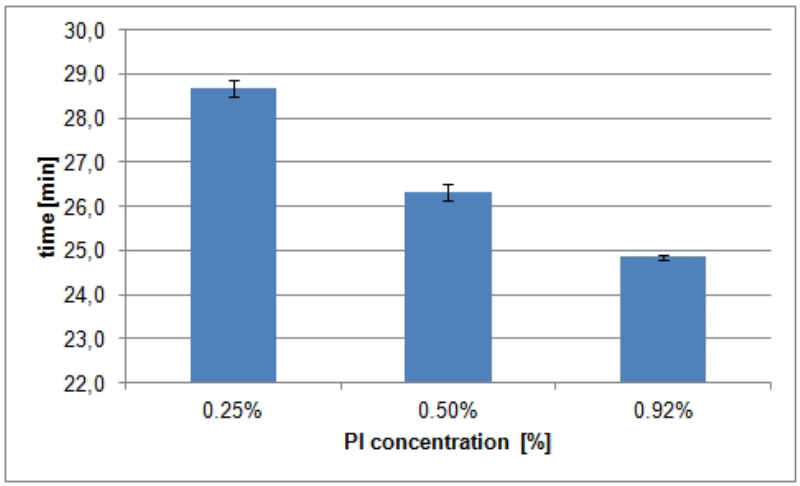

Figure G.4.39: Time after which 95% of the maximum value of G' are reached of mixtures from A20T6 with different PI concentrations

According to the last results of the increasing storage modulus, also the time that is needed to reach 95% of the maximum storage modulus is dependent on the PI concentration. This goes hand in hand with the higher reactivity of the mixtures with higher PI concentrations. In Figure G.4.39, one can clearly see the decreasing amount of time needed to reach 95% of the maximum. The higher reactivity of the mixtures can in fact be seen more clearer in the slope of the storage modulus curve. Therefore the slope was measured in the linear region and compared between the mixtures.

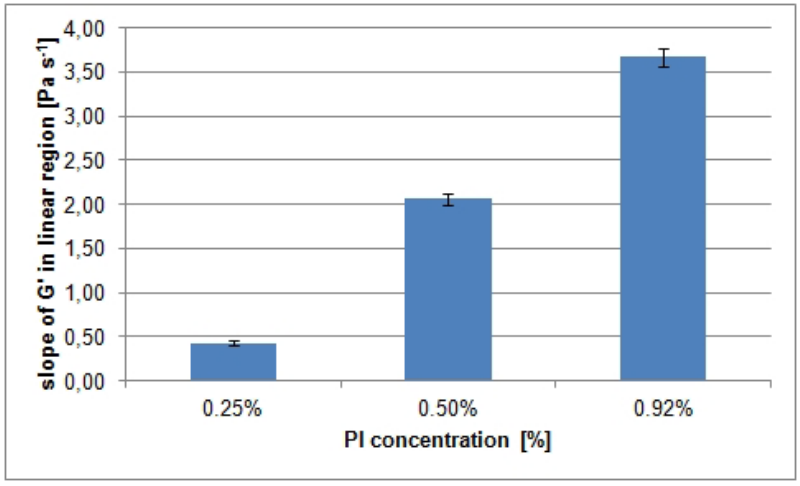

Figure G.4.40: Slope of G' in the linear region of each mixture from A20T6 with different PI concentrations

Figure G.4.40 shows that the slope of the increasing storage modulus is much higher for the systems with higher PI concentrations, indicating a higher reactivity because of higher number of radicals. From 0.25% to 0.50% an increase of the fourfold amount of the slope can be seen. From 0.5% to 0.92% only an increase of less than a twofold amount is present.

From this data it is very likely that the reactivity cannot be increased indefinitely just by increasing the PI concentration, if the solubility would not prevent it anyway.

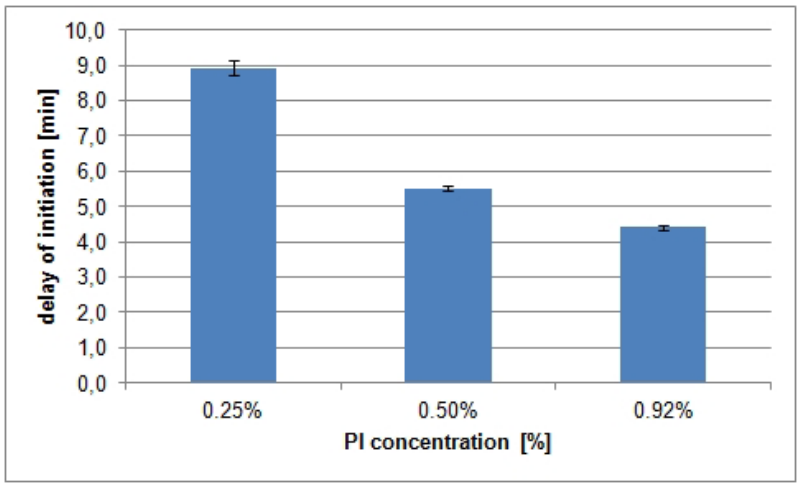

Figure G.4.41: Delay of initiation after start of irradiation of each mixture from A20T6 with different PI concentrations

Figure G.4.41 shows that the delay of initiation decreases with increasing concentration of PI in the solution. In fact, with doubled concentration, the delay of initiation is nearly halved. This data corroborate the PI-dependent reactivity of the mixtures.

4.3 Influence of the macromer concentration

To determine also the influence of the macromer content to the photorheology behavior, solutions with different macromer concentrations were produced and analysed from selected PVA-Allyl, PVA-Norbornene and PVA-Thiol derivatives. In all solutions a PI concentration of 0.5% (based on the whole formulation) was used because, as shown in Section 4.2, this concentration performs well, and problems with solubility occur less than with 0.92%.

For the analysis, mixtures with a high DS of both ene and thiol components were tested, and likewise mixtures where both DS were low; high/low DS combinations were not tested. To see the influence of the macromer concentration in case of a low molecular-weight cross linker like dithiothreitol (DTT), also an experiment with A4 and DTT was carried out.

Table G.4.7 gives information about the used PVA derivatives and the used concentrations.

Table G.4.7: Mixtures for the evaluation of the influence of the macromer concentration

Ene component	**Thiol component**	**Macromer concentration [%]**
A4	T2	3%
A4	T2	5%
A4	T2	10%
A4	T2	15%
A4	DTT	3%
A4	DTT	5%
A4	DTT	10%
A4	DTT	15%
A20	T6	3%
A20	T6	5%
A20	T6	10%
A20	T6	15%
N19	T6	3%
N19	T6	5%
N19	T6	10%
N19	T6	15%

The measurement time was 1800 s, since a plateau was reached with all formulations from 5% and above. It turned out that the 3% solution did not show any increase in storage modulus even after 5400 s, except of A4DTT which exchibited a low increase, but was not analysed further because comparing to the other samples was not possible.
On the next pages the result of these experiments will be shown.

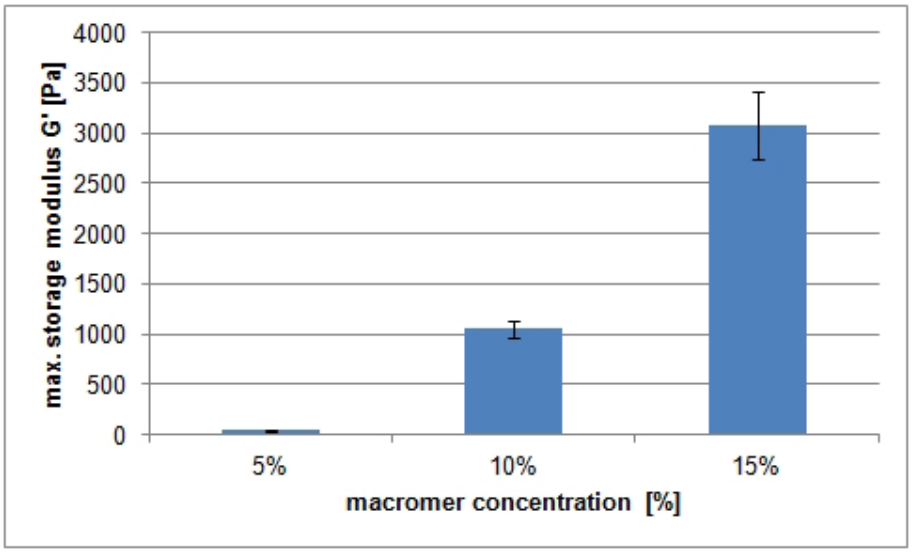

Figure G.4.42: Maximum storage modulus G' of the mixture A4T2 with different macromer concentrations

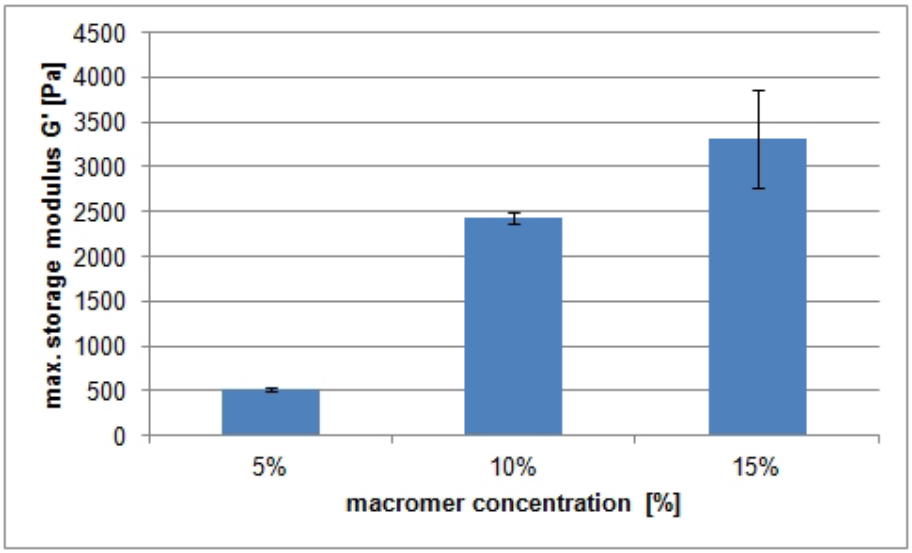

Figure G.4.43: Maximum storage modulus G' of the mixture A20T6 with different macromer concentrations

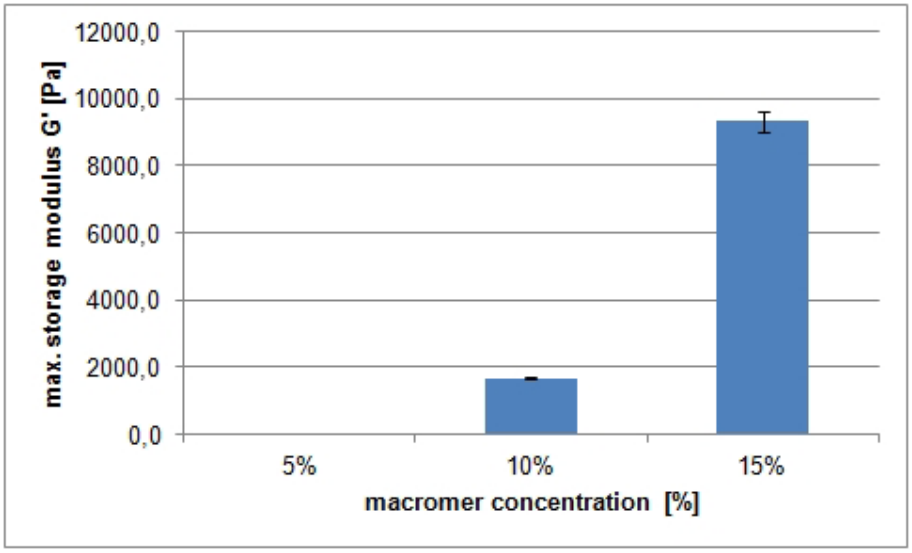

Figure G.4.44: Maximum storage modulus G' of the mixture N19T6 with different macromer concentrations

Figures G.4.42, G.4.43, G.4.44 show the maximum storage modulus G' of the mixtures A4T2, A20T6 and N19T6 as a function of macromer concentration. One can clearly see that G' is strongly dependent on the concentration of macromers in the solution. PVA-Allyl suggests a linear dependency of the macromer concentration whereas PVA-Norbornene suggests an exponential dependency. Also the absolute values of G' between the different mixtures vary strongly. PVA-Norbornene shows almost a threefold value of maximal G' as PVA-Allyl at a macromer concentration of 15%. The reason for it is probably that PVA-Norbornene is more reactive and therefore more cross-links are formed, which leads to a more rigid hydrogel.
A higher degree of substitution of the used macromers yields a higher cross-linking density, as can be seen from the results of A20T6 and A4T2.

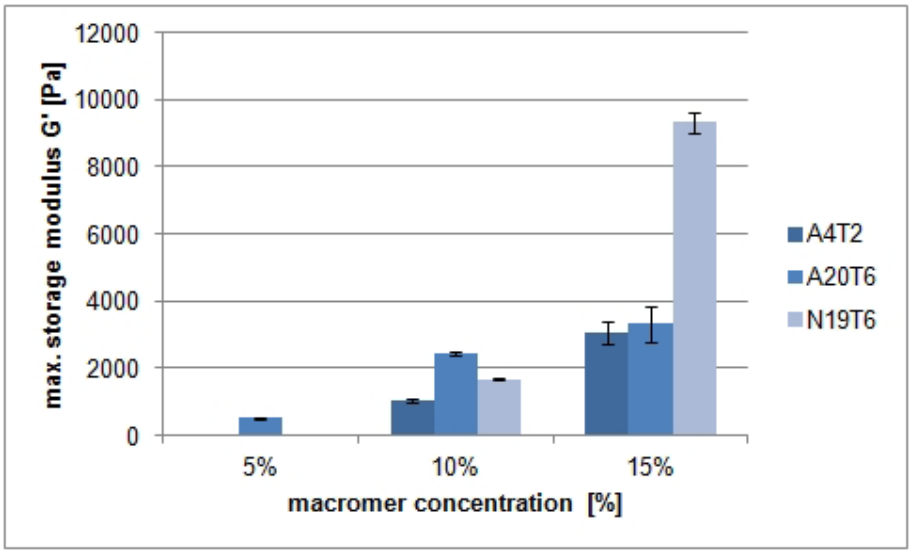

Figure G.4.45: Comparison of maximal G' of the mixtures A4T2, A20T6 and N19T6 with different macromer concentrations

Figure G.4.45 compares the mixtures A4T2, A20T6 and N19T6 concerning their maximal G' as a function of macromer concentration. Here the different dependency of cross-linking density on the macromer concentration can be seen very well, with the enormous difference of N19T6 to the other mixtures at a concentration of 15%. Also the influence of a low molecular-weight cross-linker (DTT) was analysed in this experiment in a mixture with PVA-Allyl A4. Figure G.4.46 shows the results of the measurements.

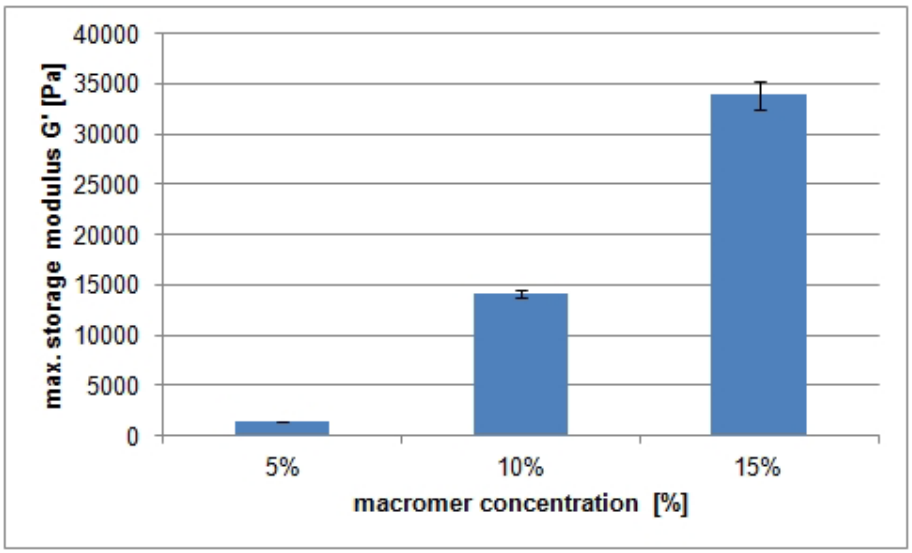

Figure G.4.46: Maximum storage modulus G' of the mixture A4DTT with different macromer concentrations

Also with DTT a linear dependency from the macromer concentration was observed with PVA-Allyl. On comparison of A4T2 and A4DTT the absolute values of G' are vastly different: A4DTT shows the tenfold value of G' compared with A4T2. The reason for this effect was already stated in section 4.1.

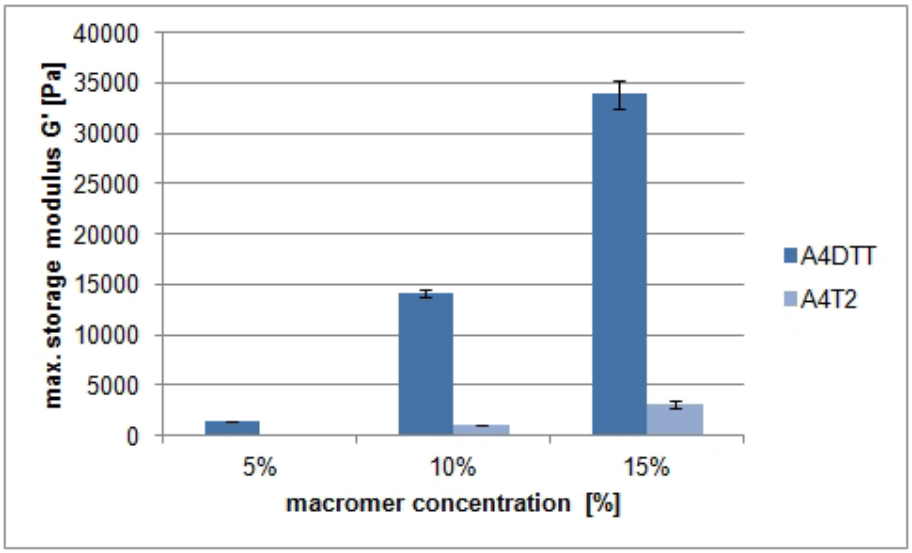

Figure G.4.47: Comparison of maximum G' of the mixtures A4T2 and A4DTT with different macromer concentrations

To visualise this vast difference, the maximal G' values of mixtures A4T2 and A4DTT are shown in Figure G.4.47.
A positive trend is linking reactivity and macromer concentration, as can be deduced by comparing the slope in the linear region of the following figures.

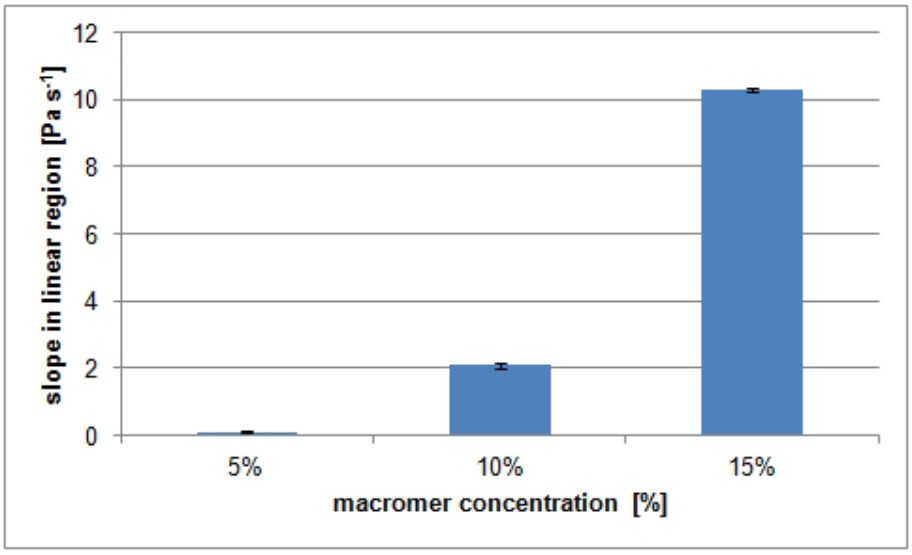

Figure G.4.48: Slope in linear region of the mixture N19T6 with different macromer concentrations

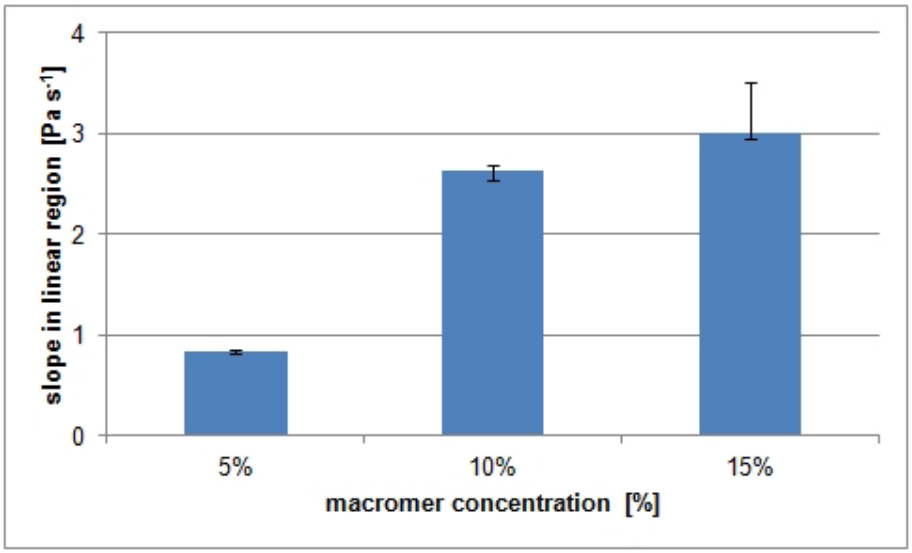

Figure G.4.49: Slope in linear region of the mixture A20T6 with different macromer concentrations

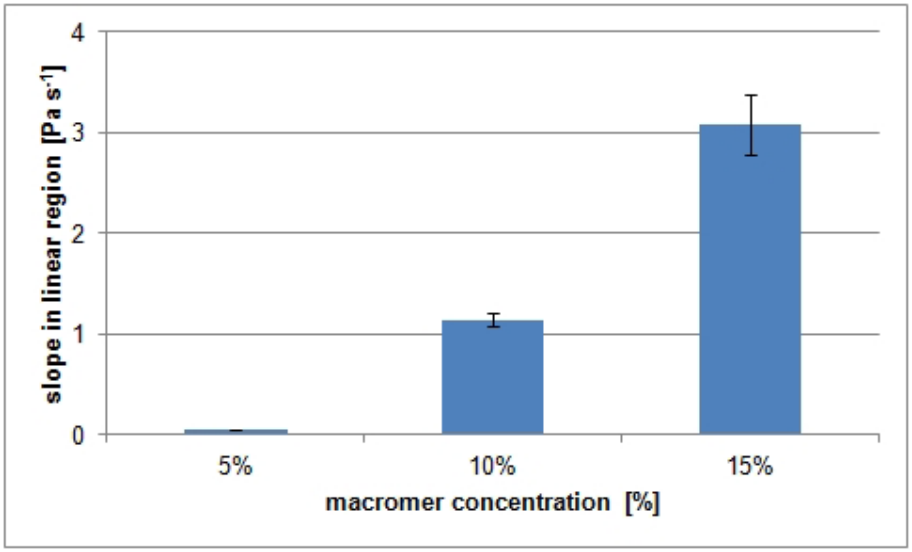

Figure G.4.50: Slope in linear region of the mixture A4T2 with different macromer concentrations

From the figures G.4.48, G.4.49 and G.4.50 one can see the different reactivities of the formulations indicated by the slope of the storage modulus increase. The absolute values of PVA-Norbornene are higher than those of PVA-Allyl at 15%. However with 10% macromer concentration A20 is slightly more reactive than N19. As before a higher dependency of the macromer concentration from PVA-Norbornene could be the reason for this phenomenon. Interestingly with decreasing DS also the dependency of the reactivity from the macromer concentration increases, which could be seen comparing Figures G.4.49 and G.4.50.
The results from the mixture of A4 with DTT are also strongly different from the three other mixtures, as can be seen in Figure G.4.51

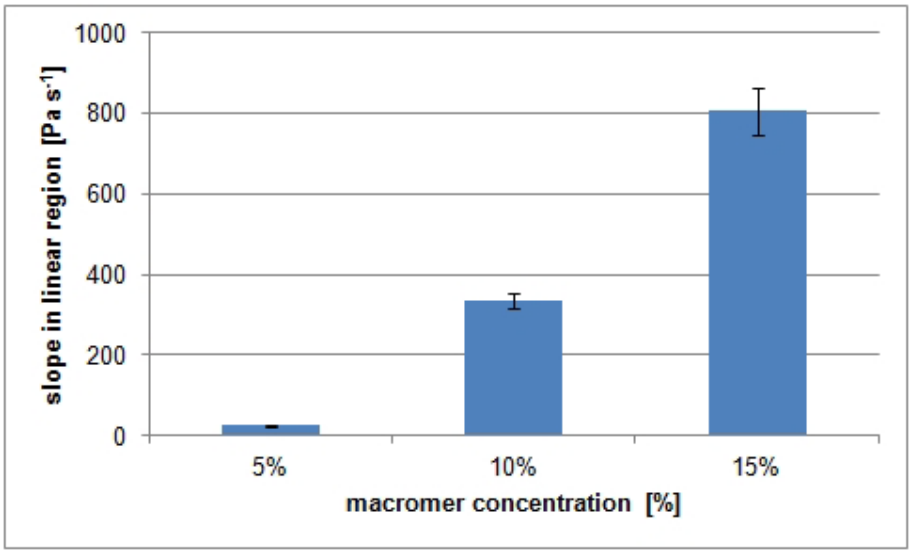

Figure G.4.51: Slope in linear region of the mixture A4DTT with different macromer concentrations

Compared to the reactivities of A4T2, A4DTT exhibits a 280-fold higher reactivity in the 15% solution and 290-fold higher reactivity in the 10% solution.

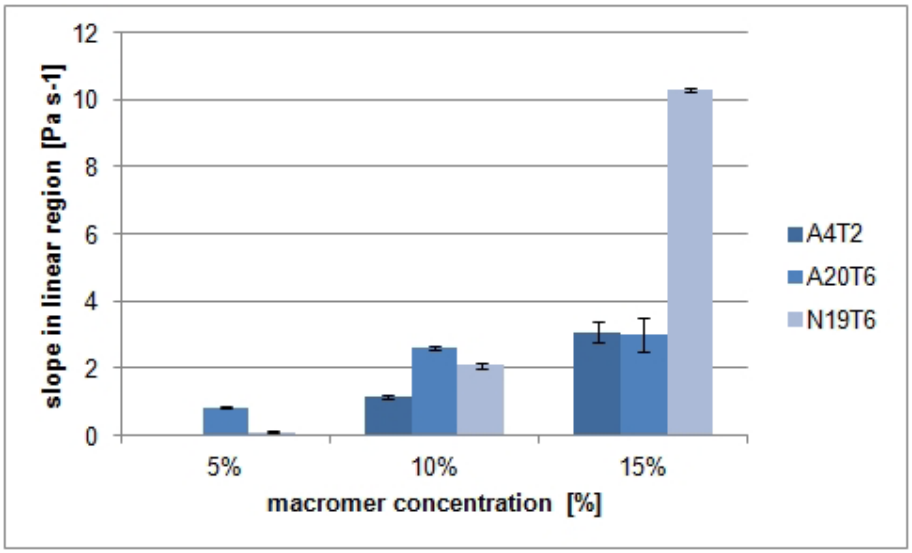

Figure G.4.52: Comparison of the slope in linear region of the mixtures A4T2, A20T6 and N19T6 with different macromer concentrations

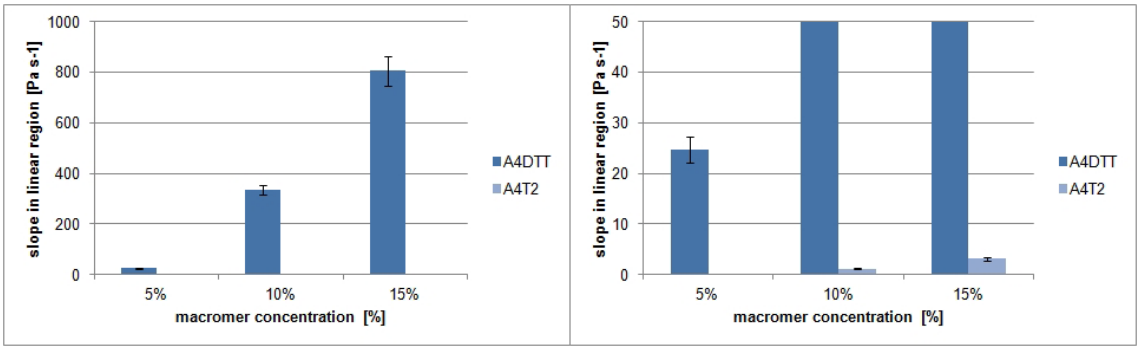

Figure G.4.53: Comparison of the slope in linear region of the mixtures A4T2 and A4DTT with different macromer concentrations. Note that scales of y-axes are different!

Figure G.4.53 compares the reactivities of PVA-Allyl A4 with PVA-Thiol T2 and DTT respectively. One can see that the difference is vast between these two mixtures. The decreased mobility of the PVA-Thiol seems to be a reason for this big difference.

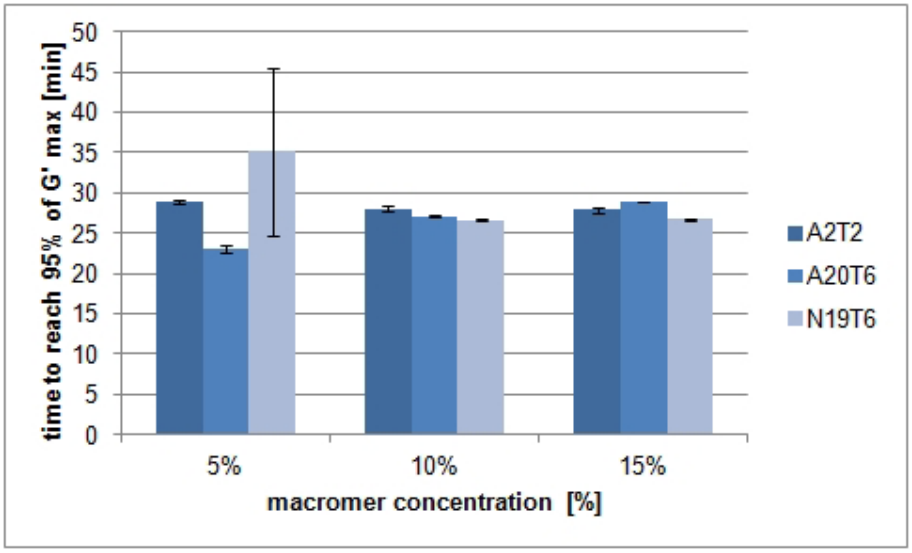

Figure G.4.54: Time after which 95% of the maximum value of G' are reached in mixtures A4T2, A20T6 and N19T6 with different macromer concentrations

The times that were needed to reach 95% of maximum G' of the mixtures A4T2, A20T6 and N19T6 with different macromer concentrations are compared in Figure G.4.54. There is no significant difference in these analysed mixtures concerning the time to reach 95% of maximum G'.

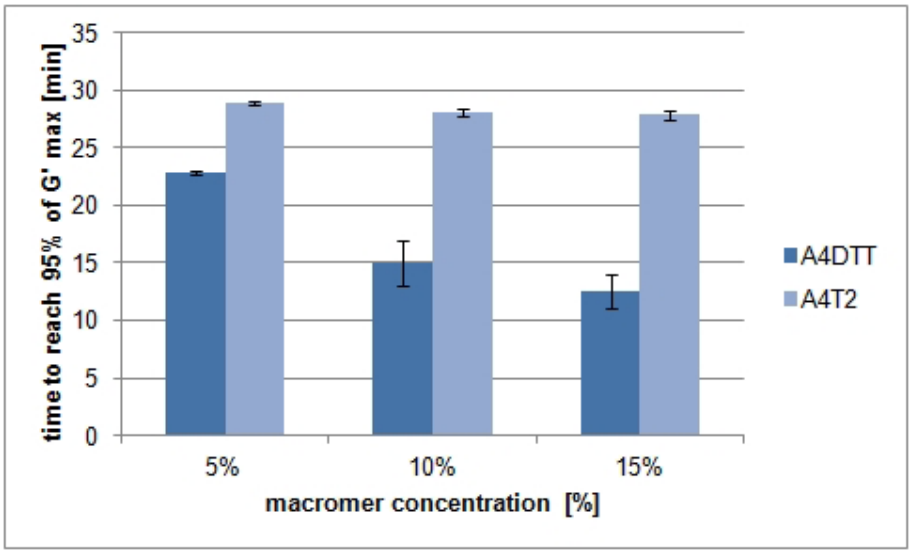

Figure G.4.55: Time after which 95% of the maximum value of G' are reached in mixtures A4T2 and A4DTT with different macromer concentrations

Contrary to the results from the comparison of mixtures A4T2, A20T6 and N19T6 the comparison of the mixtures A4T2 and A4DTT in Figure G.4.55 shows significant differences of the time that is needed to reach 95% of maximum G'. This time is more depending on the macromer concentration in mixture A4DTT than in mixture A4T2.

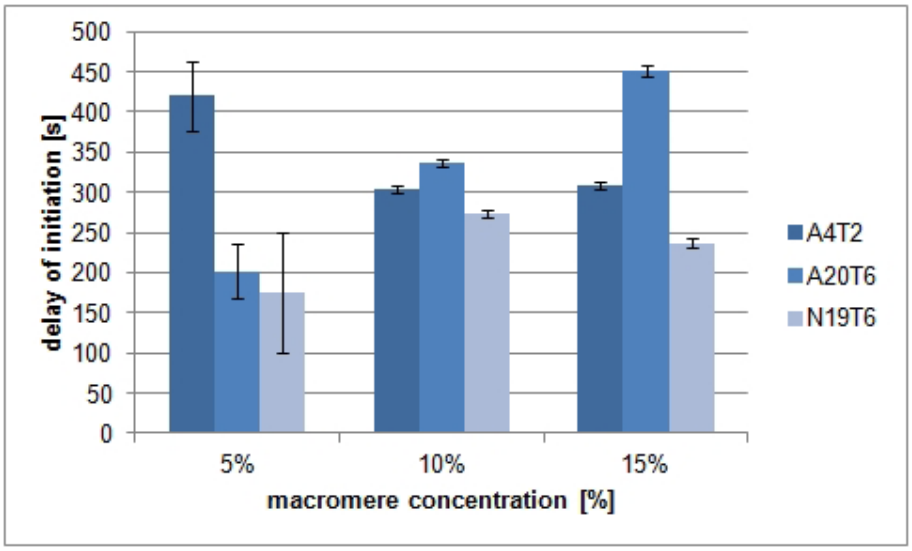

Figure G.4.56: Delay of initiation of mixtures A4T2, A20T6 and N19T6 with different macromer concentrations

In Figure G.4.56 the delay of initiation from the mixtures A4T2, A20T6 and N19T6 with different macromer concentrations are compared. There is no clear trend between DS and delay of initiation as well as macromer concentration and delay of initiation. To elucidate this phenomenon more analyses have to be done in future.

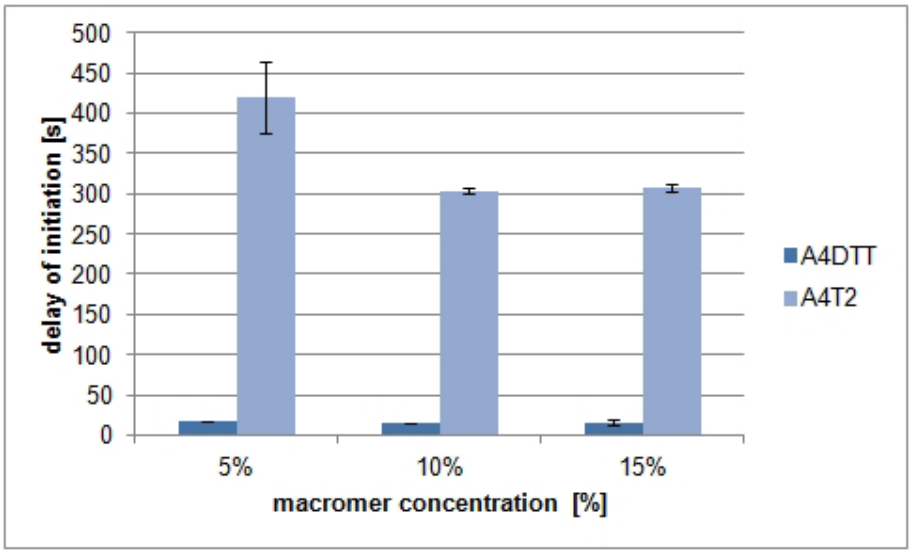

Figure G.4.57: Delay of initiation of mixtures A4T2 and A4DTT with different macromer concentrations

A significant difference can be seen on comparison of the delay of initiation from the mixtures A4T2 and A4DTT. In case of A4DTT the delay is constant over a broad macromer concentration, however the delay of initiation in mixture A4T2 is more depending on the macromer concentration.

4.4 Storage stability of the formulations

It was already mentioned that there are problems with storage stability with some thiol-ene formulations and that research was done as to which inhibitors gave good results in increasing the storage stability of such formulations. So, following to Esfandiari et al.,[37] we decided to use pyrogallol as an inhibitor for our formulations. Also we decided not to use the acid inhibitors because the PVA derivatives are in salt form and have solubility problems anyway, which would have been aggravated by the addition of acidic substances.

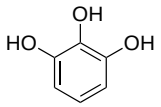

pyrogallol (pyr)

Figure G.4.58: Structure of pyrogallol

To analyse the storage stability of the produced PVA derivatives in solution, mixtures were prepared with different amounts of pyrogallol and the viscosity of the solutions was measured upon preparation, after 1 day, after 1 week and after 1 month. A change in viscosity will indicate premature gelation of the formulations. PVA-Allyl A4 was selected due to its low toxicity, which makes A4 the favorite for the application in tissue engineering. PVA-Norbornene N7 was used because of the higher reactivity of PVA-Norbornenes, which has been shown in Section 4.3. Also N7 has a similar DS compared to A4. It has already been shown, that a mixture between N7 and PVA-Thiol T2 will not form a clear solution. Therefore PVA-Thiol T6 was used for both mixtures. Table G.4.8 gives information about the analysed solutions.

Table G.4.8: Mixtures from PVA-Allyl A4, PVA-Norbornene N7 and PVA-Thiol T6 for the evaluation of the storage stability

Sample	**Inhibitor concentration [ppm]**
SS-A4T6-0	0
SS-A4T6-100	100
SS-A4T6-1000	1000
SS-N7T6-0	0
SS-N7T6-100	100
SS-N7T6-1000	1000

All mixtures had 0.5% PI concentration and 10% macromer concentration. The viscosity was measured without irradiating the samples and they were stored in brown glass vials to prevent being irradiated while stored. The results of the storage stability test are shown in the following figures.

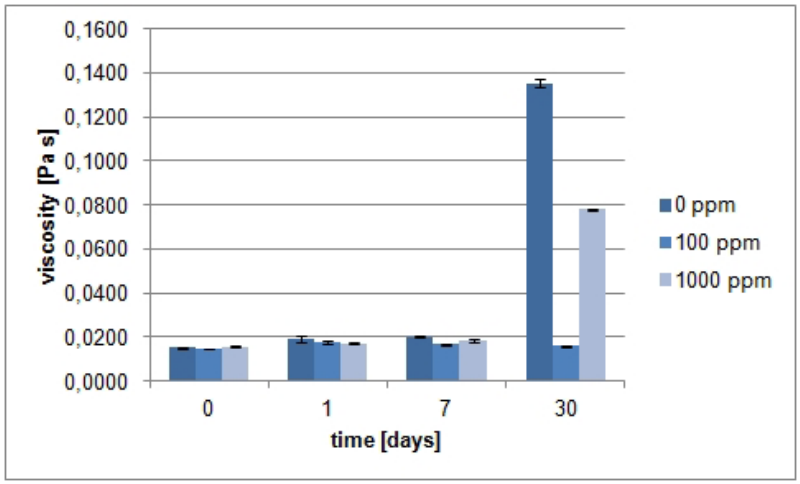

Figure G.4.59: Measured viscosities of mixtures A4T6 containing different concentrations of pyrogallol as inhibitor

The viscosities of the mixtures A4T6 with 0, 100 and 1000 ppm of pyrogallol as inhibitor were measured directly after preparation, after 1 day, 1 week and 1 month. As can be seen in Figure G.4.59 the viscosity stays almost constant for over a week. After a month the mixture without inhibitor experienced a strong increase of viscosity, whereas the viscosity of a mixture with 100 ppm of pyrogallol stays constant. Interestingly the mixture with 1000 ppm of pyrogallol exhibits a much higher viscosity after 30 days, than the mixture with only 100 ppm. An undetected evaporation of the solvent of the mixture with 1000 ppm inhibitor may explain this result.

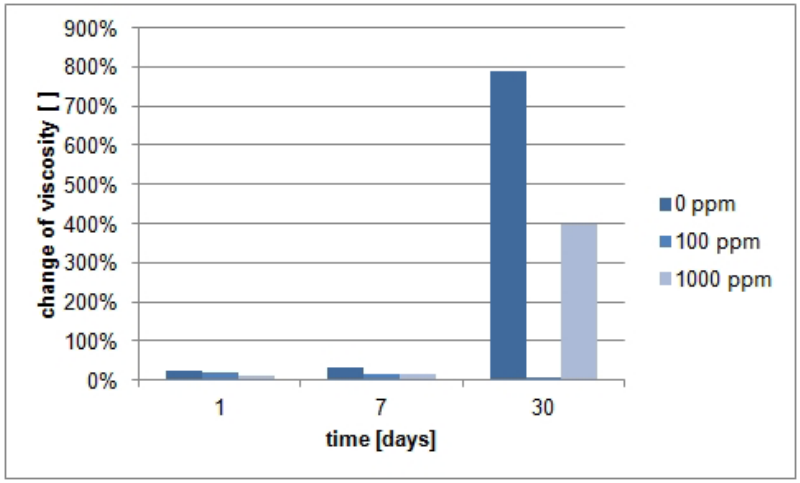

Figure G.4.60: Relative change of viscosity of A4T6 containing different concentrations of pyrogallol as inhibitor. Values are calculated relative to the value of day of preparation.

Figure G.4.60 shows the relative change of viscosity of the mixtures A4T6. An increase of about 800% with no inhibitor can be seen after 30 days, and a increase of 400% with 1000 ppm inhibitor. We can conclude, that the solutions are equally stable for a week not depending on any inhibitor. After this time that the addition of pyrogallol as inhibitor to the formulation increases the storage stability, and 100 ppm of pyrogallol seem to be

enough.
Also the storage stability of PVA-Norbornene mixtures was analysed. The results are shown in the following figure.

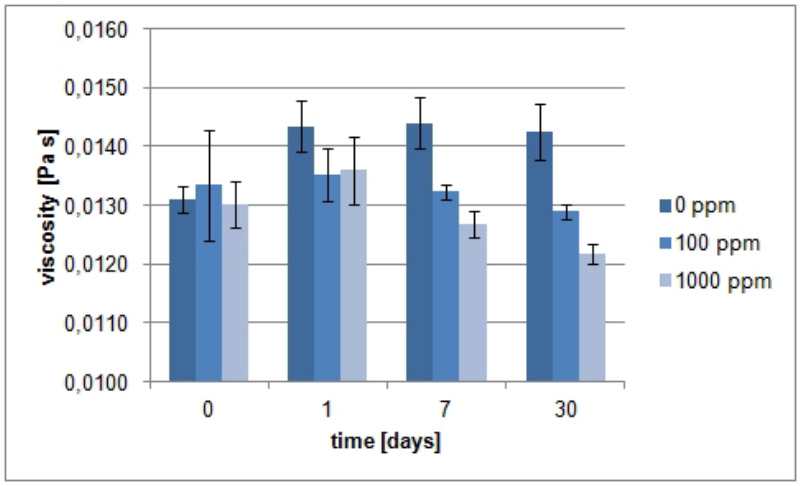

Figure G.4.61: Measured viscosities of mixtures N7T6 containing different concentrations of pyrogallol as inhibitor

The viscosities of the mixtures N7T6 with 0, 100 and 1000 ppm of pyrogallol as inhibitor was measured directly after preparation, after 1 day, 1 week and 1 month and the results are displayed in Figure G.4.61. A little increase of viscosity can be seen in the solution with no inhibitor, whereas the solutions with inhibitor do not show any significant change in viscosity. Although the reactivity of PVA-Norbornene showed to be higher compared to PVA-Allyl, the storage stability was better even without inhibitor.
We can conclude that the storage stability of the analysed mixtures of PVA derivatives over a time range of 30 days is sufficient if stored together with 100 ppm of pyrogallol.

5 Swellability

When a solvent enters a polymer network the polymer chains between the cross-link points distend and experience a stress that the polymer tries to compensate with relaxing its chains back to its entangled state. Thus an equilibrium between swelling and relaxing is formed, influenced by the length of the polymer chains between the cross-linking points. Since swelling can influence mechanical properties and solute transport activities,[93] the swelling behavior of selected PVA derivatives was analysed.

5.1 Preparation of samples

For determining the swellability of the PVA derivatives, cylindrical pellets of 6 mm diameter and 0.7 mm thickness were produced according to Qin et al.[94] Therefore solutions with different content of macromer (3, 5, 10 and 15%) were produced and transferred to a cross-linked poly(dimethylsiloxane) (PDMS) mould. The mould was put on an icebath and irradiated in a UV-chamber for a specified amount of time. After the irradiation, the mould was put in distilled water for 10 minutes and subsequently the pellets were taken out and directly transferred into a vial with exactly 1 mL of water. In this vial the specimens swelled for 2 days and were weighed after adhered water had been removed. Afterwards the samples were transferred into new vials submersed in minimal amount of water and dried via lyophylisation.
To determine the influence of the different macromer content on the swellability, hydrogel formulations from PVA-Thiol T6 and PVA-Norbornene N7 were used with a thiol to ene ratio of 0.6:1 and 0.5% PI. As shown in Section 4 mixtures with 60% thiol to ene ratio showed the best results concerning reactivity and mechanial properties. Also PVA-Norbornene showed higher reactitivy compared to PVA-Allyl. These were the reasons for the selection of the analysed compounds. Table G.5.9 shows the tested macromer contents.

Table G.5.9: Macromer content of the tested solutions for determination of hydrogel swellability

Macromer content [%]	**Pellets formed**
3%	no
5%	yes
10%	yes
15%	yes

Except from the 3% solution, which did not allow any pellet-formation, 3 pellets were produced from all mixtures, so that the analysis could be done in triplicate. To successfully form pellets also from the 5% solution the pellets were irradiated for 1600 s, because after 800 s the 5% mixture still was completely liquid.

5.2 Swellability analysis

From the dry and soaked weight, the mass swell ratio was calculated after the following formula.

$$R_{sw} = \frac{m_{wet} - m_{dry}}{m_{dry}}$$

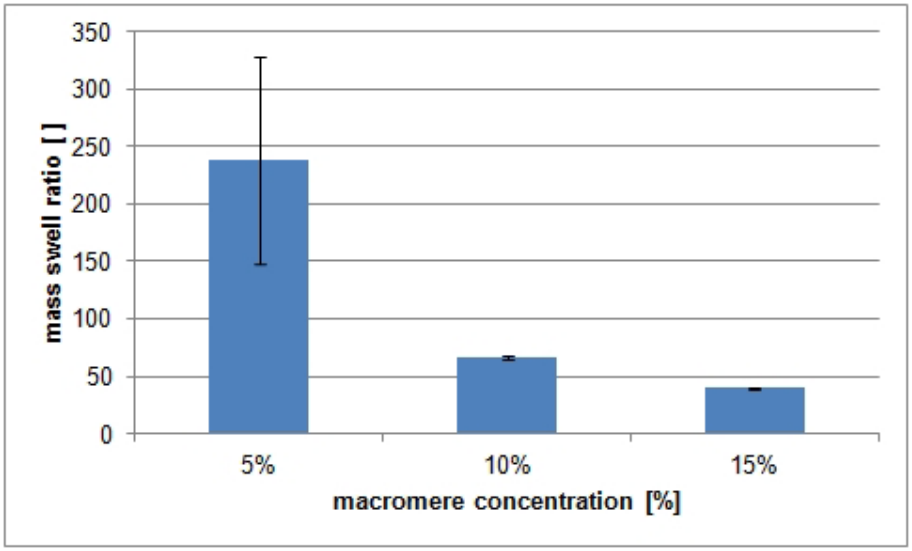

Figure G.5.62: Mass swell ratios of mixture N7T6 with different macromer concentrations

In Figure G.5.62 the mass swell ratio of the pellets formed from PVA-Norbornonen N7 and PVA-Thiol T6 in different macromer-concentrations are displayed. It can be seen that with increasing macromer concentration the mass swell ratio decreases dramatically. As shown in Section 4.3 the cross-linking density increases with increasing macromer concentration in solution. Therefore with increasing macromer content also the number of cross-links increases and this reduces the swellability.
To further examine the swelling behavior of the other derivatives, mixtures of PVA-Allyl, PVA-Norbornene and PVA-Thiol were produced of which pellets were formed.
Because the pellets with only 3% are very difficult to handle due to their really low dry weight (which also explains the high standard deviation of the results from 5% mixtures), we concluded to use a fixed macromer concentration of 10% for the rest of the swellability experiments. Table G.5.10 shows which mixtures were possible and of which pellets were formed. The same swelling experiment was carried out with them. The irradiation was here only for 800 s, because this was enough to form pellets in a good shape. Thus a direct comparison of the results from the preceding experiment is not advised, although the difference between 800 s irradiation and 1600 s irradiation of the sample N7T6 is only 5%.

Table G.5.10: Mixtures for determination of the swellability behavior of different PVA derivatives

Mixture	result
A4T2	pellets formed
A4T6	pellets formed
A20T2	no homogenous solution possible
A20T6	pellets formed
N7T2	no homogenous solution possible
N7T6	pellets formed
N19T2	no homogenous solution possible
N19T6	pellets formed

The results of this experiment is shown in Figure G.5.63.

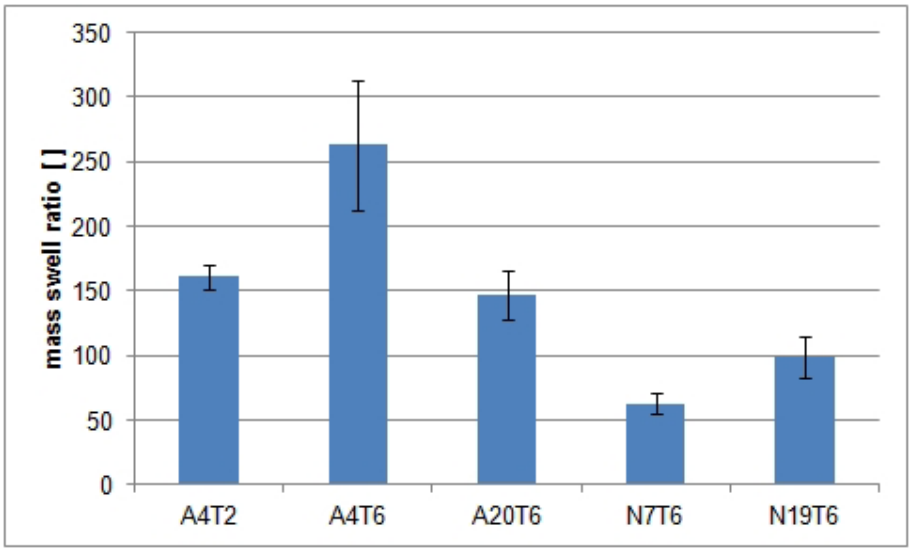

Figure G.5.63: Mass swell ratios of different PVA-Allyl, PVA-Norbornene and PVA-Thiol mixtures

As described above, with increasing cross-linking density the swellability decreases. It was already stated in Section 4.3, that the cross-linking density is also depending on the degree of substitution of the used macromers. The higher the degree of substitution, the higher the cross-linking density gets and therefore the lower the mass swell ratio of the mixture should be.
Comparing the results from mixture A4T2 and A20T6, no significant difference can be seen, although the cross-linking density of A20T6 is presumably almost doubled compared to A4T2. A possible explanation of this effect is the much higher number of carboxylate groups in the case of A20 which could take up more water due to increased hydrophilicity despite of higher network density.
Mixture A4T6 exhibits the highest mass swell ratio of all tested mixtures. One would expect a higher cross-linking if the DS is increased from 2.5% to 6%. However the lower

cross-linking density in this case, may result of a hindered reaction of the thiol groups. The more thiol groups are on one polymer backbone, the less can react before the mobility of the chain is decreased too much to react further. This effect results finally in a lower cross-linking density and also in a higher swellability of the pellet. The cross-linking density of N19T6 is a little bit lower than that of A20T6 in a 10% solution, but the mass swell ratios behave inversely to what we expect (high swell ratio at low cross-linking density). However, a direct comparison is difficult because norbornene is strongly different to allylsuccinic acid.

The overall highest mass swell ratio occurs with A4T6, whereas N7T6 has the lowest one. The cross-linking density of these mixtures have not been studied so far, so it is very difficult to compare the two values. It can be concluded that these hydrogels can absorb up to the 250-fold amount of water of their own weight and that their swelling behavior is strongly dependent on the macromer concentration used for pellet-forming.

Based on obtained values, molecular weight between cross-links M_c should be calculated using Flory-Huggins theory. This value of M_c should be compared with a M_c value obtained from rheological measurement using statistical rubber elasticity theory.

6 Two-Photon Polymerisation

6.1 Synthesis of water-soluble photoinitiators

For 3D structuring of the modified PVA, water-soluble PIs were necessary. Thus the initiators E2CK (5) and P2CK (6) were synthesised according to Li et al.[95] These two initiators have been selected because of their straightforward synthesis based only on an aldol-condensation between 4-aminobenzaldehydes with carboxylic acid salts at their terminal amino group and corresponding ketones. Compared to other methods such as Heck[96] or Sonogashira[97] coupling aldol-condensation is easy and economical.
But also the low toxicity and large processing windows exhibited by those PIs were arguments for their selection.
Furthermore, an improved method for workup and purification was developed, so that the PIs were clean enough for further toxicity studies.

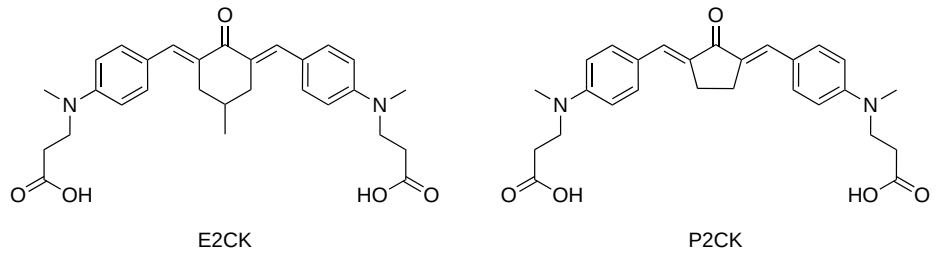

Figure G.6.64: Structures of the water-soluble PIs E2CK and P2CK

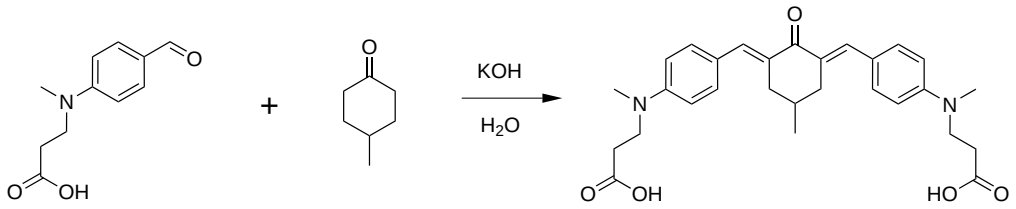

For the synthesis of E2CK, 4-methylcyclohexanon, 3-((4-formylphenyl)(methyl)amino)-propanoic acid (2 eq.) and potassium hydroxide (6 eq.) were dissolved in deionized water (110 eq.) and heated to 80°C. After 6 hours of reaction time the reaction was cooled to room temperature. Since TLC showed incomplete reaction, the mixture was stirred further for 6 days at room temperature, afterwards the reaction was cooled in an icebath and methanol was added. The product was precipitated with HCl and separated with centrifugation.
Since NMR showed up to 19% of remaining aldehyde the product was purified with column chromatography (eluent: chloroform with 3% of acetic acid) yielding a very pure product. The purity was determined via HPLC and spiking with 3-((4-formylphenyl)(methyl)amino)-propanoic acid, exhibiting a remaining impurity of only 0.27%.

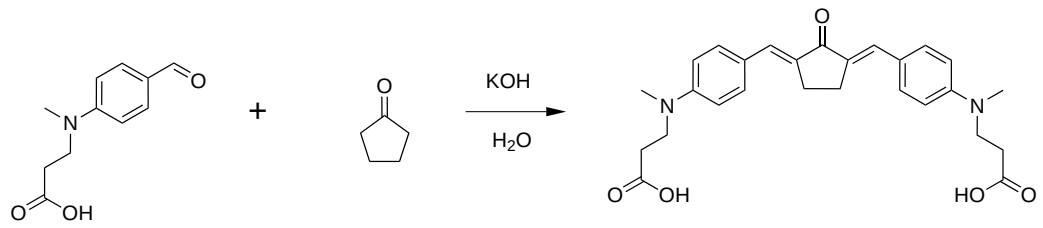

The synthesis of P2CK is almost the same as of E2CK. Cyclopentanone, 3-((4-formylphenyl)-(methyl)amino)propanoic acid (2 eq.) and potassium hydroxide (6 eq.) were dissolved in deionized water (122 eq.) and the reaction was heated to 80°C. After 6 hours of reaction time, the mixture was cooled to room temperature and stored under argon for 5 days. The product was precipitated with HCl in water. The precipitate was separated by centrifugation and dried in vacuum, resulting in 99% of theory of a dark red solid.
The purification was done by recrystallising from 2-propanol, resulting in a red, crystalline product with 1.7% of remaining aldehyde according to HPLC analysis.

6.2 Determination of processing window

Using Two Photon Polymerisation one has many choices of parameters, that can be adjusted to ones needs. The structure, the laser power, the writing speeds are just some of those. It is known that the parameters can be varied over a broad range still resulting in well shaped structures. This range is called processing window. The larger processing windows are, the better for further usage, since one has more possibilities to adjust the parameters to ones need (e.g. lowering the laser power to prevent cell damage). The size of a processing window is influenced by the reactivity of the reactants, by the effectivity and concentration of the PI, by macromer concentration and also by the limitation of the 2PP apparatus.
For determination of processing windows mixtures of PVA-Ally or PVA-Norbornene and PVA-Thiol and DTT respectively were prepared. Although PVA-Allyl A4 exhibited the lowest toxicity, the reactivity of PVA-Norbornene was superior compared to PVA-Allyl. Therefore formulations of PVA-Norbornene with PVA-Thiol T6 and DTT respectively were prepared. The macromer concentration as well as the concentration of PI was varied. Only some mixtures depending on the DS and the type of macromer were possible without precipitating of the initiator. With these samples E2CK-THEMA showed the highest compatibility.

Ene component	**Thiol component**	**PI**	**c(PI) [%]**	**c(Macromer) [%]**
N19	T6	E2CK-THEMA	0.5	20
N19	T6	E2CK-THEMA	0.1	20
A4	T2	E2CK-THEMA	0.5	10
A4	DTT	E2CK-THEMA	0.5	10

Table G.6.11: Formulations for determination of the processing windows for 2PP

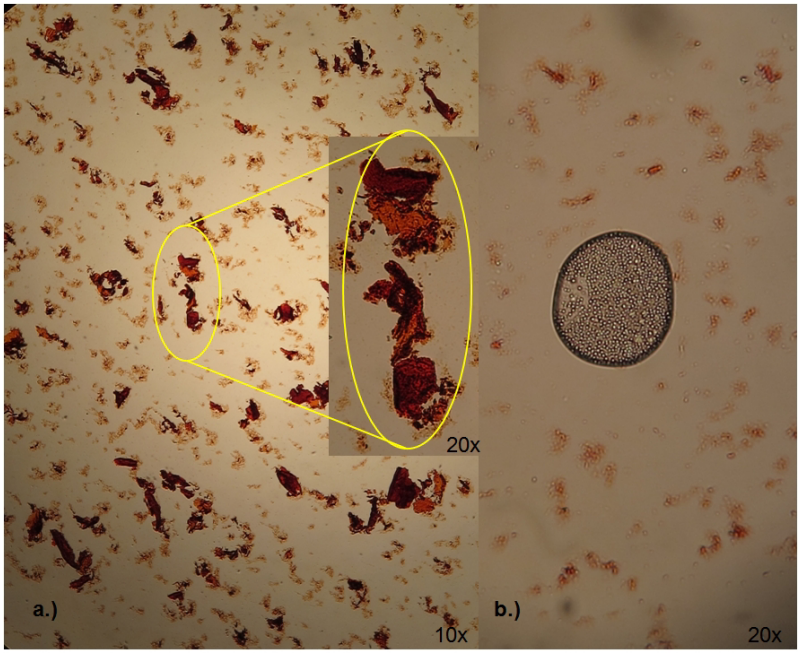

Figure G.6.65: Example of precipitated photoinitiator of a 2PP mixture. a.) shows the precipitate; b.) shows an air bubble which has, by comparison, black borders

Glass slides were prepared, similar to Goss,[98] with covalently bond thiol groups in order to attach the 3D structures to the glass. For this purpose microscopic glass slides were cleaned with a mixture of concentrated sulfuric acid and hydrogen peroxide and subsequently submersed in a solution of (3-mercaptopropyl)trimethoxysilane. These glass cover slides were sticked with transparent tape, as distance piece, to a clean microscope slide like shown in Section 6.1.
The prepared samples were put in the 2PP apparatus and standard-structures (cubes with pores) were structured in the formulation. An array of 10 times 10 cubes were produced with varying laser power on one axis and varying writing speed on the other axis. After the structuring process the samples were submersed in water to prevent evaporation and collapse of the hydrogels, which would falsify the results. Afterwards the structures were analysed under a light microscope as well with an laser scanning microscope (LSM). For the analysis with LSM it is important, that remaining PI is removed prior to analysis, because otherwise the fluorescence of the remaining PI would overlap the fluorescence of the structures. This overlapping would prevent taking of pictures with the LSM.
The analysis of the formed hydrogels resulted in structures that were well shaped, completely damaged or in between this two categories.

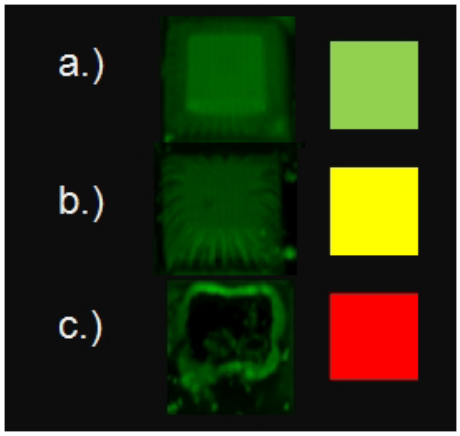

Figure G.6.66: Examples of 2PP structures a.) well shaped structure; b.) shape can be clearly identified but shows errors; c.) completely damaged structure or no structure at all

Figure G.6.66 gives examples for the quality categories of 2PP produced structures together with their colour-code. The cubes were structured from the cover slide to the resin, so that the structures were covalently bond to the cover slides and floating of the structures was prevented.

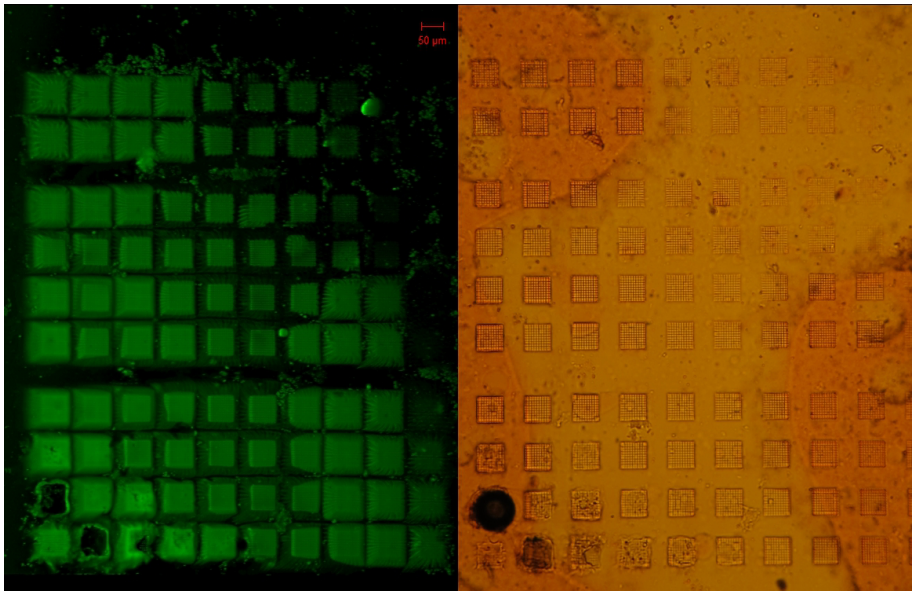

Figure G.6.67: Left: LSM 3D model, right: Photo (through light microscope) of mixture N19T6 with 20% macromer content and 0.5% PI concentration. From left to right the laser power was decreased from 100 to 10 mW and from bottom to the top the writing speed was increased from 1 to 177 mm/s

Figure G.6.67 shows an LSM 3D model on the left and a photo, taken through a light microscope, of the mixture N19T6 with 20% macromer content and 0.5% of PI E2CK-THEMA. The laser power was decreased from left to right beginning at 100 mW and ending at 10 mW. The writing speed was increased from 1 mm/s at the bottom to 177 mm/s at the top of the array. One can clearly see that in the region of high laser energy combined with low writing speed, the energy was so high that the formulation got to hot and locally

the solvent started boiling. This is the reason for the damaged structures in left, downer corner of the figure. At low laser powers (about 10 mW) and at high writing speeds the energy was not high enough to form well shaped structures, as can be seen in the right upper part of Figure G.6.67.

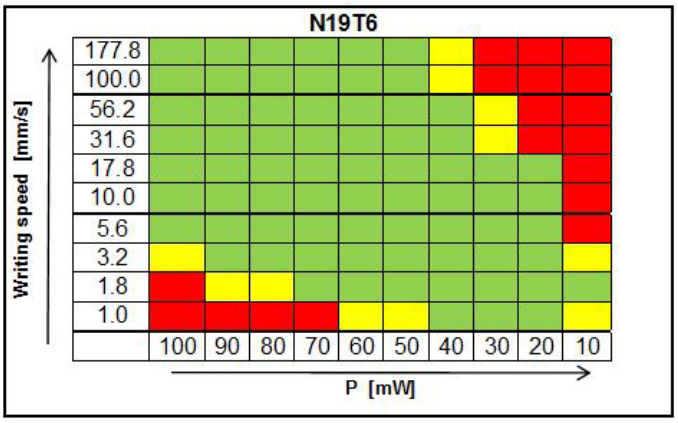

Figure G.6.68: Processing windows of mixture N19T6 with 20% macromer content and 0.5% PI concentration

Figure G.6.68 shows the processing window, with analysis of the data with the LSM model. A very large processing window is exhibited by the formulation N19T6 with 20% macromer content.
Another interesting phenomenon can be seen in the LSM model: the swelling of the structures if strongly dependent on the distance to the glass slide. That is the reason for the broadening of the structures from top to the bottom of each cube.

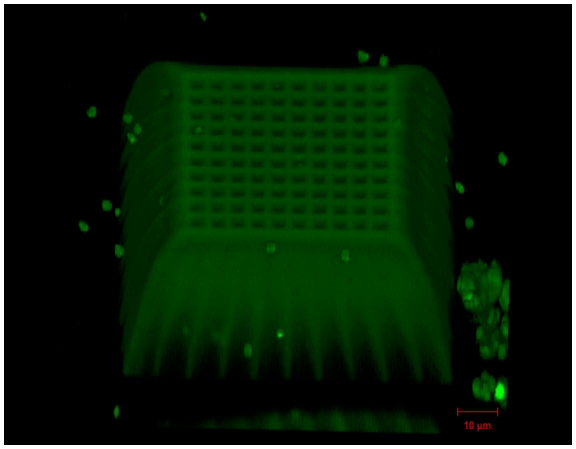

Figure G.6.69: Magnification of a single cube of the formulation N19T6 with 20% macromer content and 0.5% PI concentration

Figure G.6.69 shows a magnification of a swollen cube which widens from top to the bottom. It can be seen that the top edge of the cubes is 50 µm long were the bottom edge is about 76 µm long. A reason for the different swelling may is that water is hindered to enter the network near the glass slide.
To see what influence the PI concentration has to the processing window, the same for-

mulation but with 0.1% instead of 0.5% of E2CK-THEMA was prepared and analysed. The parameter for structuring were the same as with 0.5% PI-concentration.

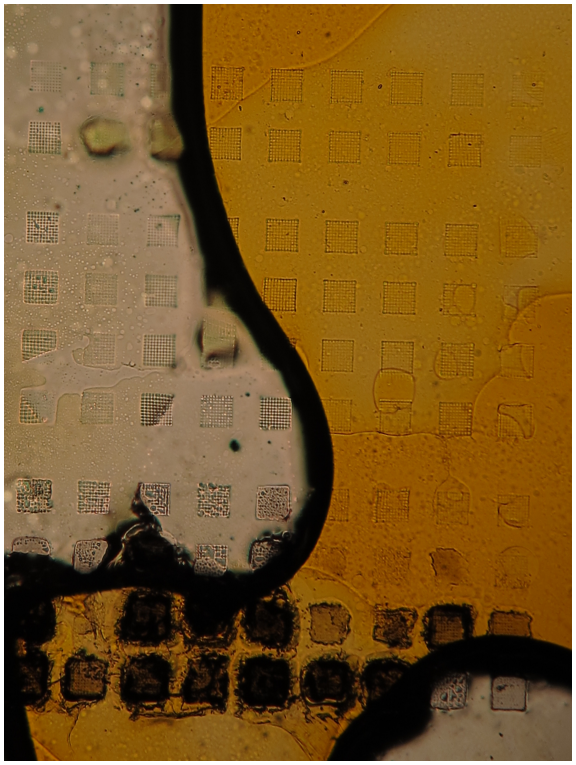

Figure G.6.70: Photo (through light microscope) of mixture N19T6 with 20% macromer content and 0.1% PI concentration

Again we can see in Figure G.6.70 regions with too high laser energy (black, damaged structures) and with too low energy (too high writing speed, respectively) in the right upper corner. Also the difference from fresh water (almost colourless) and from mixture with PI (orange) can be seen well in this picture. On analysis of the structures with the LSM almost no structures were left on the slide. This is most probably because of lower cross-linking density which leads to a higher swelling of the structures, what teared the structures apart and floated away during washing procedure.

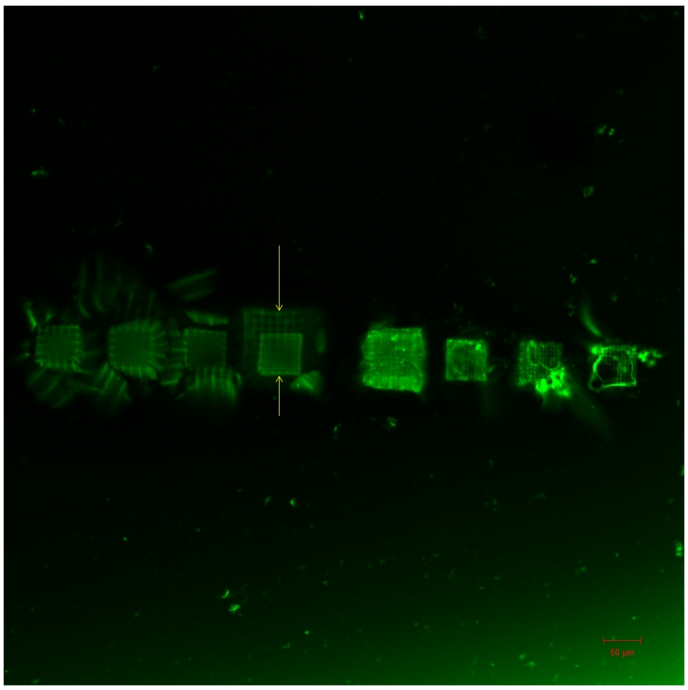

Figure G.6.71: LSM 3D model of mixture N19T6 with 10% macromer content and 0.1% PI concentration.

Figure G.6.71 shows the LSM 3D model of mixture N19T6 with 20% macromer content and 0.1% PI concentration. As can be seen, almost no structures persisted the swelling and were visible after the washing procedure. Also the enormous swelling (marked with yellow arrows) which almost doubled their volume, can be seen very well in the left structures.

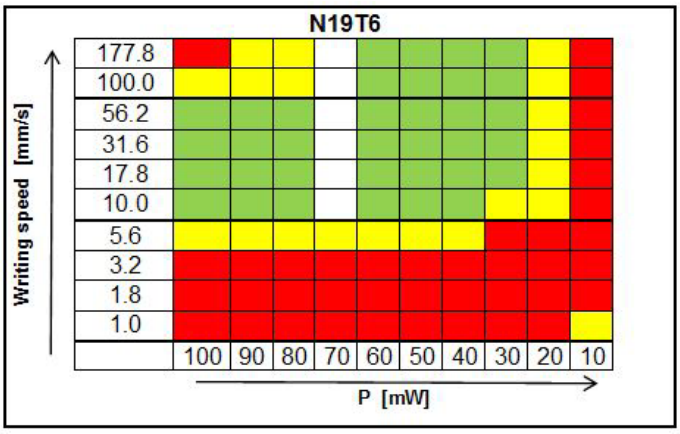

Figure G.6.72: Processing windows of mixture N19T6 with 20% macromer content and 0.1% PI concentration

Figure G.6.72 shows the processing window, with analysis of the data with light microscope. The white squares were those, where no statement about the structure quality could be made, because of the phase boundary which formed while soaking the glass slide in water between structuring and analysis. A large processing windows is exhibited by the formulation N19T6 with 20% macromer content and 0.1% PI concentration. Compared to

the formulation with 0.5%, the formulation with 0.1% exhibits a smaller processing window, but not as expected only in the region with lower energy density (power compared to speed), but especially in the regions with higher density. That suggests a higher sensibility towards radiation in formulations with lower PI concentrations. More investigations have to be done to further study this effect.

We can conclude that the PI concentration does make a difference on the degree of crosslinking and further on the swelling behavior of the formed hydrogel structures. Also we concluded that the formulation was very reactive towards 2PP and showed a very large processing window. If compared to the work from Li et al.,[95] formulations of N19 and T6 work with lower laser powers, lower macromer concentrations and lower PI concentrations while still exhibiting a larger processing window than PEGDA used by Li et al. What has to be stated here, is that the laser power in Li's paper was measured before passing the objective and in this work it was measured after passing the microscope. Thus a direct comparison of the results concerning the laser power has do be done with caution. Measuring the laser power after the objective has the advantage that the measurement is closer to the power effective in curing of the formulation.
To see if DTT would increase the reactivity of PVA-Norbornene formulations, also a processing window of PVA-Norbornene N19 and DTT was determined.

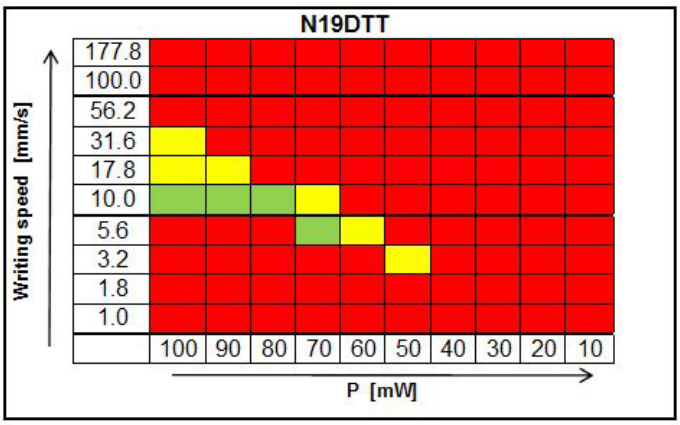

Figure G.6.73: Processing windows of mixture N19DTT with 20% macromer content and 0.5% PI concentration

As can be seen in Figure G.6.73, the processing window of N19DTT (with the same parameters as in the mixture N19T6) is much smaller. Maybe this is due to the selected hatch (5 µm) compared to the hatch Qin[94] used for hydrogels (0.1–0.5 µm). Hatch defines the horizontal distance between two polymer lines. Although a higher hatch is possible for more viscous solutions, as can be seen in mixtures N19T6, is seems that for mixtures with DTT the material is not stable enough with this high hatch. This explanation is corroborated by the fact that it was possible to create a more complex 3D structure with the above mentioned N19DTT mixture, although a hatch of 0.1 µm was used, to get finer structures (see Section 6.2.1).
Furthermore, PVA-Allyl has been tested for applicability in 2PP processes. The processing

windows of these mixtures will be discussed in the following.

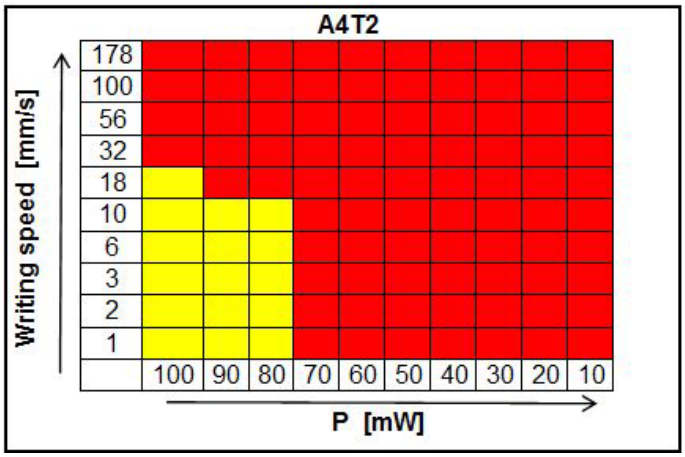

Figure G.6.74: Processing windows of mixture A4T2 with 10% macromer content and 0.5% PI concentration

Figure G.6.74 shows the processing window of the mixture A4T2 with 10% macromer content and 0.5% PI concentration. As can be seen no structures with adequate shape could be produced with these parameters. Mostly because the structures were destroyed due to evaporation of the solvent.

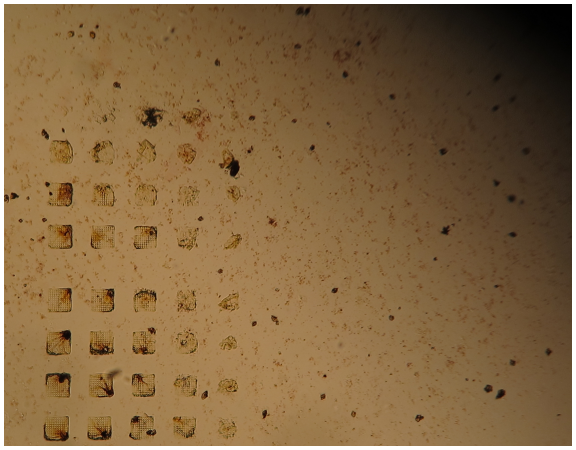

Figure G.6.75: Photo (through light microscope) of mixture A4T2 with 10% macromer content and 0.5% PI concentration

The destroyed structures from mixture A4T2 are displayed in Figure G.6.75.
To increase the reactivity of the PVA-Allyl mixtures DTT as low-molecular thiol cross-linker was used instead of PVA-Thiol. It was shown in section 4.3 that mixtures with DTT exhibited a multiple reactivity compared to those with PVA-Thiols. Additionally, the macromer content was increased to 20%, the PI concentration to 1% and the macromer was changed to PVA-Allyl A20 to achieve a higher reactivity and stability of the formed structures.

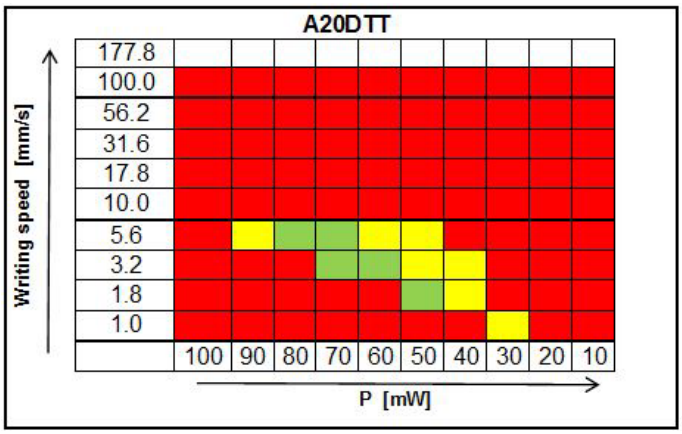

Figure G.6.76: Processing windows of mixture A20DTT with 20% macromer content and 1% PI concentration

Figure G.6.76 shows the processing window of A20DTT with 20% macromer content and 1% PI concentration. With increased reactivity of the formulation well shaped structures were finally possible, although with the drawback of a reduced quality of the structures in the area of high power with low writing speeds (high energy density). What has already been showed with mixture N19T6, applies also to PVA-Allyl: with increasing initiator concentration the regions with high energy density exhibited lower qualities of the structures.

Although this rather rough analysis of the applicability of PVA-Allyl for 2PP, we can conclude that the reactivity of PVA-Allyl is much smaller, than PVA-Norbornene. Further the use of small molecular cross-linkers like DTT can be used to increase reactivity, but not in any order. The main advantage of PVA-Allyl compared to PVA-Norbornene is the far lower cell toxicity, which is the reason for its possible application in biomedical applications like tissue engineering.

6.2.1 3D structures

As a proof of concept more complex structures have been structured with PVA-Norbornene in combination with DTT. A modell of a body centered cubic crystal structure was selected as structure, because it has dense spheres on thin connectors, which tests the stability of the formed hydrogels.

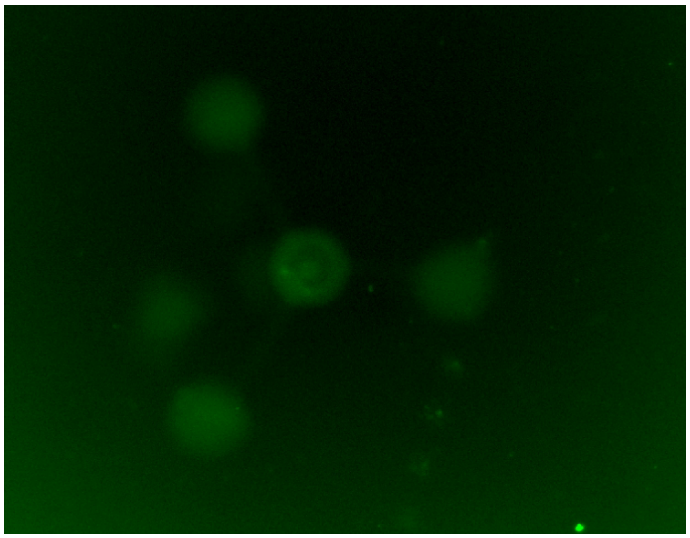

Figure G.6.77: Complex structure of a body centered cubic (bcc) crystal structure formed in a formulation of PVA-Norbornene N19 with DTT. Writing speed was 50 mm/s at a laser power of 50 mW

Figure G.6.77 shows an example of such a structure. It was produced in a mixture of PVA-Norbornene N19 with DTT with a macromer content of 20% and a PI concentration of 0.5%. E2CK-THEMA was used as PI, the writing speed of 50 mm/s with a laser power of 50 mW. Distance between to layers was 1 µm and the horizontal distance between two lines was 0.1 µm. Although the picture looks very noisy, the structuring worked very well, what can be seen in Figure G.6.78.

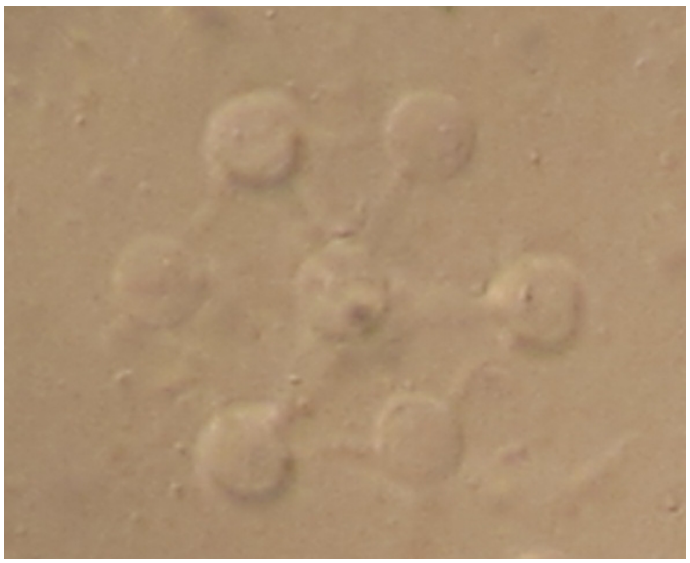

Figure G.6.78: Photo of the body centered cubic crystal structure formed in a formulation of PVA-Norbornene N19 with DTT.

In fact the PI is so easy to remove from this material that scanning with a LSM is almost impossible, because the formulation exhibits almost no fluorescence.

Experimental

1 Synthesis

1.1 Synthesis of ethylene glycoldiitaconate (1)

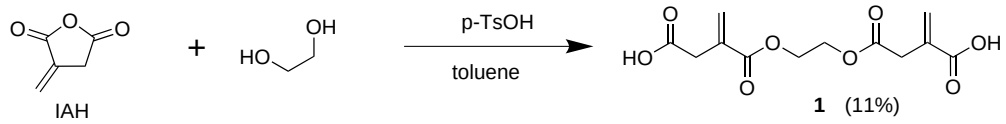

Chemical	M [g/mol]	eq. [ ]	n [mmol]	m [mg]	V [µL]
ethylenglycol	62.07	1.00	1.00	62.07	55.9
itaconic anhydride	112.08	2.25	2.25	252.18	
toluene	92.14	94.42	94.42	8700.00	10000.0
para-toluenesulfonic acid	172.20	0.25 wt%		0.63	

In a 50 mL single necked roundbottom flask with magnetic stirrer, ethylene glycol (1 mmol, 62 mg) was dissolved in 10 mL of dry toluene together with itaconic anhydride (2.25 eq., 2.25 mmol, 252 mg) and 0.25 wt% of p-TsOH (based on anhydride). The reaction was stirred under argon atmosphere at room temperature for 6 days. The reaction progress was monitored with GC-MS and TLC. After 6 days, no further conversion could be observed, so to the reaction mixture 5 mL of water were added and the mixture was extracted 3 times with about 5 mL ethylacetate each. The combined organic phases were washed with 10 mL water once and dried over anhydrous sodium sulfate. After evaporation of the solvent TLC showed still unreacted anhydride, so the product was hydrolysed with concentrated acetic acid until a pH of 2 was reached. Again 5 mL of water were added to the mixture which was extracted with ethylacetate (5 mL, 3 times), dried over sodium sulfate and the solvent was evaporated in vacuo. The solid product was dried further in fine vacuum yielding 33 mg (11% of theory) of **1** as a white solid.
As can be seen in the NMR, the product is the desired product as a mixture between the three possible regio-isomers.

^{1}H-NMR (DMSO-d_6): δ (ppm) =
12.52 (s, 2 H, HOOC-C=(CH_2)-CH_2-COO-CH_2),
6.13 (d, 2H, HOOC-C=(CH_2)-CH_2-COO-CH_2),
5.73 (d, 2H, HOOC-CH_2-C=(CH_2)-COO-CH_2),
4.20 (s, 2H -COO-CH_2-),
3.21 (s, 2H, HOOC-C=(CH_2)-CH_2-COO-CH_2)

^{13}C-NMR (DMSO-d_6): δ (ppm) =
171.97 and 167.22 (HOOC-C-C=(CH_2)-CH_2-COO-CH_2- and
HOOC-CH_2-C=(CH_2)-COO-CH_2-),

170.42 and 167.53 (HOOC-C-C=(CH_2)-CH_2-COO-CH_2- and
HOOC-CH_2-C=(CH_2)-COO-CH_2-),
135.49 and 134.58 (HOOC-CH_2-C=(CH_2)-COO-CH_2- and
HOOC-C-C=(CH_2)-CH_2-COO-CH_2-),
128.18 and 127.24 (HOOC-C-C=(-CH_2)-CH_2COO-CH_2-
and HOOC-CH_2C-=(CH_2)-COO-CH_2-),
62.06 (-COO-CH_2-),
37.47 and 36.88 (HOOC-CH_2-C=(CH_2)-COO-CH_2- and
HOOC-C-C=(CH_2)-CH_2-COO-CH_2-),

DC (PE:MeOH 1:1 + 2% HAc): R_f = 0.78
Fp (ethylacetate) = 123–128°C

1.2 Modification of PVA with allylsuccinic anhydride (PVA-Allyl)

1.2.1 Synthesis of allylsuccinic isopropylester (2)

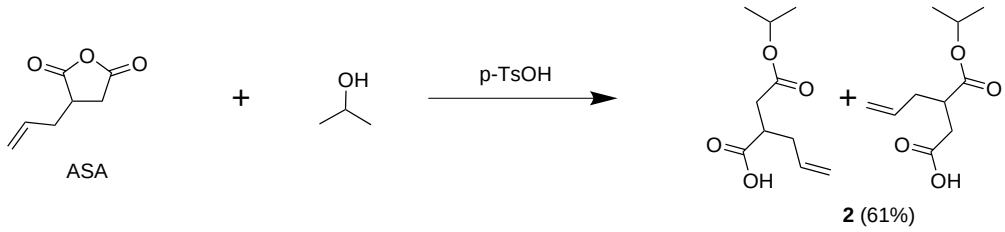

Chemical	M [g/mol]	eq. [ ]	n [mmol]	m [mg]	V [mL]
allyl succinic anhydride	140.14	1	4	560.56	
2-propanol	60.10	80	320	19232.00	25
para-toluenesulfonic acid	172.20	0.125 wt%		49.48	
pyrogallol	126.11	1000 ppm		0.56	

In a 25 mL single necked roundbottom flask equipped with reflux condenser and magnetic stirrer pyrogallol (0.56 mg, 1000 ppm based on anhydride) was added to 25 mL of 2-propanol. Subsequently, p-TsOH (49 mg, 0.25 wt% based on 2-propanol and anhydride) was added and upon solution allylsuccinic anhydride (4 mmol, 561 mg) was added dropwise. The mixture was heated to 60°C and held under argon atmosphere. The reaction progress was controlled via TLC. After 3 days no further reaction could be observed. The solvent was evaporated yielding 710 mg (88% of theory).
Since a TLC of the product showed impurities the product was purified via column chromatography (116 g silica gel, eluent $CHCl_3$ with 10% of ethylacetate and 1% acetic acid) yielding in 489 mg (61% of theory) of **2** as colourless oil.

^{1}H-NMR ($CDCl_3$): δ (ppm) =
11.19 (s, 1 H, HOOC-),
5.74 - 5.60 (m, 1 H, H_2C=CH-CH_2-),
5.07 - 4.94 (m, 3 H, H_2C=CH-CH_2- and $(CH_3)_2$-CH-O),
2.96 - 2.70 (m, 1 H, -OOC-CH-(CH_2-)-(CH_2-)-),
2.68 - 2.14 (m, 4 H, =CH-CH_2-CH- and -OOC-CH_2-CH-),
1.15 (d, 6 H, $(CH_3)_2$-CH-O)

^{13}C-NMR ($CDCl_3$): δ (ppm) =
180.55 and 178.39 (-CH_2-COOH and -CH-COOH),
173.60 and 171.38 (-CH_2-COO-CH- and -CH-COO-CH-),
134.33 and 134.21 (H_2C=CH-CH_2-CH-COOH and H_2C=CH-CH_2-CH-COO-),
118.21 and 118.05 (H_2C=CH-CH_2-CH-COOH and H_2C=CH-CH_2-CH-COO-),
68.31 and 68.13 (-CH-COO-CH-$(CH_3)_2$ and -CH_2-COO-CH-$(CH_3)_2$),
40.88 and 40.75 (HOOC-CH-CH_2- and -CH-OOC-CH-CH_2-,),
36.08 and 35.93 (-CH-CH_2-COOH and -CH-CH_2-COO-CH-),
35.30 and 35.00 (H_2C-CH-CH_2-CH-COOH and (H_2C-CH-CH_2-CH-COO-CH-),
21.79 and 21.77 ($(CH_3)_2$-CH-OOC-CH- and $(CH_3)_2$-CH-OOC-CH_2-)

DC ($CHCl_3$:EE 4:1 + 1% HAc): R_f = 0.54

n_D (20°C) = 1.4445

1.2.2 Synthesis of PVA-Allyls

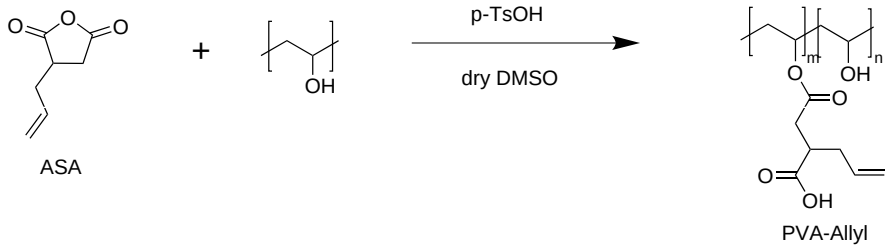

Compound	PVA [mg]	PVA [mmol]	ASA [mmol]	p-TsOH [mg]	Pyrogallol [mg]	DMSO [mL]	Yield [mg]	DS [%]
A2	220	0.01	0.2	0.60	0.028	21	268	2
A4	2200	0.100	2.0	6.20	0.280	150	2123	4
A20	2200	0.100	5.5	7.40	0.771	200	2449	20
A24	110	0.005	1.0	0.60	0.140	11	77	24
A32	220	0.010	2.0	1.30	0.280	21	129	32
A54	110	0.005	5.0	2.00	0.700	11	116	54

MW(PVA): 22000 g/mol

In a 250 mL three necked roundbottom flask with reflux condenser and magnetic stirrer PVA, p-TsOH (0.25 wt% based on anhydride and PVA) and pyrogallol (1000 ppm based on anhydride) were dissolved in dry DMSO while heating to 50°C. After about one hour all PVA had dissolved and allylsuccinic anhydride was added dropwise to the solution.

After complete addition of the anhydride, the reaction mixture was heated to 60°C and stirred for 3 days. The whole reaction was performed under argon atmosphere.
After 3 days the reaction mixture was allowed to reach room temperature and was transferred to a dialysing tube. It was dialysed against deionized water (7 water exchanges). After evaporation of the water from the dialysed solution on the rotary evaporator, the product was dried in fine vacuum.

To get water-soluble products about 1 g of the product was mixed with water (not completely dissolved) and again transferred into a dialysing tube. Now the pH in the outer dialysing vessel was adjusted with $NaHCO_3$ and Na_2CO_3 to a value between 8.0 and 9.0. After equilibrating over night, the outer solution was exchanged against deionized water (7 water exchanges) to get rid of excessive salts or bases. Again the dialysed solution was concentrated on the rotary evaporator, yielding the final product after drying in fine vacuum.

^{1}H-NMR (DMSO-d_6): δ (ppm) =
5.71 (pent, x H, CH_2-CH-CH_2-CH-),
5.05 (t, 2x H, CH_2-CH-CH_2-CH-),
4.66 and 4.46 and 4.22 (s each, 1-x, -CH_2-CH-(OH-)),
3.83 (s, 1 H, -CH_2-CH-(OH-)),
1.35 (bs, -CH_2-CH-(OH-))
x depends on degree of substitution, rest of the signals of allylsuccinic acid are overlapping with the polymer backbone's signal

IR (ATR) ν(cm^{-1}) = 3273, 2914, 1713, 1570, 1400, 1176, 1087, 915, 838, 645

1.3 Modification of PVA with norbornen anhydride (PVA-Norbornen)

1.3.1 Synthesis of norbornen isopropylester (3)

3 (26%)

Chemical	M [g/mol]	eq. [ ]	n [mmol]	m [mg]	V [mL]
cis-5-norbornene-*endo*-2,3-dicarboxylic anhydride	164.16	1	4	656.64	
2-propanol	60.10	80	320	19232.00	25
para-toluenesulfonic acid	172.20	0.125 wt%		24.86	
pyrogallol	126.11	1000 ppm		0.66	

In a 50 mL single necked roundbottom flask p-TsOH (0.125 wt% based on 2-propanol and anhydride) together with pyrogallol (1000 ppm based on amount of anhydride) was

dissolved in 25 mL (80 eq., 320 mmol) 2-propanol. Subsequently, 657 mg *cis*-5-norbornene-*endo*-2,3-dicarboxylic anhydride (4 mmol) were added in portions to the solution at room temperature. Afterwards the reaction mixture was stirred and heated to 50°C. The progress of the reaction was monitored with TLC and after 3 days, no more change could be observed. The reaction mixture was cooled to room temperature and afterwards the solvent was removed on the rotary evaporator yielding in 840 g (93% of theory) of crude, white solid. Since TLC showed impurities the product was purified with column chromatography (116 g silica gel, eluent $CHCl_3$ with 10% of ethylacetate and 1% of acetic acid) yielding in 240 mg (26% of theory) of **3** as white solid.

^{1}H-NMR ($CDCl_3$): δ (ppm) =
6.26 (m, 2 H, -CH-CH=CH-CH-),
4.92 (sept, 1 H, -O-CH-$(CH_3)_2$),
3.27 (t, 2 H, =CH-CH-CH-COO-),
3.16 (t, 2 H, =CH-CH-CH-COO-),
1.49 and 1.44 and 1.33 and 1.29 (2 H, HOOC-CH-CH_2-CH-COO-CH- and
-CH-OOC-CH-CH_2-CH-COOH),
1.17 (t, 6 H, -O-CH-$(CH_3)_2$)

^{13}C-NMR ($CDCl_3$): δ (ppm) =
178.96 (-CH_2-COOH),
171.84 (-CH_2-COO-CH-),
135.39 and 134.50 (-CH-CH=CH-CH-),
67.97 (-O-CH-$(CH_3)_2$),
48.81 and 48.15 (-CH-CH-CH=CH-CH-CH-),
48.78 (-CH-CH_2-CH-),
46.59 and 46.31 (-CH-CH-(COO-)-CH-CH-(COO-)-),
21.84 and 21.58 (-O-CH-$(CH_3)_2$)

DC ($CHCl_3$:EE 4:1 + 1% HAc): R_f = 0.50
Fp ($CHCl_3$) = 82–85°C

1.3.2 Synthesis of PVA Norb

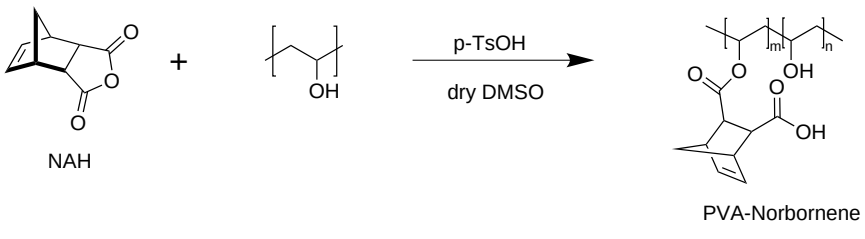

Compound	PVA [mg]	PVA [mmol]	anhydride [mmol]	p-TsOH [mg]	DMSO [mL]	Yield [mg]	Time [days]	DS [%]
N7	2640	0.12	4.8	4.0	55	837	1	7.5
N19	2200	0.10	22.5	5.5	55	3350	1	19.0
N23	2200	0.10	22.5	5.5	55	4126	2	23.0
N42	4400	0.20	50.0	16.0	110	8617	2	42.5

MW(PVA): 22000 g/mol, time refers to the reaction time of each preparation.

In a 250 mL three-necked roundbottom flask with magnetic stirrer, reflux condenser, PVA and p-TsOH (0.125 wt% based on PVA and anhydride) were dissolved in dry DMSO. For complete dissolution the mixture was heated while stirring to 50°C for about an hour. Meanwhile the *cis*-5-norbornene-*endo*-2,3-dicarboxylic anhydride was dissolved in about 10 mL of dry DMSO. After the PVA was dissolved completely, the anhydride solution was added dropwise to the reaction mixture, which was further on stirred at 50°C for a certain amount of time.

After letting the reaction mixture cool to room temperature, the mixture was transferred to a dialysis tube and dialysed against deionized water. The pH value of the solution in the outer dialysing vessel was adjusted to a range between 8.0 and 8.2, to readily yield the sodium salt of the products. The dialysis was carried out according to the standard dialysing protocol.

From the dialysed solution the water was evaporated on a rotary evaporator and the product was dried in fine vacuum. Afterwards the product was milled in the cryomill for better dissolving and easier handling.

^{1}H-NMR (D_2O): δ (ppm) =
6.22 (s, x H, -CH-CH=CH-CH-),
4.02 (s, 1H, -CH_2-CH-O-),
3.28 (s, x H, =CH-CH-(CH_2)-CH-),
3.09 (s, x H, =CH-CH-(CH_2)-CH-),
1.67 (bs, -CH_2-CH-(O-)-),
1.39 (s, x H, -CH-CH_2-CH-)
x depends on degree of substitution

IR (ATR) ν (cm^{-1}): 3319, 2937, 1712, 1563, 1400, 1183, 1073, 834

1.4 Modification of PVA with γ-Thiobutyrolactone (PVA-Thiol)

1.4.1 Synthesis of isopropyl 4-mercaptobutanoate (4)

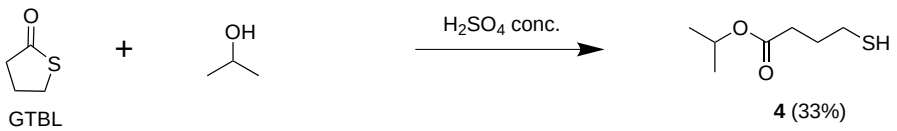

Chemical	M [g/mol]	eq. [ ]	n [mmol]	m [mg]	V [µL]
γ-thiobutyrolactone	102.16	1.0	4.00	409	346
2-propanol	60.10	65.0	260.00	15626	20033
sulfuric acid	98.08	0.6	0.57	56	103

In a single necked roundbottom flask with a reflux condenser, 15.6 g of 2-propanol (260 mmol, 65 eq.) were put, two drops of sulfuric acid were added, subsequently 409 mg (4 mmol) of γ-thiobutyrolactone were added dropwise. The apparatus was flushed with argon and heated to 90°C oilbath temperature. After 3 days of reaction, a GC-MS sample showed good conversion, so that the reaction mixture was cooled to room temperature over night, afterwards the reaction-mixture was cooled in an ice-sodiumchloride cooling bath and 0.3 g of sodiumbicarbonate were added in portions. Solid was filtered off and the solution was concentrated in vacuo resulting in 0.620 g (95% of theory) **4** as a slightly yellowish oil. The product was purified with column chromatography (petroleum ether with 10% THF) resulting in 0.219 g (33% of theory) of **4** as a slightly yellowish oil.

^{1}H-NMR ($CDCl_3$): δ (ppm) =
5.00 (sep, 1 H, $(CH_3)_2$-CH-O-)),
2.55 (qn, 2 H, -COO-CH_2-CH_2-CH_2-SH),
2.40 (t, 2 H, -COO-CH_2-CH_2-CH_2-SH)),
1.93 (p, 2 H, -COO-CH_2-CH_2-CH_2-SH)),
1.34 (t, 1 H, -COO-CH_2-CH_2-SH),
1.23 (d, 6 H, $(CH_3)_2$-CH-O-)

^{13}C-NMR ($CDCl_3$): δ (ppm) =
67.87 ($(CH_3)_2$-CH-O-),
33.18 (-COO-CH_2-CH_2-CH_2-SH),
29.29 (-COO-CH_2-CH_2-CH_2-SH),
24.18 (-COO-CH_2-CH_2-CH_2-SH),
21.96 ($(CH_3)_2$-CH-O-)

DC (PE:THF 10:1): $R_f = 0.69$
n_D (20°C) = 1.4660

1.4.2 Protocol for desiccating poly(vinyl alcohol)

15 g of PVA (MW: 22000 g/mol) were placed into a 250 mL roundbottom flask and heated in bulk on the oil bath to 95°C for 8 hours at vacuum of 0.03 mbar. The vacuum fluidises the solid very well and thus it can be stirred very well. This reduces the containing water from 5% to 3%. For further dehydration the PVA was stirred in dry DMSO until completely dissolved and then 10% of the solution was distilled of in fine vacuum. Solutions prepared in that way can be reduced to a water-content of 2%. All water-content analyses were done with Karl-Fisher like titration with a *C*A-21 moisture meter apparatus from

the company Envirotech, with original-packaged single-use syringes and cannulas. Where possible, argon atmosphere was used to prevent DMSO from absorbing humidity from the air.

1.4.3 Synthesis of PVA-Thiols

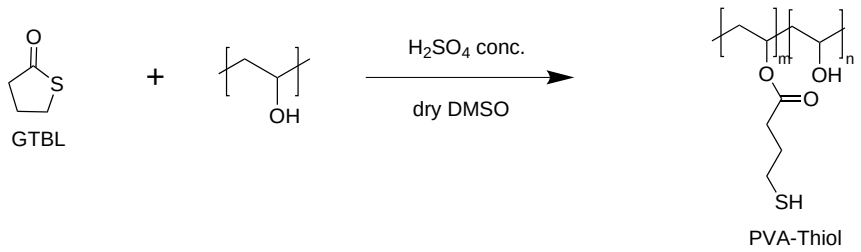

Compound	PVA [mg]	PVA [mmol]	GTBL [mmol]	H_2SO_4 conc. [mg]	H_2SO_4 [mmol]	DMSO [mL]	Yield [mg]	DS [%]
T1	2200	0.1	66.6	2800	28.55	150	1174	1.5
T2	2200	0.1	66.6	2800	28.55	150	2078	2.5
T6	2200	0.1	133.3	2800	28.55	150	2200	6.0

MW(PVA): 22000 g/mol

In a three-necked roundbottom flask with reflux condenser and magnetic stirrer, the PVA was dissolved in anhydrous DMSO at 60°C for about 30 minutes until no solid could be seen. Subsequently, concentrated sulphuric acid was added dropwise to the reaction mixture and further stirred for 10 minutes. Afterwards the γ-thiobutyrolactone (GTBL) was added dropwise and the reaction mixture was heated to 90°C for 3 days. Thereafter the reaction was cooled to room temperature. For purification the reaction mixture was dialysed after the standard dialysing protocol. Thereafter the solution was concentrated in vacuo. The result was in every case a slightly brownish solid that was milled to a fine powder in the cryomill for further handling.

^{1}H-NMR (D_2O): δ (ppm) =
4.24 and 3.98 and 3.62 (s,1 H, -CH_2-$\underline{CH}$-(O-)-),
2.77 (s, x H, -OOC-$\underline{CH_2}$-CH_2-CH_2-SH),
2.52 (t, x H, -OOC-CH_2-CH_2-$\underline{CH_2}$-SH),
2.18-1.36 (m, 2 H, -$\underline{CH_2}$-CH-(O-)-),
1.20 (t, x -OOC-CH_2-$\underline{CH_2}$-CH_2-SH)
x depends on degree of substitution

IR (ATR) ν(cm^{-1})= 3358, 2916, 1713, 1174, 1135, 1047, 641

1.5 Synthesis of E2CK (5)

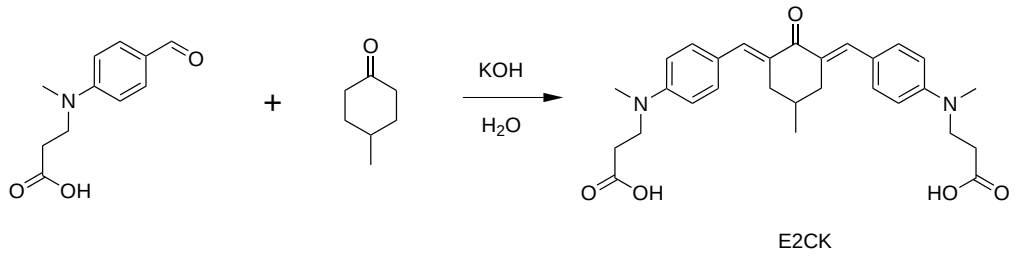

Chemical	M [g/mol]	eq. [ ]	n [mmol]	m [mg]
4-methylcyclohexane	112,17	1	4,2	471
3-((4-formylphenyl)(methyl)amino)propanoic acid	207,23	2	8,4	1741
sodium hydroxide	56,11	6	25,2	1414
water	18	110	462	8316

In a 50 mL single necked roundbottom flask with magnetic stirrer and reflux condenser, 4-methylcyclohexanone (4.2 mmol), 3-((4-formylphenyl)(methyl)amino)propanoic acid (2 eq., 8.4 mmol) and potassium hydroxide (6 eq., 25.2 mmol) were dissolved in 8.5 mL deionized water (110 eq., 462 mmol) and heated to 80°C. The reaction was performed under argon atmosphere. After 6 hours of reaction time, the reaction was cooled to room temperature. Since TLC showed incomplete reaction, the mixture was stirred further for 6 days at room temperature, afterwards the reaction was cooled in an ice bath, and 10 mL of methanol were added. Subsequently, 1 M HCl was added dropwise under vigorous stirring until a pH value of 5 was reached. The formed precipitate was separated by centrifugation, washed and dried, resulting in 1.75 g of a dark red solid.
Since NMR showed up to 19% of remaining aldehyde, the product was purified with column chromatography (eluent: chloroform with 3% of acetic acid) yielding 298 mg of perfectly clean product.
The purity was determined via HPLC and spiking with 3-((4-formylphenyl)(methyl)amino) propanoic acid, exhibiting a remaining impurity of 0.27%.

^{1}H-NMR (D_2O+NaOD): δ (ppm) =
7.43 (s, 2 H, -N-ArH-ArH-CH-C-),
7.07 (d, 4 H, -N-ArH-ArH-CH-C-),
6.37 (d, 4 H, -N-ArH-ArH-CH-C-),
3.34 (bs, 4 H, -OOC-CH_2-CH_2-N-(CH_3),
2.58 (s, 8 H, -OOC-CH_2-CH_2-N-(CH_3) and CH_3-CH-(CH_2-C-C=O)),
2.22 (t, 4 H, -OOC-CH_2-CH_2-N-(CH_3)),
1.44 (s, 1 H, CH_3-CH-(CH_2-C-C=O)),
0.85 (d, 3 H, CH_3-CH-(CH_2-C-C=O)),

^{13}C-NMR (D_2O+NaOD): δ (ppm) =

192.7 (-CH_2-C-C=O-C-CH_2-),
181.1 (-N-CH_2-CH_2-COO-),
149.6 (-CH-ArC-ArC-ArC-ArC-N-),
138.7 (-C=CH-ArC-),
133.2 (-C=CH-ArC-),
131.5 (-CH-ArC-ArC-ArC-ArC-N-),
123.5 (-CH-ArC-ArC-ArC-ArC-N-),
112.2 (-CH-ArC-ArC-ArC-ArC-N-),
49.3 (-N-CH_2-CH_2-COO-),
37.4 (-C-CH_2-CH-(CH_3)-CH-CH_2-C-),
34.4 (-N-CH_2-CH_2-COO-),
20.7 (-C-CH_2-CH-(CH_3)-CH-CH_2-C-)

DC($CHCl_3$+ 3% HAc): R_f = 0.31
E2CK was used as salt only for 2PP and therefore converted to two different salts:

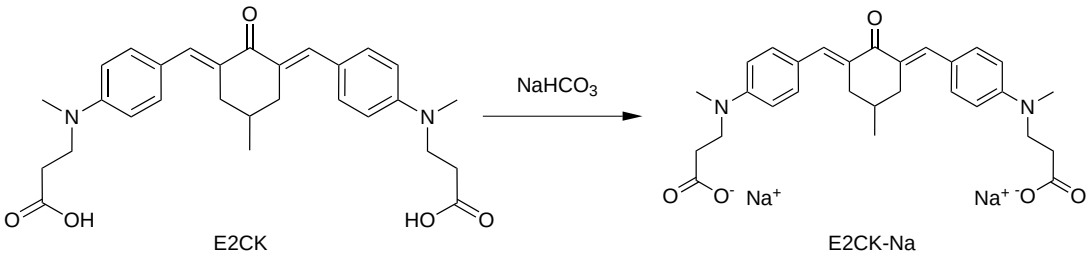

In a 10 mL three necked round bottom flask, 34 mg E2CK (0.07 mmol) were suspended in 3.6 mL of deionized water. With control of the pH value about 0.14 mmol of $NaHCO_3$ were added in portions until a pH of 7.0 was reached. The reaction was further stirred for 3 hours at room temperature and afterwards the water was removed in vacuum resulting in quantitative amounts of red crystals of E2CK disodium salt.

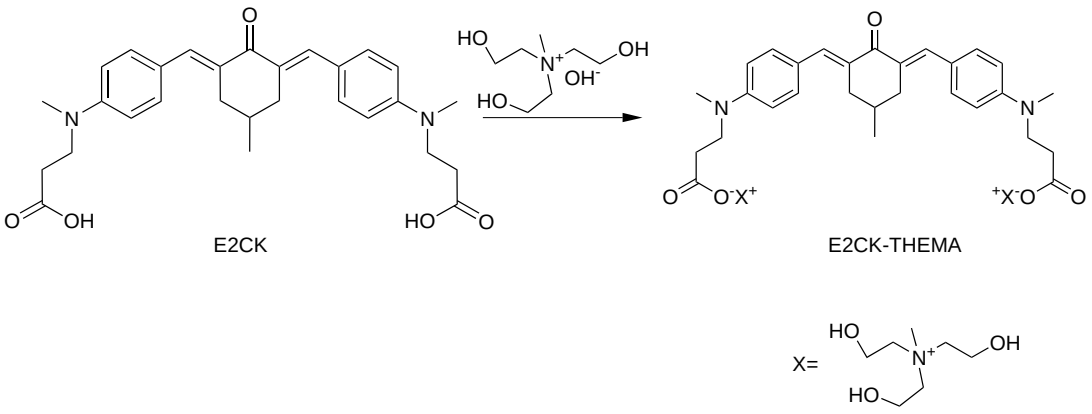

In a 25 mL three necked round bottom flask, 100 mg of E2CK (0.203 mmol) were suspended in 22 mL of deionized water. The flask was cooled with an ice bath and under pH control, about 0.406 mmol of tris(2-hydroxyethyl)methylammonium hydroxide were

added dropwise until a pH of 7.4 was reached. The reaction was allowed to reach room temperature and was stirred for further 2 hours. Afterwards, the solvent was removed on the rotary evaporator and the product was subsequently dried in fine vacuum, resulting in a highly viscous red liquid. It was stored for a week in a vacuum desiccator over phosphorus pentoxide and was still liquid.

1.6 Synthesis of P2CK (6)

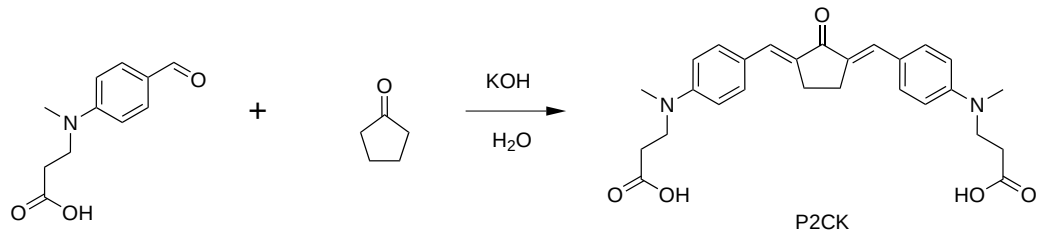

Chemical	M [g/mol]	eq. [ ]	n [mmol]	m [mg]
cyclopentanone	84.12	1	4.2	353
3-((4-formylphenyl)(methyl)amino)propanoic acid	207.23	2	8.4	1741
sodium hydroxide	56.11	6	25.2	1414
water	18.00	122	512.4	9223

In a 50 mL single necked roundbottom flask with magnetic stirrer and under argon atmosphere, cyclopentanone (4.2 mmol), 3-((4-formylphenyl)(methyl)amino)propanoic acid (2 eq., 8.4 mmol and potassium hydroxide (6 eq., 25.2 mmol) were dissolved in 9.2 mL of deionized water (122 eq., 512 mmol), and the reaction was heated to 80°C. After 6 hours of reaction time, the mixture was cooled to room temperature and stored under argon for 5 days. While vigorously stirring, the solution was acidified to a pH of 2 with 1 M HCl solution. The precipitate was separated by centrifugation and dried in vacuum, resulting in 1.93 g of dark red solid.
The purification was done by recrystallisation from 2-propanol, resulting in a red, crystalline product with 1.7% of remaining aldehyde according to HPLC analysis.

^{1}H-NMR (D_2O+NaOD): δ (ppm) =
7.15 (d, 4 H, -N-ArH-ArH-CH-C-),
6.89 (s, 2 H, -N-ArH-ArH-CH-C-),
6.34 (d, 4 H, -N-ArH-ArH-CH-C-),
3.27 (s, 4 H, -OOC-CH_2-CH_2-N-(CH_3)),
2.52 (s, 4 H, -OOC-CH_2-CH_2-N-(CH_3)),
2.43 (s, 6 H, -OOC-CH_2-CH_2-N-(CH_3)),
2.18 (s, 4 H, -CH_2-(C-C=O)),

^{13}C-NMR (D_2O+NaOD): δ (ppm) =
196.9 (-CH=C-C=O-C=CH-),

180.7 (-N-(CH_3)-CH_2-CH_2-COO-),
149.7 (-CH-ArC-ArC-ArC-ArC-N-),
135.0 (-CH=C-C=O-C=CH-),
133.3 (-CH=C-C=O-C=CH-),
132.7 (-CH-ArC-ArC-ArC-ArC-N-),
123.1 (-CH-ArC-ArC-ArC-ArC-N-),
111.9 (-CH-ArC-ArC-ArC-ArC-N-),
49.1 (-N-(CH_3)-CH_2-CH_2-COO-),
37.3 (-N-(CH_3)-CH_2-CH_2-COO-),
34.7 (-N-(CH_3)-CH_2-CH_2-COO-),
26.4 (=C-CH_2-CH_2-C=)

DC($CHCl_3$+ 5% HAc): R_f = 0.10

P2CK was used as salt only for 2PP and therefore converted to two different salts:

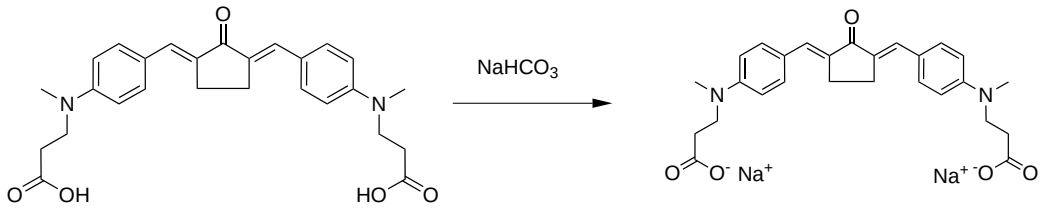

In a 25 mL three necked round bottom flask, 116 mg P2CK (0.25 mmol) were suspended in 10 mL of deionized water. With control of the pH value, about 0.5 mmol of $NaHCO_3$ were added in portions until a pH of 7.03 was reached. The reaction was stirred for further 3 hours at room temperature and afterwards the water was removed in vacuum, resulting in quantitative amounts of red crystals of P2CK disodium salt.

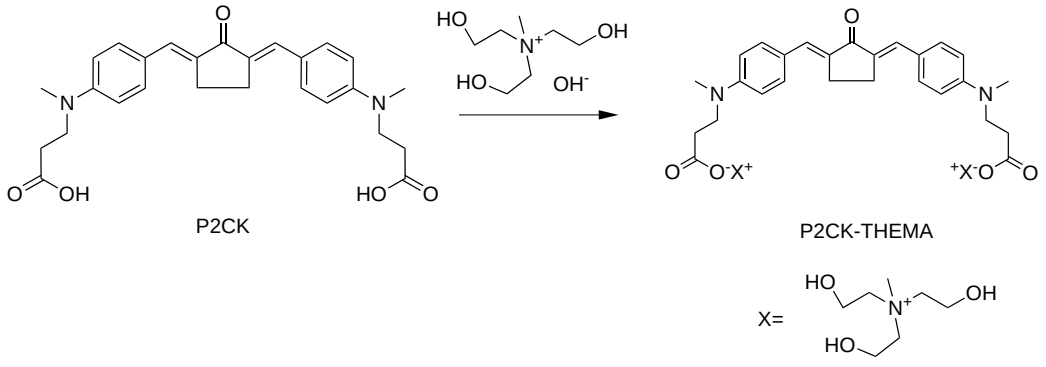

In a 25 mL three necked round bottom flask, 141 mg of P2CK (0.305 mmol) were suspended in 23 mL of deionized water. The flask was cooled with an ice bath and under pH control, about 0.61 mmol of tris(2-hydroxyethyl)methylammonium hydroxide were added dropwise until a pH value of 7.5 was reached. The reaction was allowed to reach room temperature

and was stirred for further 2 hours. Afterwards, the reaction mixture was frozen in liquid nitrogen and lyophylised over night. To remove further water, the product was stored in a vacuum dessicator over phosphorus pentoxide for a week, which removed a bit of water (gravimetrically determined), but the product was still liquid.

2 NMR Tube Experiments

2.1 Model reactions for thiol-ene polymerisation

To evaluate whether two substances undergo thiol-ene polymerisation, experiments in NMR-tubes were carried out. All preparations were done in a room blocked against radiation lower than 520 nm. The mixtures were prepared in deuterated NMR-solvents from Eurisotop in 5 mL brown glass tubes. When all components were dissolved, the solution was divided to three NMR tubes of which one was also from brown glass and two were normal (colourless) glass. The sample in the brown glass NMR tube was the blank sample, which never was irradiated with light of wavelengths that could initialize the PI. The two other samples were put into an UV-chamber INTELLI-RAY 600 from uvi tron international. The distance between sample and UV-lamp was 21 cm. Intensity and time of irradiation is stated with every experiment.
After the irradiation the NMR tubes were covered with aluminium foil until measurement at the NMR apparatus to prevent any further radiation. The analysis was done via integration of selected proton signals.

3 Toxicology tests

3.1 Method description

Murine fibroblast cells (adipocytes) from the cell line L929 were cultivated in Dulbecco's modified eagle medium (DMEM) with high glucose content (4.5 g/L) supplemented with 10% fetal bovine serum (FBS) and penicillin/streptomycin (100 IE/mL penicillin and 100 µg/mL streptomycin). The cells were provided from Professor Jürgen Stampfl from the Institute of Materials Science and Technology of the Technical University of Vienna. The medium was refreshed every second day and the cells were splitted with trypsin and EDTA once a week. The cell passage was 6 to 10.
For separation of cells and trypsin the cells were centrifuged and suspended in fresh medium. The cells were counted in a Neubauer chamber and afterwards seeded to a 96 well plate having 10 000 cells in each well.
The cells were left over night to attach to the wells and afterwards the medium was removed. The cells were stimulated with the prepared test-solutions at least in triplicate. After exactly 24 hours the medium including the samples to be tested was removed and Presto Blue in fresh medium (ratio 1:10) was added. After 30 minutes fluorescence were measured on BioTek Multiplate reader from Synergy.

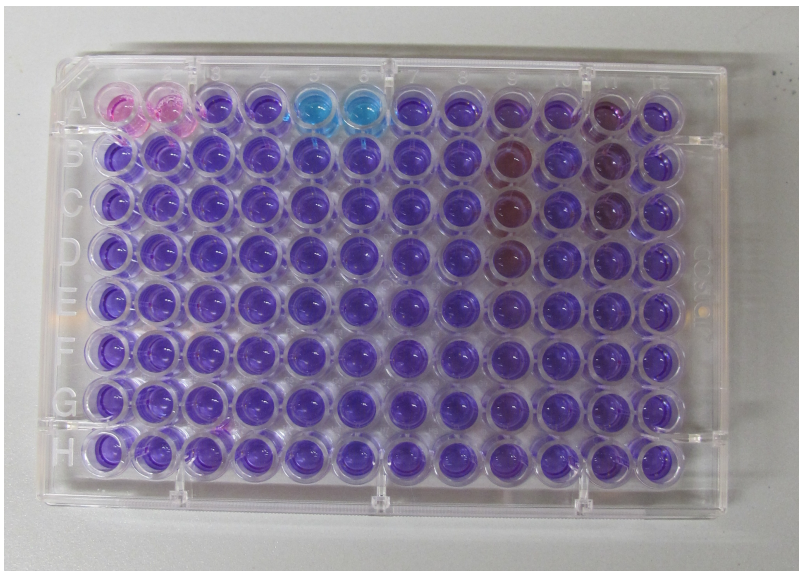

Figure E.3.1: Photo of a well plate with Presto Blue dye in it

Figure E.3.1 shows an example of such a well plate filled with PB after measuring the fluorescence. The test layout used is shown in Table E.3.1 and E.3.2.

Table E.3.1: Layout of first well plate

	1	2	3	4	5	6	7	8	9	10	11	12
A	Medium	Medium	Cells +PB	Cells + PB	Cells + DMSO	Cells + DMSO	N42 10%	N42 1%	T6 10%	T6 1%	T2 10%	T2 1%
B	N19 10%	N19 1%	N7 10%	N7 1%	T1 10%	T1 1 %	N42 10%	N42 1%	T6 10%	T6 0.1%	T2 10%	T2 0.1%
C	N19 10%	N19 1%	N7 10%	N7 1%	T1 10%	T1 1 %	N42 10%	N42 0.1%	T6 10%	T6 0.1%	T2 10%	T2 0.1%
D	N19 10%	N19 0.1%	N7 10%	N7 0.1%	T1 10%	T1 0.1%	N42 1%	N42 0.1%	T6 10%	T6 0.1%	T2 1%	T2 0.1%
E	N19 1%	N19 0.1%	N7 1%	N7 0.1%	T1 10%	T1 0.1%	N42 1%	N42 0.1%	T6 1%	T6 0.1%	T2 1%	T2 0.1%
F	N19 1%	N19 0.1%	N7 1%	N7 0.1%	T1 1%	T1 0.1%	N42 1%	N42 0.1%	T6 1%	T6 0.1%	T2 1%	T2 0.1%
G	N19 1%	N19 0.1%	N7 1%	N7 0.1%	T1 1%	T1 0.1%	N42 1%	N42 0.1%	T6 1%	T6 0.1%	T2 1%	T2 0.1%
H	N19 1%	N19 0.1%	N7 1%	N7 0.1%	T1 1%	T1 0.1%	N42 1%	N42 0.1%	T6 1%	T6 0.1%	T2 1%	T2 0.1%

Table E.3.2: Layout of second well plate

	1	2	3	4	5	6	7	8	9	10	11	12
A	A20 10%	A20 1%	A20 0.1%	A4 10%	A4 1%	A4 0.1%	N23 10%	N23 1%	N23 0.1%	-*)	-*)	-*)
B	A20 10%	A20 1%	A20 0.1%	A4 10%	A4 1%	A4 0.1%	N23 10%	N23 1%	N23 0.1%	-*)	-*)	-*)
C	A20 10%	A20 1%	A20 0.1%	A4 10%	A4 1%	A4 0.1%	N23 10%	N23 1%	N23 0.1%	-*)	-*)	-*)
D	A20 10%	A20 1%	A20 0.1%	A4 10%	A4 1%	A4 0.1%	N23 10%	N23 1%	N23 0.1%	-*)	-*)	-*)
E	A20 10%	A20 1%	A20 0.1%	-*)	A4 1%	A4 0.1%	-*)	N23 1%	N23 0.1%	-*)	-*)	-*)
F	-*)	A20 1%	A20 0.1%	-*)	A4 1%	A4 0.1%	-*)	N23 1%	N23 0.1%	-*)	-*)	-*)
G	-*)	A20 1%	A20 0.1%	-*)	A4 1%	A4 0.1%	-*)	N23 1%	N23 0.1%	-*)	-*)	-*)
H	Medium	Medium	Cells +PB	Cells + PB	Cells + DMSO	Cells + DMSO	-*)	N23 1%	N23 0.1%	-*)	-*)	-*)

*) where data are missing, this well was left empty

3.2 Sample preparation

The substances which have been analysed for toxicity were dissolved in DMEM without FBS in it. The PVA-Thiol samples (T1, T2 and T6) were heated in the medium at 60°C for several hours to yield clear solutions. In case of T6 this was not possible even after dilution to 7.2%, as the mixture was still cloudy. PVA-Allyl and PVA-Norbornene were dissolved at room temperature in the medium. Table E.3.3 lists the composition of the toxicology samples.

Table E.3.3: Mixtures for the analysis of the cell-toxicity of the PVA derivatives

Substance	**m [mg]**	**V(DMEM) [µL]**	**Conc [%]**
A4	51.1	459.9	10.0
A20	51.1	459.9	10.0
N7	50.5	455.0	10.0
N19	50.4	454.0	10.0
N23	53.0	477.1	10.0
N43	50.8	457.2	10.0
T1	59.9	549.0	9.8
T2	50.6	455.4	10.0
T6	50.2	651.8	7.2

3.3 Analysis data

Additional to the tested substances some cavities were filled with medium only, with cells and Presto Blue (positive control) or cells and DMSO (negative control). For comparison

and analysis the number of cells were averaged and normalised to the amount of cells in the positive check well. The original results are listed in Table E.3.4.

Table E.3.4: Measured intensities of fluorescence from the toxicity test

Substance	**Conc [%]**	**I well 1**	**I well 2**	**I well 3**	**I well 4**	**I well 5**	**I well 6**	**I well 7**
medium	0.0%	0	1	2	2	- *)	- *)	- *)
positive control	0.0%	732	838	720	776	- *)	- *)	- *)
negative control	0.0%	212	210	230	226	- *)	- *)	- *)
A4	10.0%	486	617	599	654	- *)	- *)	- *)
A4	1.0%	610	717	760	631	677	707	617
A4	0.1%	519	620	606	641	597	553	566
A20	10.0%	238	264	260	258	- *)	- *)	- *)
A20	1.0%	771	653	769	689	829	710	488
A20	0.1%	597	628	610	520	485	548	529
N7	10.0%	165	167	168	- *)	- *)	- *)	- *)
N7	1.0%	953	805	955	895	1080	867	- *)
N7	0.1%	723	645	617	536	659	- *)	- *)
N19	10.0%	399	257	236	- *)	- *)	- *)	- *)
N19	1.0%	417	720	697	668	985	630	- *)
N19	0.1%	654	719	780	848	477	- *)	- *)
N23	10.0%	199	193	190	192	- *)	- *)	- *)
N23	1.0%	899	824	751	786	861	751	469
N23	0.1%	597	653	906	763	723	675	683
N43	10.0%	174	179	179	- *)	- *)	- *)	- *)
N43	1.0%	669	631	587	509	557	471	614
N43	0.1%	633	574	631	682	712	608	- *)
T1	9.8%	212	486	513	408	- *)	- *)	- *)
T1	1.0%	563	712	701	614	900	544	- *)
T1	0.1%	679	721	731	723	424	- *)	- *)
T2	10.0%	426	391	353	- *)	- *)	- *)	- *)
T2	1.0%	504	679	536	403	485	667	- *)
T2	0.1%	563	460	520	615	402	464	464
T6	7.20%	274	450	453	371	- *)	- *)	- *)
T6	1%	785	473	495	571	503	- *)	- *)
T6	0.1%	512	460	532	602	557	563	541

*) where data are missing, analysis was done only in triplicate
I is fluorescence intensity [a.u.]

Table E.3.4 shows the fluorescence intensity according to well and substance that have been analysed.

4 Rheology Measurements

4.1 Parameter of measurement

As mentioned before all rheology measurements involving irradiation of the sample were carried out on an Anton-Paar Modular Compact Rheometer MCR 302 WESP. A plate-to-plate measuring system with 25 mm diameter was used for all analysis with a gap size of 50 µm. The measurements were done in oscillation mode with a shear rate of 10 Hz and a strain of 10% at a constant temperature of 25°C. Light intensity was measured directly on the top of the glass slide with a USB2000+ radiometer from Oceanoptics. The intensity was measured in the very centre and in distance of 0.6 cm and 1.25 cm from the centre, at 0°, 90°, 180° and 270°. The intensities are listed below in Table E.4.5

Table E.4.5: Measured light intensity depending on position on the glass plate of the rheometer

Position	**angle [°]**	**distance from center [cm]**	**intensity [mW·cm^{-2}]**
Center	0	0.00	11
1	0	0.60	8
2	90	0.60	8
3	180	0.60	8
4	270	0.60	9
5	0	1.25	7
6	90	1.25	6
7	180	1.25	8
8	270	1.25	7

The first 60 seconds of each measurement were done without UV irradiation and after this timespan the UV light was turned on automatically via triggering of the rheometer. Datapoints were collected after each 3 seconds.
The light output intensity was set to 1.45 W/cm^2 on the Omnicure system, which was calibrated with a Omnicure R2000 radiometer prior to usage.

4.2 Determination of optimal thiol to ene ratio

All samples for determining the optimal (for reactivity) thiol to ene ratio were mixtures between dithiothreitol (DTT), PVA-Thiol T2 (DS 2%) respectively and PVA-Allyl A20 (DS: 20%). The formulations were made in 10 wt% macromer (including DTT) concentration (based on the whole formulation) in deionized water. The photoinitiator IG 2959 was used in a final concentration of 0.5 wt% based on the whole formulation. In Table E.4.6, the used amounts of DTT and PVA-Allyl A20 are listed according to the thiol to ene ratio.

Table E.4.6: Mixtures for evaluation for the optimal thiol to ene ratio with A20 and DTT

Sample	Thiol-Ene Ratio [%]	m(DTT) [mg]	m(A20) [mg]
A20DTT-20	20	0.63	15.39
A20DTT-40	40	1.19	14.81
A20DTT-60	60	1.73	14.28
A20DTT-80	80	2.25	13.76
A20DTT-100	100	2.72	13.33
A20DTT-120	120	3.09	12.89

DTT and A20 were separately dissolved in a solution of IG2959. Upon complete dissolution, the two solutions were mixed together while being cooled on an ice-bath.
With the PVA-Thiol T2, things were more difficult because a stock solution from T2 had to be made prior to usage.

Table E.4.7: Mixtures for evaluation for the optimal thiol to ene ratio with A20 and T2

Sample	Thiol-Ene Ratio [%]	m(T2) [mg]	m(A20) [mg]
A20T2-20	20	14.8	15.2
A20T2-40	40	19.8	10.2
A20T2-60	60	22.4	7.7

The samples were stored on the ice-bath until measurement. For the measurement 60 µL were put on the rheometer plate and measured with the standard parameters mentioned in Section 4.1.

4.3 Influence of the PI concentration

To analyse the influence of the photoinitiator concentration of the photorheological properties, mixtures of PVA-Allyl A20 and PVA-Thiol T6 were prepared with PI-concentrations from 0.1 to 0.92 wt% of IG 2959 (based on the whole formulation). The value of 0.92 wt% is due to the maximum solubility of IG 2959, which in water amounts to 1.5 wt% at 20°C. Since the PVA-Thiol is only soluble in water if heated for several hours to 60°C, PVA-Thiol was dissolved in pure water to form a 20 wt% stock solution. To finally yield 300 mg (wt/wt %) of the analysed solutions, only 184.88 µL of solution were left for dissolving the PVA-Allyl and the PI IG2959, which resulted in the unusual value.
At first stock solutions of the photoinitiator IG 2959 in water where prepared, as shown in Table E.4.8.

Table E.4.8: PI stock solutions of IG2959 in water

$c(PI_{final})$[1] [%]	c(PI-conc) [%]	$c(PI\text{-}Sol_{higher})$[2] [%]	$V(PI\text{-}Sol_{higher})$[3] [µL]	$V(H_2O)$ [µL]
0,92%	1,50%	- [4]	0	500
0,50%	0,81%	1,50%	272	228
0,25%	0,41%	0,81%	250	250
0,10%	0,16%	0,41%	200	300

[1] $ci(PI_{final})$ is the final PI concentration in the ready-to-use sample for rheometer measurements
[2] $c(PI\text{-}Sol_{higher})$ is the concentration of the preceding higher concentrated stock solution used for the preparation of this solution
[3] $V(PI\text{-}Sol_{higher})$ is the volume of the preceding higher concentrated stock solution used for the preparation of this solution
[4] For the 1.5% solution the PI was directly dissolved in water.

With this stock solutions mixtures of PVA-Allyl A20 and PVA-Thiol T6 were prepared with a macromer concentration of 10 wt% in water, which are listed in detail in Table E.4.9.

Table E.4.9: Mixtures for evaluation of the influence from PI concentration

Mixture	m(A20) [mg]	m(T6) [mg]	V(T6) [µL]	V(Init.) [µL]	Conc. of Init-Sol. [%]	Final PI conc. [%]
PI-A20T6-M10-0.1	12.95	17.02	85.1	185	0.16%	0.10%
PI-A20T6-M10-0.25	12.96	17.02	85.1	185	0.41%	0.25%
PI-A20T6-M10-0.5	13.05	17.02	85.1	185	0.81%	0.50%
PI-A20T6-M10-0.92	13.03	17.02	85.1	185	1.50%	0.92%

Init. refers to the PI stocksolution of IG 2959

For the measurement 60 µL were put on the rheometer plate and measured with the standard parameters mentioned in Section 4.1.

4.4 Influence of the macromer concentration

For analysing the influence of macromer concentration on the photorheological behavior the mixtures were prepared from stock solutions. From PVA-Allyl T6, a 20% stock solution was prepared in deionized water, which was only possible when heating it to 60°C for several hours. PVA-Allyl A20 and PVA-Norbornene N19 were also used as stock solutions of 20% concentration in deionized water. The PI IG 2959 was prepared as 1.5% solution in deionized water. Table E.4.10 shows the mixtures of PVA-Allyl A20 and PVA-Thiol T6 with content and concentrations.

Table E.4.10: Mixtures of A20 and T6 for the evaluation of the influence of the macromer concentration

Mixture	m(A20) [mg]	V(A20) [µL]	m(T6) [mg]	V(T6) [µL]	V(Init.) [µL]	$V(H_2O)$ [µL]
M-A20T6-3%	3.89	19.47	5.11	25.5	100.0	146.0
M-A20T6-5%	6.49	32.44	8.51	42.6	100.0	110.0
M-A20T6-10%	12.98	64.88	17.02	85.1	100.0	20.0
M-A20T6-15%	19.49	- *)	25.53	127.7	100.0	27.3

*) Mixture A20T6-15% was not prepared from a A20 stock solution, instead A20 was directly dissolved in the initiator solution.
Init. refers to the PI stocksolution of IG 2959

Table E.4.11: Mixtures of N19 and T6 for the evaluation of the influence of the macromer concentration

Mixture	m(N19) [mg]	V(N19) [µL]	m(T6) [mg]	V(T6) [µL]	V(Init.) [µL]	V(H_2O) [µL]
M-N19T6-3%	3.90	19.52	5.10	25.5	100.0	146.00
M-N19T6-5%	6.51	32.54	8.49	42.5	100.0	110.00
M-N19T6-10%	13.02	65.08	16.98	84.9	100.0	20.00
M-N19T6-15%	19.53	- *)	25.48	127.4	100.0	27.60

*) Mixture N19T6-15% was not prepared from a N19 stock solution, instead N19 was directly dissolved in the initiator solution. Init. refers to the PI stocksolution of IG 2959

4.5 Storage stability

The storage stability of selected PVA derivative mixtures was analysed using their viscosity as indicator for premature gelation. For this purpose, solutions with 0 ppm, 100 ppm and 1000 ppm of pyrogallol (based on the whole formulation) were prepared. PVA-Allyl A4, PVA-Norbornene N7 and PVA-Thiol T2 were chosen for this mixtures. All mixtures had a macromer-content of 10% in water.
The viscosity was measured immediately after preparation, after one day, one week and finally after one month.
The PVA-Thiol was used as 20 wt% solution in deionized water, which had to be stored in an oven at 60°C for about 6 hours until fully dissolved. The needed PVA-Norbornene and PVA-Allyl amounts were weighed in brown glass vials and stock solutions of pyrogallol or water in the case of 0 ppm, respectively were added. The mixtures were mechanically stirred with a thin glass capillary (on one side closed) until they formed a clear solution. Afterwards the PVA-Thiol solution was added and again the solution was stirred with a capillary. Detailed information about the used compounds and amounts is given in Tables E.4.12 and E.4.13.

Table E.4.12: Composition of the storage stability samples with PVA-Allyl A4 and PVA-Thiol T6 with different amounts of pyrogallol as inhibitor

Mixture	m(A4) [mg]	m(T6) [mg]	V(T6) [µL]	V(Pyr-Sol.) [µL]	V(H_2O) [µL]
SS-A4T6-0	39.39	15.63	93.8	20	146.6
SS-A4T6-100	39.38	15.63	93.8	20	146.6
SS-A4T6-1000	39.41	15.63	93.8	20	146.6

Table E.4.13: Composition of the storage stability samples with PVA-Norbornene N7 and PVA-Thiol T6 with different amounts of pyrogallol as inhibitor

Mixture	m(N7) [mg]	m(T6) [mg]	V(T6) [µL]	V(Pyr-Sol.) [µL]	V(H_2O) [µL]
SS-N7T6-0	33.01	22.02	110.1	20	136.7
SS-N7T6-100	32.96	22.02	110.1	20	136.7
SS-N7T6-1000	32.97	22.02	110.1	20	136.7

Table E.4.14 lists the used inhibitor stock solutions.

Table E.4.14: Inhibitor stock solutions of pyrogallol in water

Inhibitor	**m(Pyrogallol) [mg]**	**V(H_2O) [µL]**
100 ppm	6.27	2083.73
1000 ppm	29.77	962.33

For determining the viscosity 60 µL of a solution were put on the rheometer plate and measured in rotation mode with a constant shear rate of 100 s^{-1}. Measuring points were recorded every 10 s. The measuring was done with a cone-to-plate measuring system with 25 mm diameter (CP-25), with a gapsize of 50 µm at a constant temperatute of 20°C. Each solution was measured 3 times and the mean was calculated from the results. The results of the viscosity measurements are listed in tabular form in Table E.4.15.

Table E.4.15: Averaged values of the viscosity measured of the storage stability samples

Sample	**η(0d) [Pa·s]**	**η(1d) [Pa·s]**	**η(7d) [Pa·s]**	**η(30d) [Pa·s]**
SS-A4T6-0	0.0152	0.0190	0.0201	0.1352
SS-A4T6-100	0.0148	0.0178	0.0168	0.0159
SS-A4T6-1000	0.0156	0.0172	0.0183	0.0782
SS-N7T6-0	0.0131	0.0143	0.0144	0.0142
SS-N7T6-100	0.0133	0.0135	0.0132	0.0129
SS-N7T6-1000	0.0130	0.0136	0.0127	0.0122

5 Swellability

5.1 Sample preparation for swellability analysis

In a micro centrifugation tube, PVA-Norbornene was dissolved in 33.3 µL of an aqueous solution (1.5%) of the PI IG2959 and additional water, depending on the composition. The solid was mixed with a thin and on the lower part closed glass-capillary until completely dissolved. Stirring with a magnetic stirrer and ultrasound bath won't succeed here. Subsequently a solution of PVA-Thiol in water was added and again mixed with a glass-capillary.

Table E.5.16: Mixtures of PVA-Norbornene N7 and PVA-Thiol T6 for analysing the influence of the macromer concentration concerning the swellability

Sample	**m(N7) [mg]**	**m(T6) [mg]**	**V(T6-solution 20%) [µL]**	**V(H_2O) [µL]**
SW-N7T6-M3	1.80	1.20	6.00	58.90
SW-N7T6-M5	3.00	2.00	10.00	53.70
SW-N7T6-M10	6.00	4.00	20.00	40.70
SW-N7T6-M15	8.99	6.01	30.00	27.60

Table E.5.16 lists the mixtures that were used for determining the swellability behavior of PVA-Norbornen N7 and PVA-Thiol T6 based on different macromer concentrations.
The total amount of each solutions from Table E.5.16 was 100 mg, they all had a final PI concentration of 0.5% (based on the whole formulation) and were irradiated for 1600 s. From the mixture SW-N7T6-M3, no pellet could be formed even after 1600 s of irradiation. The mixtures for analysing the swelling behavior depending on different DS and substances are listed in Table E.5.17.

Table E.5.17: Mixtures of A20, A4, N19 together with T2 and T6 for analysing the swellability with 10% macromer content

Sample	**m(A20) [mg]**	**m(T6) [mg]**	**V(T6-solution 20%) [µL]**	**V(H_2O) [µL]**
SW-A20T6-M10	4.27	5.67	28.4	38.3
Sample	**m(A4) [mg]**	**m(T6) [mg]**	**V(T6-solution 20%) [µL]**	**V(H_2O) [µL]**
SW-A4T6-M10	7.13	2.84	14.2	52.5
Sample	**m(A4) [mg]**	**m(T2) [mg]**	**V(T2-solution 20%) [µL]**	**V(H_2O) [µL]**
SW-A4T2-M10	5.36	4.70	23.5	43.2
Sample	**m(N19) [mg]**	**m(T6) [mg]**	**V(T6-solution 20%) [µL]**	**V(H_2O) [µL]**
SW-N19T6-M10	4.38	5.66	28.3	38.4
Sample	**m(N7) [mg]**	**m(T6) [mg]**	**V(T6-solution 20%) [µL]**	**V(H_2O) [µL]**
SW-N7T6-M10	6.00	4.00	20.00	40.70

The total amount of each solution from Table E.5.17 was 100 mg, they all had a final PI concentration of 0.5% (based on the whole formulation) and were irradiated for 800s. All solutions had a macromer concentration of 10% based on the whole formulation and PVA-Allyl and PVA-Norbornene was in 33.3 µL PI-solution.

Beside the mentioned combinations in Table E.5.17 also the mixtures N7T2, N19T2 and A20T2 were prepared with a macromer-concentration of 10% but they did not dissolve completely which prevented formation of pellets.
To form the pellets a mold made from poly(dimethylsiloxane) (PDMS) with cylindrical cavities of 6 mm diameter and 1 mm in height was used, as shown in Figure E.5.2.

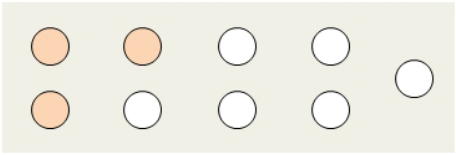

Figure E.5.2: Scheme of the used PDMS mold for production of the swellability pellets, partially filled with samples

As is shown in Figure E.5.3 the mold was put between two microscope cover glass slides to cover the samples on both sides of the mold.

Figure E.5.3: PDMS mold between two cover glass slides

Three of the cavities were filled by 25 µL of the prepared solutions. Afterwards the mold was put on a crystallising dish filled with crushed ice and transferred together with the crystallising dish to the UV chamber.
The samples were irradiated at 100% intensity in a distance of 14 cm (from the lamp) for a certain amount of time as shown in Figure E.5.4.

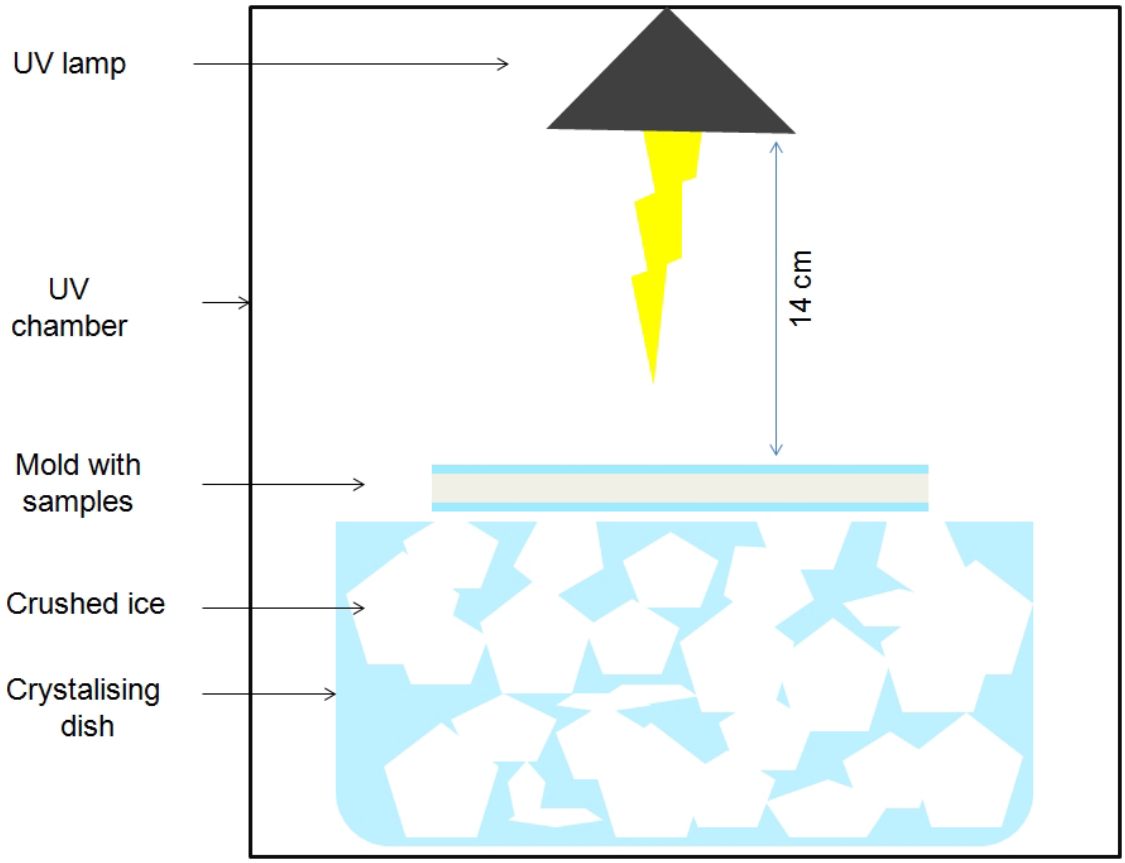

Figure E.5.4: Scheme of the used setup for producing the swellability samples

After this time the mold was taken out and put into a beaker with deionized water for about 10 minutes.
To remove the formed pellets from the mold, one of the glass plates was removed very gently with a scalpel. The formed pellets were transferred to a microcentrifugation tube with exactly 1 mL of deionized water in it. They were allowed to swell in water for 3 days. After the swelling time the supernatant water was removed and adhered water was removed with a towel. The samples were weighed and afterwards every sample was put into another microcentrifugation tube, where three holes were punched out of the cover lid. Just enough water was added to completely submerse the sample.
For freeze-drying the samples were frozen at -90°C in liquid nitrogen–acetone slurry for about one minute and then put into a round bottom flask to connect them to the lyophylisation apparatus. Water was removed over night with the lyophylisator, and the samples were weighed again.

5.2 Analysis of the samples

From the weights before (w_{wet}) and after drying (w_{dry}) the weight of the pellet itself and the weight of the absorbed water was determined. All analysis were done in triplicate and are displayed with standard deviation. The mass ratio of swelling was calculated according

to the following formula.

$$R_{sw} = \frac{m_{wet} - m_{dry}}{m_{dry}}$$

Tables E.5.18 and E.5.19 list the original measured values and averaged values that were used to calculate the mass swellability ratio from the samples N7T6 with macromer concentrations between 5 and 15%.

Table E.5.18: Dry– and wet–weights together with the mass swelling ratio of the N7T6 samples with different macromer content

Sample	$\mathbf{m_{wet}}$ **[mg]**	$\mathbf{m_{dry}}$ **[mg]**	$\mathbf{R_{sw}}$ **[ ]**
SW-N7T6-M5-1	77.95	0.23	337.91
SW-N7T6-M5-2	60.66	0.37	162.95
SW-N7T6-M5-3	95.65	0.44	216.39
SW-N7T6-M10-1	85.05	1.23	68.15
SW-N7T6-M10-2	117.77	1.75	66.30
SW-N7T6-M10-3	121.55	1.9	62.97
SW-N7T6-M10-4	116.37	1.72	66.66
SW-N7T6-M15-1	119.30	2.88	40.42
SW-N7T6-M15-2	113.19	2.86	38.58
SW-N7T6-M15-3	100.81	2.39	41.18

Table E.5.19: Averaged values of R_{sw} with standard deviation of the N7T6 samples with different macromer content

Sample	**averaged** $\mathbf{R_{sw}}$ **[ ]**	**SD of** $\mathbf{R_{sw}}$ **[ ]**
SW-N7T6-M5	239	90
SW-N7T6-M10	66	2
SW-N7T6-M15	40	1

Values were rounded to one digit before the comma

Tables E.5.20 and E.5.21 list the original measured values and averaged values that were used to calculate the mass swell ratio from the samples with different DS and different substances.

Table E.5.20: Dry– and wet–weights together with the mass swelling ratio of the samples with 10% macromer content

Sample	$\mathbf{m_{wet}}$ **[mg]**	$\mathbf{m_{dry}}$ **[mg]**	$\mathbf{R_{sw}}$ **[ ]**
SW-A4T2-M10-1	166.89	1.11	149.35
SW-A4T2-M10-2	206.57	1.26	162.94
SW-A4T2-M10-3	140.53	0.88	158.69
SW-A4T2-M10-4	194.79	1.11	174.49
SW-A4T6-M10-1	213.69	0.87	244.62
SW-A4T6-M10-2	196.26	0.87	224.59
SW-A4T6-M10-3	157.14	0.49	319.69
SW-A20T6-M10-1	192.22	1.41	135.33
SW-A20T6-M10-2	227.91	1.40	161.79
SW-A20T6-M10-3	152.80	1.19	127.40
SW-A20T6-M10-4	138.05	0.83	165.33
SW-N7T6-M10-1	103.34	1.91	53.10
SW-N7T6-M10-2	119.81	1.99	59.21
SW-N7T6-M10-3	120.69	1.83	64.95
SW-N7T6-M10-4	87.36	1.18	73.03
SW-N19T6-M10-1	93.26	0.89	103.79
SW-N19T6-M10-2	188.51	1.69	110.54
SW-N19T6-M10-3	34.38	0.45	75.40
SW-N19T6-M10-4	178.58	1.65	107.23

Table E.5.21: Averaged values of R_{sw} with standard deviation

Sample	**averaged** $\mathbf{R_{sw}}$ **[ ]**	**SD of** $\mathbf{R_{sw}}$ **[ ]**
SW-A4T2-M10	161	10
SW-A4T6-M10	263	50
SW-A20T6-M10	147	19
SW-N7T6-M10	63	8
SW-N19T6-M10	99	16

Values were rounded to one digit before the comma

6 Two-Photon Polymerisation

6.1 Sample preparation

Microscope cover slides were modified with covalently bond thiol groups to allow the covalently binding of the hydrogels to the glass surface. The protocol was adapted from the product information of 3-(trimethoxysilyl)propyl methacrylate[99] as well as from Goss's paper.[98] For cleaning of the slides, they were submersed for 10 minutes in piranha solution (concentrated sulfuric acid and hydrogen peroxide (30%) in a ratio of 5:1). Afterwards the glass slides were washed with water and subsequently with ethanol. The slides were dried by holding them in a nitrogen stream. The thiolation mixture was prepared right before usage and consisted of 1 mL (3-mercaptopropyl)trimethoxysilane in 200 mL of ethanol and 6 mL of dilute acetic acid (1:10 glacial acetic acid-water). For the modification the slides were submersed in the thiolation mixture for 30 minutes. Afterwards excessive solution was poured off and the slides were rinsed with ethanol and put in a 100°C oven over night. For the preparation of the sample holder the modified glass slides were mounted on a microscope glass with adhesive tape as a spacer.
A stripe of UV-resistant adhesive tape from the company Tesa was adhered to both long edges of a microscope slide, so that there was about 1 cm space between the two tape stripes. On this tape a microscope cover slip was fixed again with two stripes of the adhesive tape.

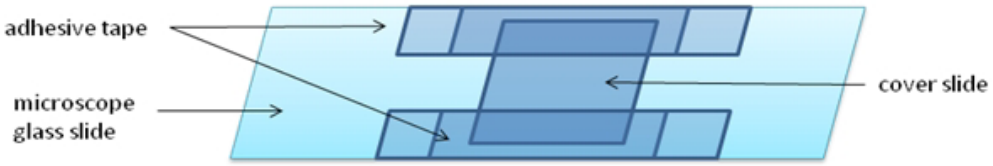

Figure E.6.5: Microscope slide ready for sample uptake: top view

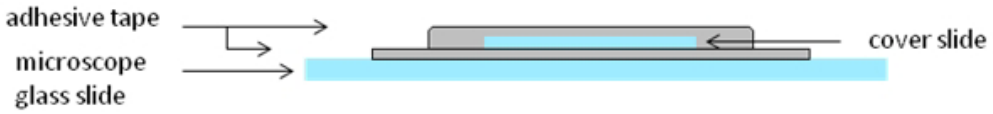

Figure E.6.6: Microscope slide ready for sample uptake: side view

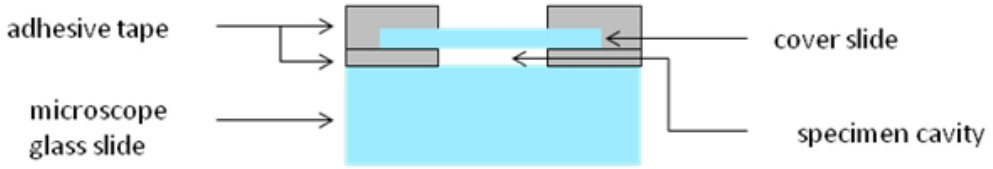

Figure E.6.7: Microscope slide ready for sample uptake: front view

The result was a microscope slide with a hollow part were the liquid formulation was transferred to via capillary action. This slide is outlined in Figures E.6.5, E.6.6 and E.6.7.

After the formulation was loaded, the two open ends were also closed with tape and so the device was ready for structuring.

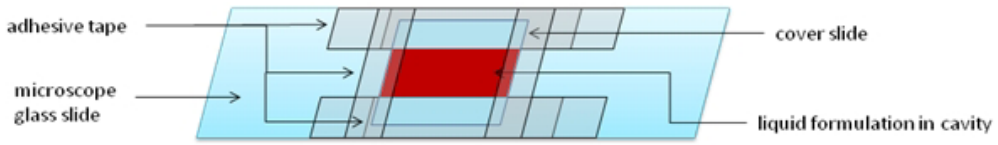

Figure E.6.8: Microscope slide with injected sample: top view

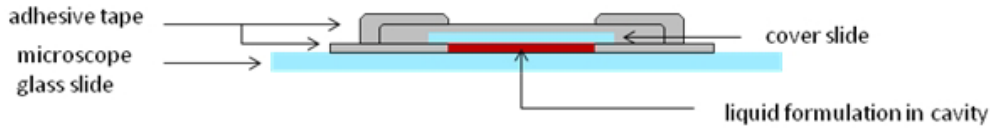

Figure E.6.9: Microscope slide with injected sample: side view

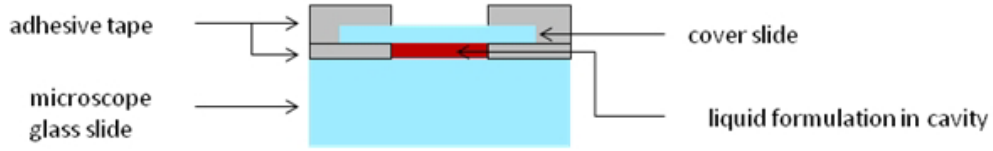

Figure E.6.10: Microscope slide with injected sample: front view

Figures E.6.8, E.6.9 and E.6.10 show the microscope slide from all views with the loaded sample, ready for structuring.
The following tables show the content of the mixtures, used for 2PP.

Table E.6.22: Composition of mixtures used for 2PP containing PVA-Allyl A4

Mixture	**m(A4) [mg]**	**V(A4) [µL]**	**m(T2) [mg]**	**V(T2) [µL]**	**c(T2-sol) [%]**	**V(PI-sol) [µL]**	**c(PI-sol) [%]**	**V(Pyr-sol) [µL]**	**c(Pyr-sol) [%]**	**V(H_2O) [µL]**
2PP-A4T2	5.3	26.5	4.7	23.5	20	25	2	6.67	0.15	8.3
Mixture	**m(A4) [mg]**	**V(A4) [µL]**	**m(DTT) [mg]**	**V(DTT) [µL]**	**c(DTT-sol) [%]**	**V(PI-sol) [µL]**	**c(PI-sol) [%]**	**V(Pyr-sol) [µL]**	**c(Pyr-sol) [%]**	**V(H_2O) [µL]**
2PP-A4DTT	9.64	48.2	0.35	7.1	5	10	5	10	0.1	14.7

PI-Conc: 0.5%, macromere concentration: 10%, Pyr-sol = pyrogallol stock solution
c(A4 stock solution): 20%

For the following mixtures were all prepared with a pyrogallol stock solution (Pyr-sol) with a concentration of 0.15%, as PI E2CK-THEMA was always used.

Table E.6.23: Composition of mixtures used for 2PP containing PVA-Norbornene N19 with 0.5% PI concentration

Mixture	**m(N19) [mg]**	**V(N19) [µL]**	**m(T6) [mg]**	**V(T6) [µL]**	**V(PI) [µL]**	**V(Pyr-sol) [µL]**	**V(H_2O) [µL]**
2PP-N19T6	8.65	-	11.32	56.6	6.7	6.7	10.1
Mixture	**m(N19) [mg]**	**V(N19) [µL]**	**m(T6) [mg]**	**V(T6) [µL]**	**V(PI) [µL]**	**V(Pyr-sol) [µL]**	**V(H_2O) [µL]**
2PP-N19T6	8.66	-	11.32	56.6	6.7	6.7	10.1
Mixture	**m(N19) [mg]**	**V(N19) [µL]**	**m(DTT) [mg]**	**V(DTT) [µL]**	**V(PI) [µL]**	**V(Pyr-sol) [µL]**	**V(H_2O) [µL]**
2PP-N19DTT	17.82	-	2.16	10.8	6.7	6.7	55.9

PI-Conc: 0.5%, macromere concentration: 20%, Pyr-sol = pyrogallol stock solution
c(N19 stock solution): 20%, c(T6 stock solution): 20%, c(DTT stock solution): 20%, c(PI stock solution): 7.5%

Table E.6.24: Composition of mixtures used for 2PP containing PVA-Allyl A20 and DTT with macromere content of 20% and 1% PI concentration

Mixture	**m(A20) [mg]**	**V(A20) [µL]**	**m(DTT) [mg]**	**V(DTT) [µL]**	**V(PI) [µL]**	**V(Pyr-sol) [µL]**	**V(H_2O) [µL]**
2PP-A20DTT	17.88	-	2.16	10.8	10	6.67	52.5

PI-Conc: 1.0%, macromere concentration: 20%, Pyr-sol = pyrogallol stock solution
c(A20 stock solution): 20%, c(DTT stock solution): 20%, c(PI stock solution): 10%

Table E.6.25: Composition of mixtures used for 2PP containing PVA-Norbornene N19 and PVA-Thiol T6 with macromere content of 20% and 0.1% PI concentration

Mixture	**m(N19) [mg]**	**V(N19) [µL]**	**m(T6) [mg]**	**V(T6) [µL]**	**V(PI) [µL]**	**V(Pyr-sol) [µL]**	**V(H_2O) [µL]**
2PP-N19T6	8.67	-	11.32	56.6	10	6.67	6.7

PI-Conc: 0.1%, macromere concentration: 20%, Pyr-sol = pyrogallol stock solution
c(N19 stock solution): 20%, c(T6 stock solution): 20%, c(PI stock solution): 1%

6.2 Structuring

For the structuring the loaded sample was put in the specimen holder and moved until the focal point of the objective was in formulation. This was possible due to the fluorescence of the initiator, when it was irradiated by the laser. Afterwards the slide was adjusted in x, y and z axis until a proper area for structuring was found. The parameter for the structuring (laser power, writing speed, structure that should be produced, distances to the adjacent structures, height of a structured line) were configured with the software. After the setup was done the structuring was carried out and could be monitored with use of a CCD camera.

After structuring the microscope glass was analysed with a light microscope. To analyse the sample with a laser scanning microscope (LSM), remaining PI had to be washed away prior to analysis. For this purpose the two last added adhesive tape stripes were removed (opening of the cavity to the surrounding solution) and microscope slide with cover slide was submersed in water. After the initiator was removed completely the structures were analysed with an LSM.

Summary

The aim of this work was the development of novel, low toxic PVA derivatives that can be photopolymerised via thiol-ene chemistry. The cross-linking should be carried out via two photon polymerisation (2PP). Thus PVA was successfully modified with allylsuccinic anhydride, *cis*-5-norbornene-*endo*-2,3-dicarboxylic anhydride and γ-thiobutyrolactone yielding in macromers with different degrees of substitution based on amount of reagent and reaction time.

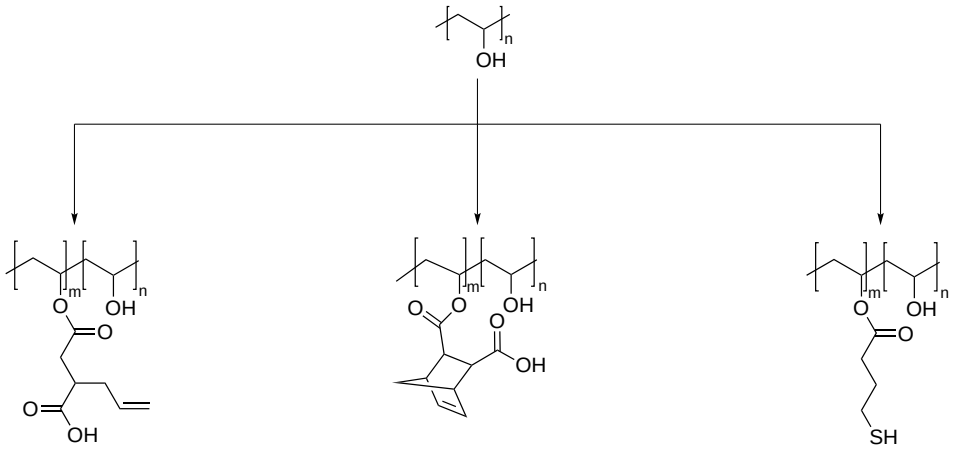

Toxicity of the synthesised PVA derivatives was tested with murine fibroblastic cells. It showed that the toxicity of PVA-Norbornene and PVA-Allyl was strongly dependent on the concentration and exhibited almost no toxicity if used in 1% solution or below. PVA-Thiols showed less dependency on the macromer concentration and also exhibited a low toxicity at 1% and below. In concentrations of 10% PVA-Norbornene was almost as cell-toxic as DMSO, PVA-Allyl with a DS of 4% showed the least toxicity of all tested derivatives.

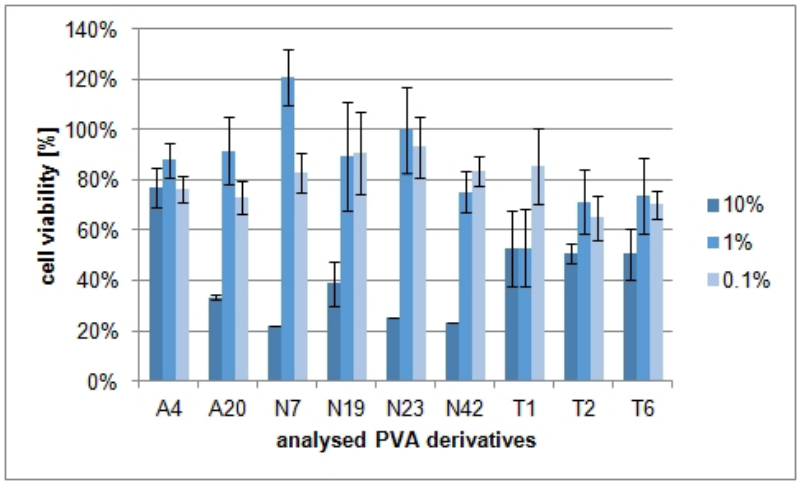

Figure S.1.1: Results from the cell-toxicity analysis of the PVA derivatives with different macromer concentrations

The mechanical properties of the cross-linked hydrogels were analysed based on their thiol

to ene ratio, their macromer content and the photoinitiator (PI) concentration in the formulation. It showed that a thiol to ene ratio of 0.6:1 gave the best results concerning reactivity and cross-linking density, therefore all further studies have been performed with this ratio. The influence of the macromer concentration in the formulation showed that the difference between the low-molecular cross-linker dithiothreitol and the high-molecular cross-linker PVA-Thiol is enormous. For the analysis the maximum storage modulus G', the slope in the linear region of the increase of G', the time until 95% of max. value G' is reached and finally the delay of initiation were determined.

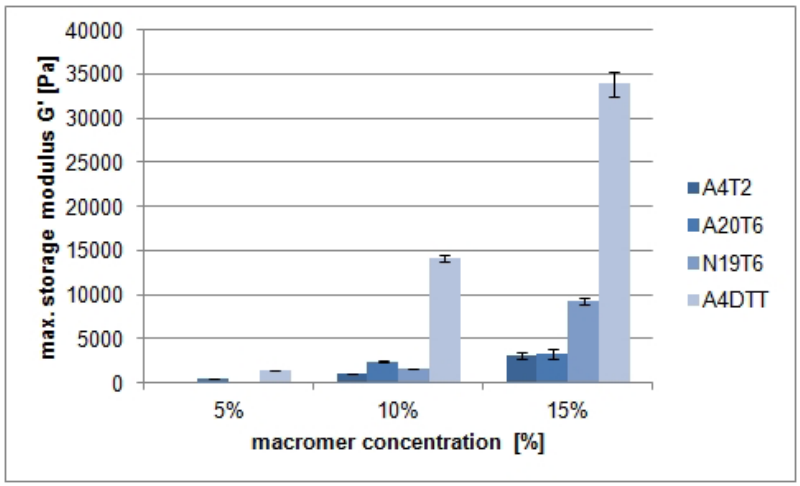

Figure S.1.2: Maximum storage modulus G' of the analysed mixtures with different macromer concentrations

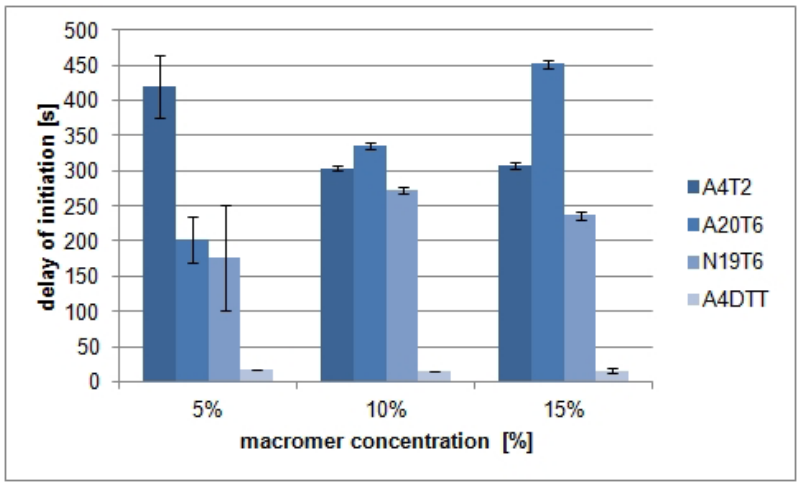

Figure S.1.3: The delay of initiation of the analysed mixtures with different macromer concentrations

Up to 290-fold higher reactivity was achieved with mixtures of PVA-Allyl in combination with DTT compared to mixtures containing PVA-Allyl and PVA-Thiol. This vast difference is mostly because of decreased mobility of the high-molecular thiol cross-linker. PVA-Norbornene showed in general a higher reactivity than PVA-Allyl, which was already predicted by Hoyle et al.[38]

The storage stability of the formulation was analysed with different concentrations of pyrogallol as inhibitor of premature gelation. It showed that the storage stability of the analysed PVA derivative formulations was sufficient over 30 days if stored with 100 ppm or pyrogallol.
Also the swelling behaviour of selected formulations was studied. It showed that the mass swell ratio increased strongly with decreasing macromer content. Although the cross-linking density of mixtures with high DS is almost doubled compared to those with a low DS, no significant difference could be observed. This is most probably due to a higher number of carboxylate groups in the case of the PVA-Allyl macromer with the high DS, which makes the polymer more hydrophilic and leads to higher swellability of those hydrogels. This dependency of the mass swell ratio from the DS could not be observed with PVA-Norbornen. In their case swellability increased with a higher DS, in contrast to what we expected. Further studies to swelling behaviour of these compounds have to be done in the future.

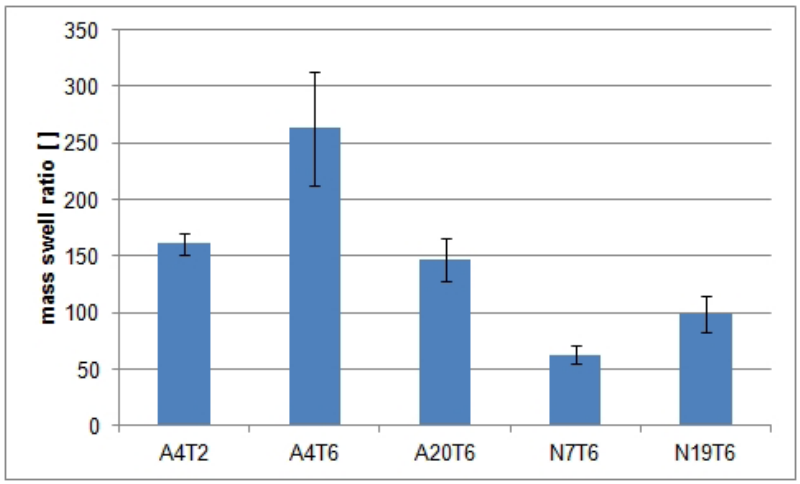

Figure S.1.4: Mass swell ratios of different PVA-Allyl, PVA-Norbornene and PVA-Thiol mixtures

Currently we can conclude that the formed pellets can absorb up to the 250-fold amount of water of their own weight and their swelling behaviour is strongly dependent on the macromer concentration used for pellet-forming.
The applicability of the synthesised PVA derivatives for 2PP was tested and showed that PVA-Norbornene exhibited a large processing window, in which writing speed and laser power can be adjusted while still getting well shaped structures.

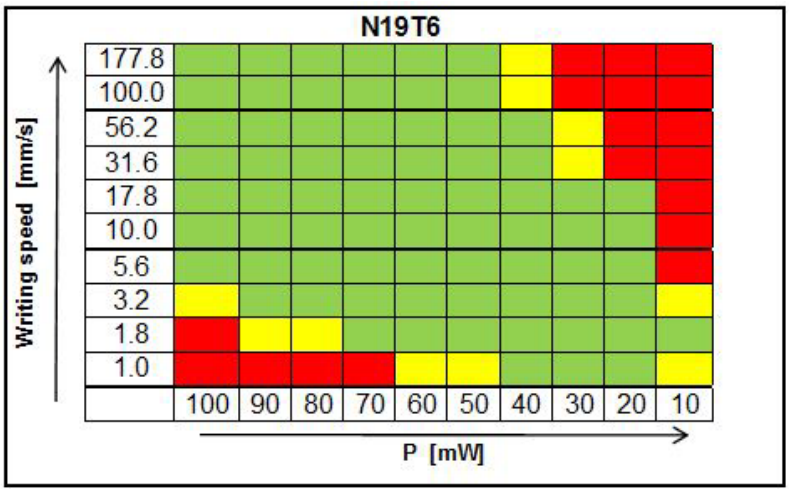

Figure S.1.5: Processing windows of mixture N19T6 with 20% macromer content and 0.5% PI concentration

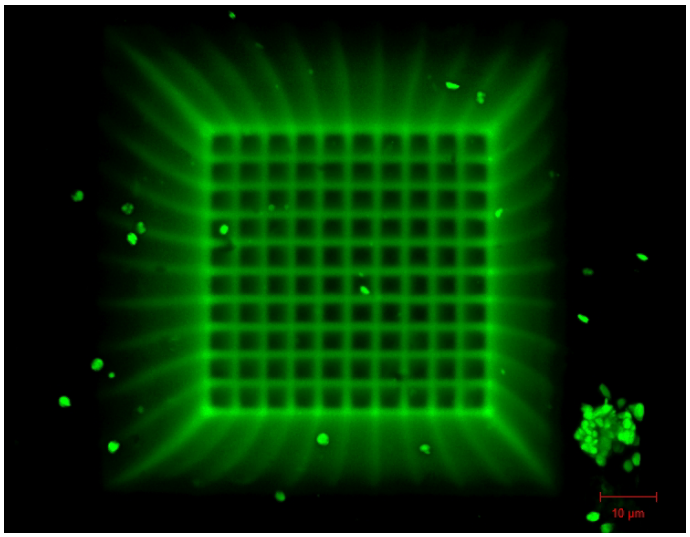

Figure S.1.6: LSM 3D model of partly swollen PVA-Norbornen/PVA-Thiol hydrogel structured via 2PP. The structure broadens with increasing distance from the glass slide, it was polymerised to, due to easier entering of the solvent

Also we showed that the processing window of the developed PVA derivatives is dependent on the PI concentration, which decreases the processing window with decreasing concentration of the PI. Like already estimated from the photorheology results, the reactivity of PVA-Allyl was far less than PVA-Norbornen. Interestingly DTT did not increase the reactivity of PVA-Allyl formulations used in 2PP the way it did with formulations used in one photon polymerisation.
PVA-Norbornene and PVA-Thiol showed excellent reactivity and are potential candidates for being used in biomedical applications.
Experiments concerning the reactivity of norbornene modified PVA with the exo isomer should be carried out in the future, because the endo isomer could be less reactive due to steric effects. Concerning the toxicology studies tests should be done with PVA-Thiol and Presto Blue without cells, to see if the proposed reduction of Presto Blue by the

thiol groups happens without metabolising. Also tests with encapsulating cells and cell-viability tests on cross-linked hydrogels have to be carried out in future. The storage stability should be observed for a longer period of time also in combination with different initiators. Finally, based on the obtained values from swellability determination, the molecular weight between cross-links M_c should be calculated using Flory-Huggins theory. These M_c values can be compared to the M_c values obtained from photorheological measurements using statistical rubber elasticity theory.

Material and Methods

If not otherwise mentioned, all commercially available reagents and solvents were used without further purification. Borontrifluoride-etherate, ethylene glycol, sodiumbicarbonate and PVA (22000 g/mol) were purchased from Merck. Anhydrous DMSO, (3-mercaptopropyl)-trimethoxysilane, γ-thiobutyrolactone, itaconic anhydride, and *cis*-5-norbornene-*endo*-2,3-dicarboxylic anhydride were purchased from Sigma-Aldrich. Itaconic acid, para-toluenesulfonic acid, cyclopentanone and acetic acid were purchased from Fluka. Sodium carbonate was purchased from Acros. Chloroform was purchased from Brenntag. Toluene, tetrahydrofurane, ethyl acetate and 2-propanol were purchased from Donauchem. Allylsuccinic anhydride was purchased from TCI Chemicals Europe. 4-Methylcycloxehanone was purchased from SAFC. Deuterated solvents were purchased from Eurisotop and deuterated sodium hydroxide was purchased from Dr. Glaser AG Basel.
All solvents (except anhydrous DMSO) were distilled prior to usage.

Chromatographical methods

Thin-layer-chromatography was done on aluminium TLC-plates from Merck (Silicagel 60, F254). Column-Chromatography was carried out on a B°chi Sepacore Flash System (Buechi pump module C-605, Buechi control unit C-620, Buechi UV-Photometer C-635, Buechi fraction collector C-660). Glass and polyethylene columns were used, packed with Silicagel 60 (Merck, 40-64 μm). The used eluents are mentioned at the purification section of each substance.

NMR

NMR spectra were recorded on a Bruker DPX-200 Fourier transform spectrometer at 200 MHz for ^{1}H and 50 MHz for ^{13}C. The signals are noted according to their shifts in comparison to trimethylsilane (δ= 0 ppm) and were always referenced on the used NMR-solvent (^{1}H: $CDCl_3$: 7.26 ppm, D_2O: 4.79 ppm, DMSO-d_6: 2.50 ppm,
^{13}C: $CDCl_3$: 77.16 ppm, DMSO-d_6: 39.52 ppm, CD_3OD: 49.00 ppm
The chemical shifts were reported in ppm (s = singlet, d = doublet, t = triplet, q = quartet, qn = quintet, sep = septet, m = multiplet, bs = broad singlet). Analysis of the spectra was carried out with the program TopSpin (Version 2.1) from Bruker.

Cryomill

For grinding the substances to fine powders (increase of solubility and simplification of handling), a Retsch Cryomill was used. The precooling-time at 5 Hz was set to automatic, so that the apparatus determinates the necessary cooling time itself. The precooling was followed by three mill-cycles of two minutes with 25 Hz, with intermediate cooling of 30 seconds at 5 Hz. After the milling process the grinding beaker was put into a 60 °C oven for 2 hours (PVA-Thiol and PVA-Allyl) or rewarmed to room temperature over night

(PVA-Norbornene). This was necessary to prevent condensation of humidity on the inner parts of the grinding beaker, which would have resulted in a gluelike product.

Rheology

Photorheology data were recorded on an Anton-Paar Modular Compact Rheometer MCR 302 WESP. As lightsource, a OmniCure 2000 from EXFO with high pressure mercury lamp was used in combination with a two-headed lightguide. The lamp was triggered by the rheometer and therefore a constant radiation time could be achieved. The Omnicure 2000 lightsource was calibrated with an R2000 radiometer from EXFO.
The light intensity was measured directly on the glas plate with an Ocean Optics USB2000+ radiometer. The results of this measurement are listed in Section 4.1. All measurements were carried out at a constant temperature of 25°C and in plate–to–plate mode with a 25 mm diameter steel plate measuring system (PP25 measuring system). To assure reproducibility the planarity of the glass plate was checked before each measurement series, at least once a day. The exact parameters are described at every experiment.

Viscosity of the samples (for storage stability experiments) was measured on an Anton-Paar Modular Compact Rheometer MCR 300. All measurements were carried out at a constant temperature of 20°C and in cone–to–plate mode with a 25 mm diameter steel cone (CP25 measuring system). Since the plate could not be exchanged in this setup, no planarity check was performed for this system.

Two-Photon Structuring

For the two-photon-polymerisation (2PP) structuring experiments the 2PP-apparatus "Lexi" from the Institute of Materials Science and Technology of the Vienna Technical University was used.

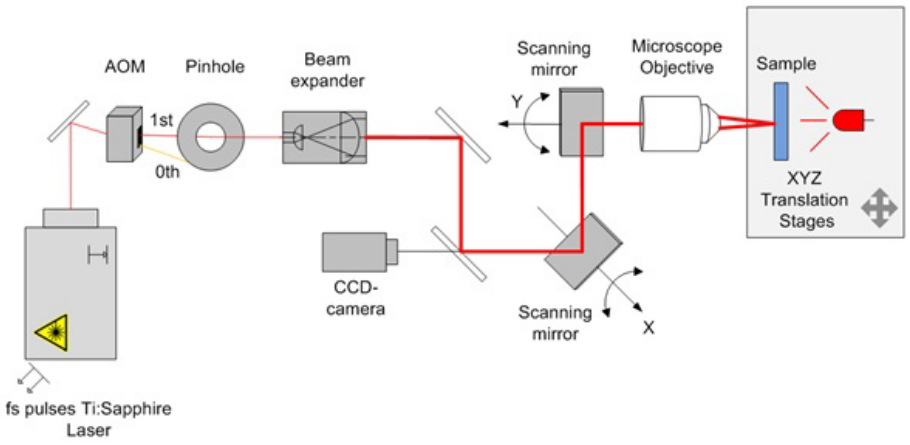

Figure M.1.1: Setup of the 2PP-apparatus Lexi

In the setup, the laser beam passed through an acustic optical modulator (AOM) leaving

the first order of diffraction for the structuring. The beam could be switched and controlled in its intensity by applying waves of different amplitudes inside the crystal. A pinhole blocked the other beam orders from further propagation in the setup. Leaving the pinhole, the beam was expanded six times of its initial 1.8 mm diameter. The galvanoscanner deflected the beam before focusing it with a microscope objective. To create 3D polymeric structures, the rotating mirrors of the galvanoscanner traced the focal point inside the formulation. A clamp carried the formulation container and was mounted to a linear XYZ axes system. For online process observation, a CCD camera monitored the polymerisation process. The whole setup was mounted on a hard stone frame to damp vibrations. The laser power was measured behind the AOM.

Microscope

An Axioskop microscope from Zeiss with an LD Achroplan (20x) objective was used for analysing the 2PP samples for homogeneity prior to usage.
For the laser scanning microscopic (LSM) pictures of the 2PP structures a Axio Observer Z1 from Zeiss was used in combination with an LSM 700 scanning head. The excitation-wavelength was 488 nm and for data processing ZEN 2011 software from Zeiss was used. The following objectives were used in combination with the LSM: 10x EC Plan Neofluar 10x/03, 20x EC Plan Neofluar 20x/05, 63x Plan Achromat 63x/1.40 with immersion oil.

UV chamber

For the preparation of swellability samples and for irradiation of NMR tube experiments a UV-chamber INTELLI-RAY 600 from uvi tron international was used. The distance from lamp to sample as well as irradiation time and intensity is stated in the corresponding section.

Ultrasonic bath

To accelerate dissolving of substances, an ultrasonic bath Sonorex Digitec from the company Bandelin was used.

Dialysis

For purification of the synthesized polymer substances dialysis was used. The dialysing tubes were ZelluTrans from Roth with a nominal molecular weight cutoff (MWCO) of 3500 g/mol.
Dialysis was performed according to the following protocol:
The dialysing tubes were soaked for at least 15 minutes in dialysed water and washed thoroughly with deionized water. Afterwards one side of the tube was reverted and clamped to seal this end of the tube. The solution or suspension to be dialysed was transferred with a funnel into the dialysis tube to a maximum of 2/3 of the volume of the tube. Afterwards

the air was removed by hand before reverting and clamping the second side of the tube. The sealed dialysis tube was put into a 5000 mL beaker with deionized water which was stirred with a magnetic stirrer. Water exchange was done every two hours at least 7 times in a row.
If salt formation was preferred sodium bicarbonate and sodium carbonate were added to the deionized water in the beaker to yield a pH value between 8.0 and 9.0. Because of the moderate pH value and the low temperature a cleavage of the ester bond could be prevented. If bases like sodium carbonate were added, this was done within the first water exchanges and at least the last 3 ones were done with deionized water to be sure that no excessive base would stay in the product.
After the dialysis was completed one end of the tube was opened and the solution was transferred to a flask from which the solvent was evaporated on a rotary evaporator.

Lyophylisation

For removing the water from the swellability samples a Lyophilisation (freeze drying) apparatus FreeZone 2.5 plus from the company Labconco was used. There the water was sublimated at a pressure of 0.01 mbar and a temperature of the cooling coils of -89°C.

IR ATR

FTIR-ATR was measured on a Spectrum 65 FTIR-ATR spectroscope from Perkin-Ellmer.

Abbreviations

2PP	two-photon polymerisation
ACC	N-acetyl-cysteine
AMT	additive manufacturing technology
ASA	allyl succinic anhydride
ATR	attenuated total reflection
$CDCl_3$	deuterated chloroform
DMAP	4-dimethylaminopyridin
DMEM	Dulbecco's modified eagle medium
DMSO	dimethylsulfoxide
DMSO-d_6	hexadeuterated dimethylsulfoxide
DS	degree of substitution
DTT	dithiothreitol
ECM	extra cellular matrix
EE	ethyl acetate
eq.	equivalent(s)
FBS	fetal bovine serum
GC-MS	gas chromatography-mass spectrometry
GTBL	γ-thiobutyrolactone
HAc	acetic acid
IA	itaconic acid
IAH	itaconic anhydride
IG819	Irgacure 819
IG2959	Irgacure 2959
IR	infrared spectroscopy
LD	lethal dose
LSM	laser scanning microscope
MeOH	methanol
NAH	*cis*-5-norbornene-*endo*-2,3-dicarboxylic anhydride
NMR	nuclear magnetic resonance
OPA	one-photon absorption
PDMS	poly(dimethylsiloxane)
PE	petroleum ether (boiling point 45–60°C)
PEG	poly(ethylene glycol)
PETMP	pentaerythritol tetra-3-mercaptopropionate
PI	photoinitiator
PVA	poly(vinylalcohol)
Pyr	pyrogallol
p-TsOH	para-toluenesulfonic acid
TEA	triethylamine
THEMA	tris(hydroxyethyl)methylammonium (salt)

THF	tetrahydrofurane
TLC	thin layer chromatography
TPA	two-photon absorption
UV	ultra-violet

Bibliography

[1] Eurotransplant, Annual Report 2013 from Eurotransplant. `http://www.eurotransplant.org/cms/mediaobject.php?file=AR2012.pdf`, access on 24.09.2013.

[2] Zopf, D. A.; Hollister, S. J.; Nelson, M. E.; Ohye, R. G.; Green, G. E. *New England Journal of Medicine* **2013**, *368*, 2043–2045.

[3] Langer, R. *Advanced Materials* **2009**, *21*, 3235–3236.

[4] Peppas, N. A.; Huang, Y.; Torres-Lugo, M.; Ward, J. H.; Zhang, J. *Annual Review of Biomedical Engineering* **2000**, *2*, 9–29.

[5] Peppas, N.; Hilt, J.; Khademhosseini, A.; Langer, R. *Advanced Materials* **2006**, *18*, 1345–1360.

[6] Bae, K. H.; Wang, L.-S.; Kurisawa, M. *Journal of Materials Chemistry B* **2013**, *1*, 5371–5388.

[7] Langer, R.; Tirrell, D. A. *Nature* **2004**, *428*, 487–492.

[8] Slaughter, B. V.; Khurshid, S. S.; Fisher, O. Z.; Khademhosseini, A.; Peppas, N. A. *Advanced Materials* **2009**, *21*, 3307–3329.

[9] Alberts, B.; Bray, D.; Hopkin, K.; Johnson, A.; Lewis, J.; Raff, M.; Roberts, K.; Walter, P. In *Lehrbuch der Molekularen Zellbiologie*; Nover, L., von Koskull-Doering, P., Eds.; Wiley-VCH Verlag GmbH & Co. KGaA, 2004; Vol. 3; pp 752–754.

[10] Wichterle, O.; Lim, D. *Nature* **1960**, *185*, 117–118, 10.1038/185117a0.

[11] Agrawal, C. M.; Carter, J.; Ong, J. L. *Journal of ASTM International* **2006**, *3*.

[12] Williams, D. *The Williams' Dictionary of Biomaterials*; Liverpool University Press, 1999.

[13] Shin, H.; Mikos, A. *Biomaterials* **2003**, *24*, 4353–4364.

[14] Hersel, U.; Dahmen, C.; Kessler, H. *Biomaterials* **2003**, *24*, 4385–4415.

[15] Cruise, G.; Hegre, O.; Lamberti, F.; Hager, S.; Hill, R.; Scharp, D. *Cell Transplantation* **1999**, *8*, 293–306.

[16] Nguyen, K. T.; West, J. L. *Biomaterials* **2002**, *23*, 4307 – 4314.

[17] Melchels, F. P. W.; Feijen, J.; Grijpma, D. W. *Biomaterials* **2010**, *31*, 6121–6130.

[18] Felzmann, R.; Gruber, S.; Mitteramskogler, G.; Tesavibul, P.; Boccaccini, A. R.; Liska, R.; Stampfl, J. *Advanced Engineering Materials* **2012**, *14*, 1052–1058.

[19] Ovsianikov, A.; Deiwick, A.; Van, V. S.; Pflaum, M.; Wilhelmi, M.; Dubruel, P.; Chichkov, B. *Materials* **2011**, *4*, 288–299.

[20] Torgersen, J. Novel biocompatible materials for in situ two-photon polymerisation. Ph.D. thesis, Technical University of Vienna, 2013.

[21] Göppert-Mayer, M. *Annalen der Physik* **1931**, *401*, 273–294.

[22] Denk, W.; Svoboda, K. *Neuron* **1997**, *18*, 351–357.

[23] Amos, B. Laboratory for Optical and Computational Instrumentation - Multiple-photon Excitation Fluorescence Microscopy. `http://loci.wisc.edu/optical-sectioning/multiple-photon-excitation-fluorescence-microscopy`, accessed on 25.09.2013.

[24] Schuster, M.; Turecek, C.; Kaiser, B.; Stampfl, J.; Liska, R.; Varga, F. *Journal of Macromolecular Science, Part A: Pure and Applied Chemistry* **2007**, *44*, 547–557.

[25] Sawhney, A. S.; Pathak, C. P.; Hubbell, J. A. *Macromolecules* **1993**, *26*, 581–587.

[26] Elisseeff, J.; McIntosh, W.; Anseth, K.; Riley, S.; Ragan, P.; Langer, R. *Journal of Biomedical Materials Research* **2000**, *51*, 164–171.

[27] Matsuda, T.; Moghaddam, M. J.; MlWa, H.; Sakurai, K.; Iida, F. *ASAIO Journal* **1992**, *38*, M154–M157.

[28] Kim, S.-H.; Chu, C.-C. *Journal of Biomedical Materials Research* **2000**, *49*, 517–527.

[29] Posner, T. *Berichte der Deutschen Chemischen Gesellschaft* **1905**, *38*, 646–657.

[30] Gou, L.; Opheim, B.; Coretsopoulos, C.; Scranton, A. *Chemical Engineering Communications* **2006**, *193*, 620–627.

[31] Bowman, C. N.; Peppas, N. A. *Macromolecules* **1991**, *24*, 1914–1920.

[32] Decker, C. *Macromolecular Rapid Communications* **2002**, *23*, 1067–1093.

[33] Simon, G. P.; Allen, P. E. M.; Bennett, D. J.; Williams, D. R. G.; Williams, E. H. *Macromolecules* **1989**, *22*, 3555–3561.

[34] Kolb, H. C.; Finn, M. G.; Sharpless, K. B. *Angewandte Chemie International Edition* **2001**, *40*, 2004–2021.

[35] Hoyle, C. E.; Bowman, C. N. *Angewandte Chemie International Edition* **2010**, *49*, 1540–1573.

[36] Kade, M. J.; Burke, D. J.; Hawker, C. J. *Journal of Polymer Science Part A: Polymer Chemistry* **2010**, *48*, 743–750.

[37] Esfandiari, P.; Ligon, S. C.; Lagref, J. J.; Frantz, R.; Cherkaoui, Z.; Liska, R. *Journal of Polymer Science Part A: Polymer Chemistry* **2013**, *51*, 4261–4266.

[38] Hoyle, C. E.; Lee, T. Y.; Roper, T. *Journal of Polymer Science Part A: Polymer Chemistry* **2004**, *42*, 5301–5338.

[39] Black, M.; Rawlins, J. W. *European Polymer Journal* **2009**, *45*, 1433–1441.

[40] Hallensleben, M. L. *Ullmann's Encyclopedia of Industrial Chemistry*; Wiley-VCH Verlag GmbH & Co. KGaA, 2000.

[41] Nair, B. *International Journal of Toxicology* **1998**, *17*, 67–92.

[42] Lindemann, M. K. Vinyl alcohol polymers. Poly(vinyl alcohol). 1971; pp 149–207.

[43] Finch, C. A. Chemical properties of poly(vinyl alcohol). 1973; pp 183–202.

[44] Pritchard, J. G. *Poly(Vinyl Alcohol): Basic Properties and Uses*; Macdonald, 1970.

[45] Stauffer, S. R.; Peppast, N. A. *Polymer* **1992**, *33*, 3932–3936.

[46] Purss, H. K.; Qiao, G. G.; Solomon, D. H. *Journal of Applied Polymer Science* **2005**, *96*, 780–792.

[47] Ruiz, J.; Mantecón, A.; Cádiz, V. *Journal of Applied Polymer Science* **2003**, *87*, 693–698.

[48] Giménez, V.; Mantecón, A.; Ronda, J. C.; Cádiz, V. *Journal of Applied Polymer Science* **1997**, *65*, 1643–1651.

[49] Chaouat, M.; Le Visage, C.; Baille, W. E.; Escoubet, B.; Chaubet, F.; Mateescu, M. A.; Letourneur, D. *Advanced Functional Materials* **2008**, *18*, 2855–2861.

[50] Fernández, M. D.; Fernández, M. J. *Journal of Applied Polymer Science* **2008**, *107*, 2509–2519.

[51] Giménez, V.; Mantecón, A.; Cádiz, V. *Journal of Polymer Science Part A: Polymer Chemistry* **1996**, *34*, 925–934.

[52] Ossipov, D. A.; Hilborn, J. *Macromolecules* **2006**, *39*, 1709–1718.

[53] Ossipov, D. A.; Brännvall, K.; Forsberg-Nilsson, K.; Hilborn, J. *Journal of Applied Polymer Science* **2007**, *106*, 60–70.

[54] Ossipov, D. A.; Piskounova, S.; Hilborn, J. *Macromolecules* **2008**, *41*, 3971–3982.

[55] Tsuda, M. *Die Makromolekulare Chemie* **1964**, *72*, 174–182.

[56] Krauch, H. *Reaktionen der organischen Chemie*; Hüthig: Heidelberg, 1997.

[57] Mühlebach, A.; Müller, B.; Pharisa, C.; Hofmann, M.; Seiferling, B.; Guerry, D. *Journal of Polymer Science Part A: Polymer Chemistry* **1997**, *35*, 3603–3611.

[58] Nuttelman, C. R.; Henry, S. M.; Anseth, K. S. *Biomaterials* **2002**, *23*, 3617 – 3626.

[59] Bourke, S.; Al-Khalili, M.; Briggs, T.; Michniak, B.; Kohn, J.; Poole-Warren, L. *AAPS Journal* **2003**, *5*, 101–111.

[60] Martens, P.; Holland, T.; Anseth, K. S. *Polymer* **2002**, *43*, 6093 – 6100.

[61] OECD, OECD SIDS Methylene butanedioic acid. http://www.eeaa.gov.eg/cmuic/cmuic_pdfs/generalpub/Butanedioic%20acid,%20methylene.htm, accessed on 05.09.2013.

[62] Klement, T.; Buechs, J. *Bioresource Technology* **2013**, *135*, 422–431.

[63] Milovanovic, M. B.; Trifunovic, S. S.; Katsikas, L.; Popovic, I. G. *Journal of the Serbian Chemical Society* **2007**, *72*, 1507–1514.

[64] Ramos, M.; Huang, S. J. *Polym. Prepr. (Am. Chem. Soc., Div. Polym. Chem.)* **2000**, *41*, 1806.

[65] Ohnishi, M.; Taguchi, N.; Gotoh, J.; Uno, T.; Kubo, M.; Itoh, T. *Polymer Bulletin (Heidelberg, Germany)* **2009**, *62*, 761–776.

[66] Huang, S. J.; Wallach, J. A. *Polym. Prepr. (Am. Chem. Soc., Div. Polym. Chem.)* **2004**, *45*, 416.

[67] Leonard, E. C. *Vinyl and diene monomers*; High polymers ; 24; Interscience Publ.: New York, NY, 1970; p 477 S.

[68] Tate, B. E. **1967**, *5*, 214–232.

[69] Tate, B. E. *Die Makromolekulare Chemie* **1967**, *109*, 176–193.

[70] Elbert, R.; Folda, T.; Ringsdorf, H. *Journal of the American Chemical Society* **1984**, *106*, 7687–7692.

[71] Wathier, M.; Johnson, C. S.; Kim, T.; Grinstaff, M. W. *Bioconjugate Chemistry* **2006**, *17*, 873–876.

[72] Gou, P.; Zhu, W.; Shen, Z. *Polymer Chemistry* **2010**, *1*, 1205–1214.

[73] Baldwin, A. D.; Robinson, K. G.; Militar, J. L.; Derby, C. D.; Kiick, K. L.; Akins, J., Robert E. *Journal of Biomedical Materials Research, Part A* **2012**, *100A*, 2106–2118.

[74] Song, J.; Chen, L.; Wang, Y.; Chen, W.; Wang, R. *Frontiers of Chemical Science and Engineering* **2008**, *2*, 390–395.

[75] Tacx, J.; Schoffeleers, H.; Brands, A.; Teuwen, L. *Polymer* **2000**, *41*, 947–957.

[76] Patel, P.; Rodriguez, F.; Moloney, G. *Journal of Applied Polymer Science* **1979**, *23*, 2335–2342.

[77] GESTIS-Stoffdatenbank, GESTIS-Stoffdatenbank Maleinsäure. http://gestis.itrust.de/nxt/gateway.dll/gestis_de/014640.xml?f=templates$fn=default.htm$3.0, accessed on 11.09.2013.

[78] Sabitha, G.; Srividya, R.; Yadav, J. *Tetrahedron* **1999**, *55*, 4015–4018.

[79] Mundi, C.; Back, M.; Back, R. *Journal of Photochemistry and Photobiology A: Chemistry* **1992**, *67*, 13–22.

[80] TCI-Chemicals, Material safety data sheet Allylsuccinic acid TCI Chemicals. `http://www.tcichemicals.com/eshop/en/be/catalog/detail/msds/de/A1283/`, access on 09.09.2013.

[81] Northrop, B. H.; Coffey, R. N. *Journal of the American Chemical Society* **2012**, *134*, 13804–13817.

[82] Ito, O.; Hoteiya, K.; Watanabe, A.; Matsuda, M. *Bulletin of the Chemical Society of Japan* **1991**, *64*, 962–965.

[83] Fairbanks, B. D.; Schwartz, M. P.; Halevi, A. E.; Nuttelman, C. R.; Bowman, C. N.; Anseth, K. S. *Advanced Materials* **2009**, *21*, 5005–5010.

[84] De Gregori, A.; Jommi, G.; Sisti, M.; Gariboldi, P.; Merati, F. *Tetrahedron* **1988**, *44*, 2549–2568.

[85] Huckstep, M.; Taylor, R. J. K.; Caton, M. P. L. *Synthesis* **1982**, 881–882.

[86] Sigma-Aldrich, Material safety data sheet Gamma-Thiobutyrolactone Sigma Aldrich. `http://www.sigmaaldrich.com/MSDS/MSDS/DisplayMSDSPage.do?country=AT&language=de&productNumber=105449&brand=ALDRIC`, access on 12.09.2013.

[87] Crawford, J. M.; Braunwald, N. S. *In Vitro Cellular & Developmental Biology - Animal* **1991**, *27*, 633–638.

[88] Mautner, A.; Qin, X.; Wutzel, H.; Ligon, S. C.; Kapeller, B.; Moser, D.; Russmueller, G.; Stampfl, J.; Liska, R. *Journal of Polymer Science Part A: Polymer Chemistry* **2013**, *51*, 203–212.

[89] Desroches, M.; Caillol, S.; Lapinte, V.; Auvergne, R.; Boutevin, B. *Macromolecules* **2011**, *44*, 2489–2500.

[90] Bryant, S. J.; Nuttelman, C. R.; Anseth, K. S. *Journal of Biomaterials Science, Polymer Edition* **2000**, *11*, 439–457.

[91] Williams, C. G.; Malik, A. N.; Kim, T. K.; Manson, P. N.; Elisseeff, J. H. *Biomaterials* **2005**, *26*, 1211 – 1218.

[92] Claudino, M.; Johansson, M.; Jonsson, M. *European Polymer Journal* **2010**, *46*, 2321–2332.

[93] Drury, J. L.; Mooney, D. J. *Biomaterials* **2003**, *24*, 4337 – 4351.

[94] Qin, X.-H.; Torgersen, J.; Saf, R.; Mühleder, S.; Pucher, N.; Ligon, S. C.; Holnthoner, W.; Redl, H.; Ovsianikov, A.; Stampfl, J.; Liska, R. *Journal of Polymer Science Part A: Polymer Chemistry* **2013**, *51*, 4799–4810.

[95] Li, Z.; Torgersen, J.; Ajami, A.; Muhleder, S.; Qin, X.; Husinsky, W.; Holnthoner, W.; Ovsianikov, A.; Stampfl, J.; Liska, R. *RSC Advances* **2013**, *3*, 15939–15946.

[96] Lin, T.-C.; Hsu, C.-S.; Hu, C.-L.; Chen, Y.-F.; Huang, W.-J. *Tetrahedron Letters* **2009**, *50*, 182–185.

[97] Li, Z.; Siklos, M.; Pucher, N.; Cicha, K.; Ajami, A.; Husinsky, W.; Rosspeintner, A.; Vauthey, E.; Gescheidt, G.; Stampfl, J.; Liska, R. *Journal of Polymer Science Part A: Polymer Chemistry* **2011**, *49*, 3688–3699.

[98] Goss, C. A.; Charych, D. H.; Majda, M. *Analytical Chemistry* **1991**, *63*, 85–88.

[99] Sigma-Aldrich, Product Information 3-(Trimethoxysilyl)propyl methacrylate. `http://www.sigmaaldrich.com/etc/medialib/docs/Sigma/Product_Information_Sheet/1/m6514pis.pdf`, access on 13.10.2013.